TECHNICAL REPORT HSM-R111-68

OCTOBER 7, 1968

# STUDY PROGRAM OF LOCAL ANGLE-OF-ATTACK EFFECTS ON VEHICLE DYNAMIC RESPONSE



SPACE DIVISION CHRYSLER CORPORATION

HUNTSVILLE OPERATIONS

TECHNICAL REPORT HSM-R111-68
NAS8-21290

# STUDY PROGRAM OF LOCAL ANGLE-OF-ATTACK EFFECTS ON VEHICLE DYNAMIC RESPONSE

By

George F. McCanless, Jr.
Dale Bradley

OCTOBER 7, 1968

SPACE DIVISION CHRYSLER CORPORATION
HUNTSVILLE OPERATIONS

## FOREWORD

This report was prepared by the Aero-Space Mechanics Branch, Structures and Mechanics Engineering Department, Huntsville Operations, Chrysler Corporation. The work reported was authorized by NASA Contract NAS8-21290 issued by the Dynamics Analysis Branch, Dynamics and Flight Mechanics Division, Aero-Astrodynamics Laboratory, Marshall Space Flight Center. Mr. James G. Papadopoulos was the program Contracting Officer's Representative. The theoretical derivations and the numerical analyses were conducted by the authors. These numerical analyses were programmed on Chrysler's G. E. 415 computer by Miss Nancy J. Tate. The purpose of the study reported herein was to determine methods of computing the effects of the aerodynamic loading caused by variations in the local angle-of-attack on the dynamic response of launch vehicles. The methods were then applied to the Saturn V launch vehicle. Suggestions are made for including additional phenomena in the analysis.

# ABSTRACT

This report describes a study in which the effects of flexible body aerodynamics on launch vehicles are determined. The First Order Method For Flexible Bodies was developed to determine the aerodynamic forces that act on vehicles. A method of determining the structural flexing response to these forces is included. An analysis of vehicle dynamic response in the low frequency range is developed. Sample calculations of the Saturn V vehicle are given. Recommendations for further refining these theoretical methods are discussed.

## TABLE OF CONTENTS

## LIST OF ILLUSTRATIONS

LIST OF ILLUSTRATIONS (CONTD)

## NOMENCLATURE

| Symbol | |
|---|---|
| $A$ | Axial force, lb |
| $A_n$ | Axial force on the section $(x_{n+1} - x_{n-1})/2$, lb |
| $A_k$ | Parameter at station $x_k$ defined by equation (3-61), ft/rad |
| $\bar{A}_k$ | Parameter at station $x_k$ defined by equation (3-58), 1/rad |
| $\bar{\bar{A}}_k$ | Parameter at station $x_k$ defined by equation (3-55), 1/ft rad |
| $B_k$ | Parameter at station $x_k$ defined by equation (3-62), slug ft/lb |
| $\bar{B}_k$ | Parameter at station $x_k$ defined by equation (3-59), slug /lb |
| $\bar{\bar{B}}_k$ | Parameter at station $x_k$ defined by equation (3-56), slug /lb ft |
| $C_p$ | Pressure coefficient |
| $EI$ | Bending stiffness, lb ft$^2$ |
| $F$ | Gimbaled thrust, lb |
| $F_{w,v}(\omega)$ | Frequency response function of wind velocity to vehicle normal acceleration, 1/sec |
| $F_{\beta,v}(\omega)$ | Frequency response function of wind velocity to engine gimbal angle, rad sec/ft |
| $F_{\phi,v}(\omega)$ | Frequency response function of wind velocity to vehicle yaw angle, rad sec/ft |
| $G_{Ak}$ | Integration constant defined by equation (3-58), 1/rad |
| $G_{Bk}$ | Integration constant defined by equation (3-59), slug /lb |
| $H_{Ak}$ | Integration constant defined by equation (3-61), ft/rad |

| Symbol | |
|---|---|
| $H_{Bk}$ | Integration constant defined by equation (3-62), slug ft/lb |
| I | Moment of inertia, slug $ft^2$ |
| $IA_k$ | Parameter at station k defined by equation (3-67), slug ft/rad |
| $IAX_k$ | Parameter at station k defined by equation (3-68), slug $ft^2$/rad |
| $IB_k$ | Parameter at station k defined by equation (3-69), $slug^2$ ft/lb |
| $IBX_k$ | Parameter at station k defined by equation (3-70), $slug^2$ $ft^2$/lb |
| $IM_k$ | Parameter at station k defined by equation (3-71), slug |
| $IML_k$ | Parameter at station k defined by equation (3-72), slug ft |
| $IMLL_k$ | Parameter at station k defined by equation (3-73), slug $ft^2$ |
| L | Length of vehicle, ft |
| LCG | Distance from nose to the center of gravity of the vehicle, ft |
| $M_\infty$ | Free stream Mach number |
| $M_k$ | Vehicle bending moment at station $x_k$, ft lb |
| MF | Pitching moment about the center of gravity, ft lb |
| $MA_k$ | Flexible body pitching moment about the center of gravity for the $k^{th}$ iteration, ft lb |
| $\frac{\partial MA_k}{\partial \alpha_r}$ | Derivative of the rigid body pitching moment about the center of gravity with respect to the rigid body angle-of-attack, ft lb /rad |
| $\frac{\partial MA_k}{\partial \alpha_r}$ | Derivative of the incremental pitching moment about the center of gravity caused by bending due to the aerodynamic loading with respect to the rigid body angle-of-attack for the $k^{th}$ iteration, ft lb /rad |
| $\frac{\partial MA_k}{\partial \dot{w}}$ | Derivative of the incremental pitching moment about the center of gravity caused by bending due to the acceleration loading with respect to the vehicle normal acceleration for the $k^{th}$ iteration, lb $sec^2$ |

Symbol

$N_k$ — Flexible body normal force for the $k^{th}$ iteration, lb

NF — Normal force, lb

$N_n'$ — Local normal force at station $x_n$, lb /ft

$N_r'$ — Local rigid body normal force, lb /ft

$\frac{\partial N_r}{\partial \alpha_r}$ — Derivative of the rigid body normal force with respect to rigid body angle-of-attack, lb /rad

$\frac{\partial N_k}{\partial \alpha_r}$ — Derivative of the incremental normal force caused by bending due to the aerodynamic loading with respect to the rigid body angle-of-attack for the $k^{th}$ iteration, lb /rad

$\frac{\partial N_k}{\partial \ddot{w}}$ — Derivative of the incremental normal force caused by bending due to the acceleration loading with respect to the vehicle normal acceleration for the $k^{th}$ iteration, lb $sec^2$/ft

$\frac{\partial N_r'}{\partial \alpha_r}$ — Derivative of the rigid body local normal force with respect to rigid body angle-of-attack, lb /ft rad

$\frac{\partial N_k'}{\partial \alpha_r}$ — Derivative of the incremental local normal force caused by bending due to the aerodynamic loading with respect to the rigid body angle-of-attack for the $k^{th}$ iteration, lb /ft rad

$\frac{\partial N_r'}{\partial \ddot{w}}$ — Derivative of the incremental local normal force caused by bending due to the acceleration loading with respect to the vehicle normal acceleration for the $k^{th}$ iteration, lb $sec^2/ft^2$ rad

$P_k(x)$ — Parameter defined by equation (3-76) for the $k^{th}$ iteration, ft/rad

$\overline{P}_k(x)$ — Parameter defined by equation (3-74) for the $k^{th}$ iteration, 1/rad

$Q_k(x)$ — Parameter defined by equation (3-77) for the $k^{th}$ iteration, slug ft/lb

$\overline{Q}_k(x)$ — Parameter defined by equation (3-75) for the $k^{th}$ iteration, slug /lb

R — Body radius, ft

$R_1$ — Parameter defined by equation (4-39), rad

$R_2$ — Parameter defined by equation (4-39), rad

| Symbol | |
|---|---|
| $R_3$ | Parameter defined by equation (4-39), rad |
| $S_1$ | Parameter defined by equation (4-20), ft lb /rad |
| $S_2$ | Parameter defined by equation (4-21), lb $sec^2$ |
| $S_3$ | Parameter defined by equation (4-22), ft lb /rad |
| $T_1$ | Parameter defined by equation (4-23), lb /rad |
| $T_2$ | Parameter defined by equation (4-24), lb $sec^2/ft$ |
| $T_3$ | Parameter defined by equation (4-25), lb /rad |
| $V$ | Vehicle velocity, ft/sec |
| $V_\infty$ | Free stream velocity, ft/sec |
| $V_w$ | Wind velocity, ft/sec |
| $V_{wo}$ | Steady state component of wind velocity, defined by equation (4-31), ft/sec |
| $V_{w1}$ | Harmonic component of wind velocity, defined by equation (4-31), ft/sec |
| $X_{n,i}$ | Parameter defined by equation (2-55) |
| $Y_{n,i}$ | Parameter defined by equation (2-56) |
| $Z_{n,i}$ | Parameter defined by equation (2-76) |
| $a_o$ | Control gain defined by equation (4-5) |
| $a_1$ | Control gain defined by equation (4-5), sec |
| $a_i$ | Parameter defined by equation (2-52), ft/sec |
| $b_i$ | Parameter defined by equation (2-70), ft/sec |
| $f$ | Supersonic source strength, $ft^2/sec$ |
| $f'$ | Derivative of supersonic source strength with respect to distance, ft/sec |

Symbol

| | |
|---|---|
| $f''$ | Second derivative of supersonic source strength with respect to distance, 1/sec |
| $i$ | Body station index |
| $m$ | In section II, supersonic doublet strength, $ft^2/sec$ |
| $m$ | In sections III and IV, mass of vehicle, slug |
| $m'$ | In section II, derivative of supersonic doublet strength with respect to distance, ft/sec |
| $m''$ | In section II, second derivative of supersonic doublet strength with respect to distance, 1/sec |
| $m'$ | In sections III and IV, mass distribution, slug/ft |
| $n$ | Station index |
| $p$ | Arbitrary point in space |
| $q$ | Dynamic pressure, lb $/ft^2$ |
| $r$ | Radial coordinate in flexible body coordinate system, ft |
| $r_n$ | Radial coordinate at station, $x_n$, ft |
| $r_1$ | Parameter defined by equation (4-39), 1/sec |
| $r_2$ | Parameter defined by equation (4-39), 1/sec |
| $u$ | Disturbance velocity in the x direction, ft/sec |
| $\overline{u}$ | Disturbance velocity in the $\overline{x}$ direction, ft/sec |
| $v$ | Disturbance velocity in the r direction, ft/sec |
| $\overline{v}$ | Disturbance velocity in the $\overline{y}$ direction, ft/sec |
| $w$ | Disturbance velocity in the $\theta$ direction, ft/sec |
| $\overline{w}$ | Disturbance velocity in the $\overline{z}$ direction, ft/sec |
| $\ddot{w}$ | Normal acceleration of the vehicle, $ft/sec^2$ |

Symbol

| | |
|---|---|
| $\ddot{w}_T$ | Transient component of the normal vehicle acceleration defined in equation (4-35), ft/sec$^2$ |
| $\ddot{w}_1$ | Harmonic component of vehicle normal acceleration defined in equation (4-35), ft/sec$^2$ |
| $\ddot{w}_2$ | Harmonic component of vehicle normal acceleration defined in equation (4-35), ft/sec$^2$ |
| $x$ | Flexible body axial coordinate, ft |
| $x_n$ | Flexible body axial coordinate at the $n^{th}$ index, ft |
| $\overline{x}$ | In section II, cartesian coordinate, ft |
| $\overline{x}$ | In section IV, distance from vehicle nose to angular sensor, ft |
| $x_{cg}$ | Distance from vehicle nose to vehicle center of gravity, ft |
| $y$ | Cartesian coordinate used in beam analysis, ft |
| $\overline{y}$ | Cartesian coordinate, ft |
| $\dot{z}$ | Normal vehicle velocity, ft/sec |
| $\overline{z}$ | Cartesian coordinate, ft |
| $\Delta z$ | Flexible displacement from the $\overline{x}$ axis, ft |
| $\alpha$ | Angle-of-attack, rad |
| $\alpha_r$ | Rigid body angle-of-attack, rad |
| $\alpha_w$ | Contribution of the wind vector to the vehicle angle-of-attack, rad |
| $\beta$ | In section II, Mach number parameter |
| $\beta$ | In sections III an IV, engine gimbal angle, rad |
| $\beta_T$ | Transient component of engine gimbal angle defined in equation (4-62), rad |
| $\beta_1$ | Harmonic component of engine gimbal angle defined in equation (4-62), rad |

| Symbol | |
|---|---|
| $\beta_2$ | Harmonic component of engine gimbal angle defined in equation (4-62), rad |
| $\theta$ | In section II, flexible body circumferential coordinates, rad |
| $\theta_{\ddot{w},v}$ | Phase angle of the wind velocity to normal acceleration frequency response function, rad |
| $\theta_{\beta,v}$ | Phase angle of the wind velocity to engine gimbal angle frequency response function, rad |
| $\theta_{\phi,v}$ | Phase angle of the wind velocity to body yaw angle frequency response function, rad |
| $\varepsilon$ | Distance along body axis, ft |
| $\phi$ | In section II, disturbance velocity potential, $ft^2/sec$ |
| $\phi$ | In sections III and IV, vehicle yaw angle, rad |
| $\dot{\phi}$ | Vehicle angular velocity in yaw plane, rad/sec |
| $\ddot{\phi}$ | Vehicle angular acceleration in yaw plane, $rad/sec^2$ |
| $\phi_T$ | Transient component of vehicle yaw angle defined in equation (4-32), rad |
| $\dot{\phi}_T$ | Time derivative of transient component of yaw angle defined in equation (4-33), rad/sec |
| $\ddot{\phi}_T$ | Second time derivative of transient component of yaw angle defined in equation (4-34), $rad/sec^2$ |
| $\phi_1$ | Harmonic component of vehicle yaw angle defined in equation (4-32), rad |
| $\phi_2$ | Harmonic component of vehicle yaw angle defined in equation (4-32), rad |
| $\phi_a$ | Axial flow disturbance velocity potential, $ft^2/sec$ |
| $\psi_c$ | Cross flow disturbance velocity potential |
| $\psi_{n,i}$ | Parameter defined by equation (2-48) |
| $\omega$ | Circular frequency, rad/sec |

# I. INTRODUCTION

Numerous studies have been made of various aspects of the static and dynamic characteristics of launch vehicle control systems and structures. The objective of these studies has been to determine whether vehicle control systems would properly control the vehicles or whether vehicle structures would fail. In many of these studies the incremental aerodynamic forces generated by vehicle flexing were not considered, since some other aspect of vehicle dynamics was being scrutinized. When the incremental aerodynamic forces were considered, the general practice of describing these forces was to use the rigid body local normal force derivatives with respect to the rigid body angle-of-attack multiplied by the local angle-of-attack caused by flexing. This approach implicitly assumes that the local normal force acting at a given body station on a flexed body is the same as the local normal force that would act at this station if that portion of the vehicle forward of the station were rigid, and were at the same angle-of-attack as the vehicle at the station being considered.

In this study a method of computing the local aerodynamics forces acting on a launch vehicle is derived that includes the effects of a flexed forebody. The need for this study was recognized by James G. Papadopoulos, and this study is an outgrowth of his work in references 1 and 2. It also utilizes an earlier study by Werner K. Dahm, described in reference 3, in which he included the effects of gross body flexing in the Slender Body Method. The technique derived here is a development of the First Order Method of supersonic aerodynamics described by Antonio Ferri in reference 4 and Milton D. Van Dyke in reference 5. The significance of the First Order Method for Flexible Bodies, which includes the effects of forebody displacement, can be seen in the fifth figure of section II. In this case calculations were made by the method developed in this study for a 10-degree half-angle cone whose forebody is at 0.1 radian angle-of-attack and the aft portion (due to flexing) is at zero angle-of-attack. The forebody induces a large negative normal force on the afterbody, which is greater in magnitude than the positive normal force acting on the forebody. If the rigid normal force coefficient derivatives were used to predict the aerodynamic loading on this bent cone, the normal force on the forebody would be zero. This approach not only would result in errors in accuracy but also would fail to describe the aerodynamic phenomena that are acting on the body. Therefore, the First Order Method for Flexible Bodies that was developed in this study provides valuable insight into the mechanism of launch vehicle behavior, besides improving the accuracy of numerous control and structural calculations.

This study also includes an analysis of structural bending response of vehicles to aerodynamic forces. The deflections are shown to be determined by three terms. The first is the rigid body aerodynamic loading. The second is the incremental aerodynamics loading caused by vehicle flexing which is due to aerodynamic loading. The third term is the aerodynamic loading caused by the vehicle flexing which is due to the D'Alembert, or inertia, forces. An iterative procedure between the aerodynamic analysis is required to determine these two incremental aerodynamic loads due to flexing. This procedure results in equations representing the aeroelastic vehicle deflections, slopes, and bending moments that are linear in terms of the angle-of-attack of the rigid center line of a vehicle and the normal acceleration of the vehicle. This simple representation reduces the analysis of the integrated dynamics of a vehicle to manageable proportions.

The integrated dynamics of a vehicle is the third analysis performed under this study. This analysis is highly simplified and is included to illustrate how the results of the previous two analyses can be utilized in a more general dynamic analysis of a vehicle. It also indicates the significance of the incremental aerodynamic loading on vehicle dynamics in a limited frequency range. The analysis consists of four equations that describe body yawing, normal body translations, engine gimbal, and bending. Frequency response functions are derived that are applicable below the control frequency of a vehicle.

## II. DETERMINATION OF THE AERODYNAMIC FORCES ACTING ON A FLEXIBLE VEHICLE

A method of computing the aerodynamic forces that act on a flexible axially symmetric body is developed in this section. The flexing of the body results in a variation in angle-of-attack along the body. The analysis is applicable when the cross flow along the body caused by winds is uniform and the variation in angle-of-attack is due only to gross body flexing. It is also restricted to supersonic cases where aerodynamic terms can be assumed to be independent of time. The aerodynamic effects of body fins are included by increasing the body diameter.

The analysis is based on the well-known First Order Method of aerodynamics described by Ferri in reference 4 and Van Dyke in reference 5. The exact tangency condition and the exact pressure relation are used here. The usual First Order Method, which is applicable to supersonic attached flow fields about bodies of revolution, is based on a cylindrical coordinate system. In deriving the First Order Method for Flexible Bodies, the equation of the velocity potential is written in cartesian coordinates. It is then transformed into the flexible body cylindrical coordinate system. The First Order Method is then developed to satisfy this equation and the flexible body boundary conditions. This yields the disturbance velocity potential from which the velocity components are obtained. The velocity components yield the pressures on the body surface. These pressures are then used to compute the aerodynamic forces and moments that act on the body.

Consider the cartesian coordinate system ($\overline{x}$, $\overline{y}$, and $\overline{z}$) of Figure 2-1. The free stream velocity, $V_\infty$, lies in the $\overline{y} = 0$ plane. The angle-of-attack with respect to the x axis is the angle in the $\overline{y} = 0$ plane between the free stream velocity vector and the x axis. The velocity components ($\overline{u}$, $\overline{v}$, and $\overline{w}$) in the $\overline{x}$, $\overline{y}$, and $\overline{z}$ directions are given by:

$$\overline{u} = V \cos\alpha + \frac{\partial \phi}{\partial \overline{x}} \qquad (2\text{-}1)$$

$$\overline{v} = \frac{\partial \phi}{\partial \overline{y}} \qquad (2\text{-}2)$$

$$\overline{w} = V \sin\alpha + \frac{\partial \phi}{\partial \overline{z}} \qquad (2\text{-}3)$$

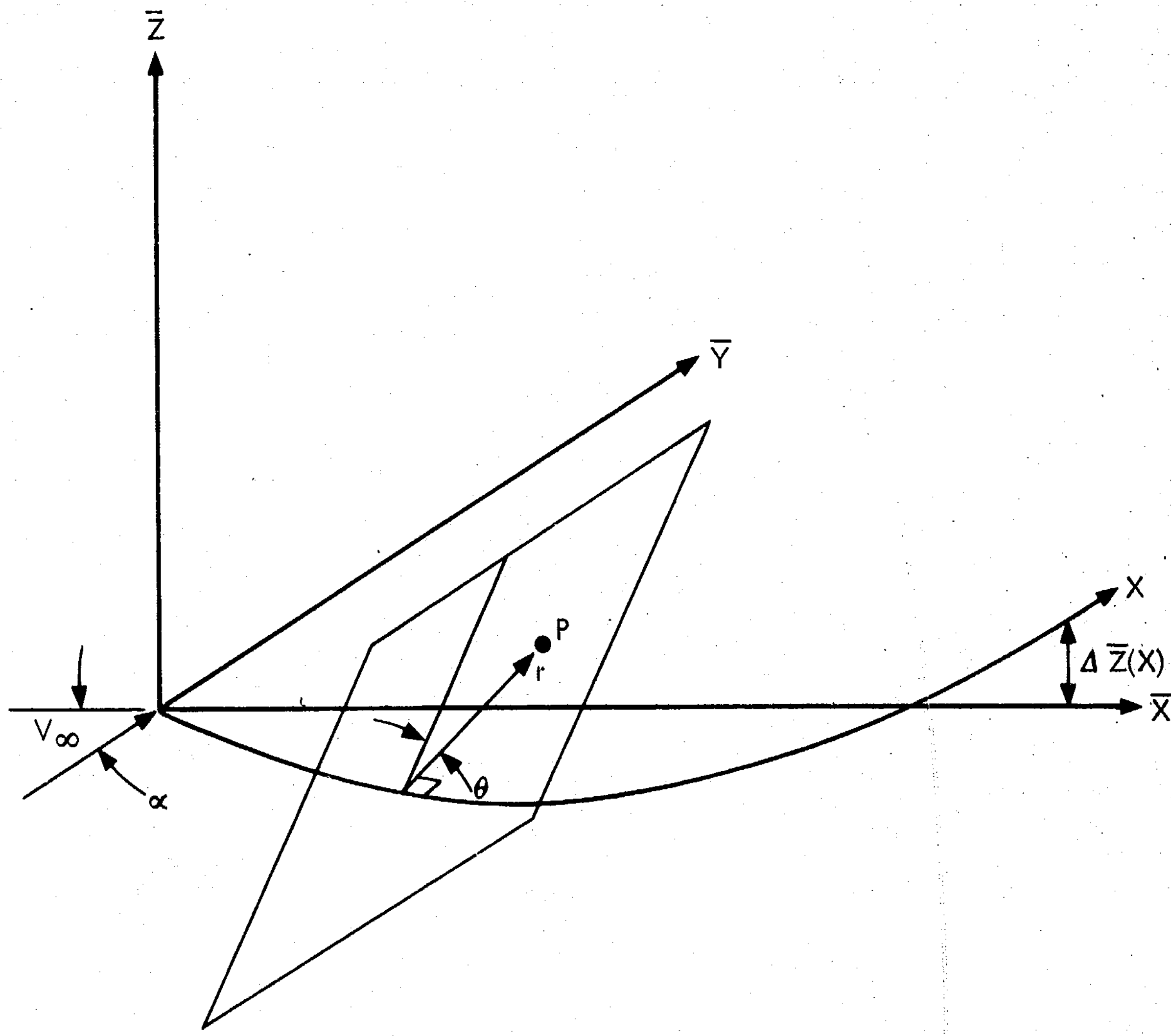

Figure 2-1. Flexible Body Coordinate System

where $\phi$ (x, y, z) is the disturbance velocity potential. The disturbance potential must satisfy the equation of the velocity potential;

$$-\beta^2 \frac{\partial^2 \phi}{\partial \bar{x}^2} + \frac{\partial^2 \phi}{\partial \bar{y}^2} + \frac{\partial^2 \phi}{\partial \bar{z}^2} = 0 \tag{2-4}$$

where

$$\beta = \sqrt{M_\infty^2 - 1} \tag{2-5}$$

The velocity potential must also satisfy boundary conditions imposed by a body that is placed in the coordinate system.

A cartesian or cylindrical coordinate system is a convenient choice for a rigid body. However, in determining the aerodynamic characteristics of a flexible body, it is more convenient to use the inherent coordinate system of the flexible body as shown in figure 2-1. This coordinate system will be defined in terms of the $\bar{x}$, $\bar{y}$, $\bar{z}$ cartesian coordinate system, and the equation of the velocity potential will be transformed into the flexible body coordinate system.

Let the body flex in the $\bar{y} = 0$ plane and let the nose of the body remain at the origin of the $\bar{x}$, $\bar{y}$, $\bar{z}$ coordinate system. Further restrict the deflections of the center line of the flexible body, $\Delta \bar{z}(\bar{x})$, to be small compared to the body radius. Consider a point, p. Pass a plane through point p perpendicular to the flexible body center line. The distance along the center line of the flexible body to this plane is the x coordinate. The distance, in the constructed plane, from the x coordinate to point p, is the r coordinate. Now consider a line defined by the intersection of the constructed plane and the $\bar{y} = 0$ plane. The angle between this line and the r coordinate is the $\theta$ coordinate.

The flexible body coordinates (x, r, $\theta$) are given in terms of the rigid body coordinates ($\bar{x}$, $\bar{y}$, $\bar{z}$) by the following equations. These equations are restricted to cases where the slopes of the flexing body, $\left(\frac{\bar{z}}{\bar{x}}\right)_{r=0}$, and the body center line deflections, $\Delta \bar{z}$, are small.

$$x = \bar{x} + \left(\frac{d\bar{z}}{d\bar{x}}\right)_{r=0} \bar{z} \tag{2-6}$$

$$r = +\sqrt{\bar{y}^2 + \bar{z}^2} \tag{2-7}$$

$$\theta = \tan^{-1} \frac{\bar{y}}{\bar{z}} \tag{2-8}$$

The derivatives of the bent body coordinates with respect to the rigid body coordinates are:

$$\frac{\partial x}{\partial \bar{x}} = 1 + \left(\frac{d^2 \bar{z}}{d\bar{x}^2}\right)_{r = 0} \bar{z} \qquad (2\text{-}9)$$

$$\frac{\partial r}{\partial \bar{x}} = 0 \qquad (2\text{-}10)$$

$$\frac{\partial \theta}{\partial \bar{x}} = 0 \qquad (2\text{-}11)$$

$$\frac{\partial x}{\partial \bar{y}} = 0 \qquad (2\text{-}12)$$

$$\frac{\partial r}{\partial \bar{y}} = \sin \theta \qquad (2\text{-}13)$$

$$\frac{\partial \theta}{\partial \bar{y}} = \frac{\cos \theta}{r} \qquad (2\text{-}14)$$

$$\frac{\partial x}{\partial \bar{z}} = \left(\frac{d\bar{y}}{d\bar{x}}\right)_{r = 0} \qquad (2\text{-}15)$$

$$\frac{\partial r}{\partial \bar{z}} = \cos \theta \qquad (2\text{-}16)$$

$$\frac{\partial \theta}{\partial \bar{z}} = -\frac{\sin \theta}{r} \qquad (2\text{-}17)$$

In order to obtain the velocity potential equation, equation (2-4), in terms of the bent body coordinates, the partial derivatives of the potential in terms of the bent body coordinates will be derived. From the chain rule:

$$\frac{\partial \phi}{\partial \bar{x}} = \frac{\partial x}{\partial \bar{x}} \frac{\partial \phi}{\partial x} + \frac{\partial r}{\partial \bar{x}} \frac{\partial \phi}{\partial r} + \frac{\partial \theta}{\partial \bar{x}} \frac{\partial \phi}{\partial \theta} \qquad (2\text{-}18)$$

From equations (2-9), (2-10), and (2-11), this reduces to

$$\frac{\partial \phi}{\partial \bar{x}} = \left[ 1 + \left( \frac{d^2 \bar{z}}{d \bar{x}^2} \right)_{\substack{\bar{z} \\ r = 0}} \right] \frac{\partial \phi}{\partial x} \tag{2-19}$$

The second partial derivative with respect to $\bar{x}$ is:

$$\frac{\partial^2 \phi}{\partial \bar{x}^2} = \left[ 1 + \left( \frac{d^2 \bar{z}}{\partial \bar{x}^2} \right)_{\substack{\bar{z} \\ r = 0}} \right]^2 \frac{\partial^2 \phi}{\partial x^2} + \frac{\partial \left( \frac{d^2 \bar{z}}{d \bar{x}^2} \right)_{r=0}}{\partial x} \bar{z} \left[ 1 + \left( \frac{d^2 \bar{z}}{d \bar{x}^2} \right)_{r=0} \bar{z} \right] \frac{\partial \phi}{\partial x} \tag{2-20}$$

Restricting this to small values of curvature, $\frac{d^2 \bar{z}}{d \bar{x}^2}$, yields:

$$\frac{\partial^2 \phi}{\partial \bar{x}^2} = \frac{\partial^2 \phi}{\partial x^2} + \frac{\partial \left( \frac{\partial^2 \bar{z}}{\partial \bar{x}^2} \right)_{r=0}}{\partial x} \bar{z} \frac{\partial \phi}{\partial x} \tag{2-21}$$

For the partial derivatives with respect to $\bar{y}$, consider

$$\frac{\partial \phi}{\partial \bar{y}} = \frac{\partial x}{\partial \bar{y}} \frac{\partial \phi}{\partial x} + \frac{\partial r}{\partial \bar{y}} \frac{\partial \phi}{\partial r} + \frac{\partial \theta}{\partial \bar{y}} \frac{\partial \phi}{\partial \theta} \tag{2-22}$$

Substituting equations (2-13) and (2-14)

$$\frac{\partial \phi}{\partial \bar{y}} = \sin \theta \frac{\partial \phi}{\partial r} + \frac{\cos \theta}{r} \frac{\partial \phi}{\partial \theta} \tag{2-23}$$

Taking the second derivative of equation (2-23)

$$\begin{aligned} \frac{\partial^2 \phi}{\partial \bar{y}^2} = {} & \sin^2 \theta \frac{\partial^2 \phi}{\partial r^2} + \frac{\sin\theta \cos\theta}{r} \frac{\partial^2 \phi}{\partial r \partial \theta} - \frac{\sin\theta \cos\theta}{r^2} \frac{\partial \phi}{\partial \theta} \\ & + \frac{\cos\theta \sin\theta}{r} \frac{\partial^2 \phi}{\partial \theta \partial r} + \frac{\cos^2\theta}{r} \frac{\partial \phi}{\partial r} + \frac{\cos^2 \theta}{r^2} \frac{\partial^2 \phi}{\partial \theta^2} \\ & - \frac{\cos\theta \sin\theta}{r^2} \frac{\partial \phi}{\partial \theta} \end{aligned} \tag{2-24}$$

This reduces to

$$\frac{\partial^2 \phi}{\partial \bar{y}^2} = \sin^2\theta \frac{\partial^2 \phi}{\partial r^2} + \frac{\cos^2\theta}{r} \frac{\partial \phi}{\partial r} + \frac{2 \sin\theta \cos\theta}{r} \frac{\partial^2 \phi}{\partial r \partial \theta}$$

$$+ \frac{\cos^2\theta}{r^2} \frac{\partial^2 \phi}{\partial \theta^2} - \frac{2 \cos\theta \sin\theta}{r^2} \frac{\partial \phi}{\partial \theta} \tag{2-25}$$

For the partial derivatives with respect to the $\bar{z}$ coordinate

$$\frac{\partial \phi}{\partial \bar{z}} = \frac{\partial x}{\partial \bar{z}} \frac{\partial \phi}{\partial x} + \frac{\partial r}{\partial \bar{z}} \frac{\partial \phi}{\partial r} + \frac{\partial \theta}{\partial \bar{z}} \frac{\partial \phi}{\partial \theta} \tag{2-26}$$

From equations (2-15), (2-16), and (2-17)

$$\frac{\partial \phi}{\partial \bar{z}} = \left(\frac{d \bar{z}}{d \bar{x}}\right)_{r=0} \frac{\partial \phi}{\partial x} + \cos\theta \frac{\partial \phi}{\partial r} - \frac{\sin\theta}{r} \frac{\partial \phi}{\partial \theta} \tag{2-27}$$

Taking the second derivative yields:

$$\frac{\partial^2 \phi}{\partial \bar{z}^2} = \left(\frac{d \bar{z}}{d \bar{x}}\right)_{r=0} \frac{\partial}{\partial x}\left[\left(\frac{d \bar{z}}{d \bar{x}}\right)_{r=0} \frac{\partial \phi}{\partial x} + \cos\theta \frac{\partial \phi}{\partial r} - \frac{\sin\theta}{r} \frac{\partial \phi}{\partial \theta}\right]$$

$$+ \cos\theta \frac{\partial}{\partial r}\left[\left(\frac{d \bar{z}}{d \bar{x}}\right)_{r=0} \frac{\partial \phi}{\partial x} + \cos\theta \frac{\partial \phi}{\partial r} - \frac{\sin\theta}{r} \frac{\partial \phi}{\partial \theta}\right]$$

$$- \frac{\sin\theta}{r} \frac{\partial}{\partial \theta}\left[\left(\frac{d \bar{z}}{d \bar{x}}\right)_{r=0} \frac{\partial \phi}{\partial x} + \cos\theta \frac{\partial \phi}{\partial r} - \frac{\sin\theta}{r} \frac{\partial \phi}{\partial \theta}\right] \tag{2-28}$$

$$\frac{\partial^2 \phi}{\partial \bar{z}^2} = \left(\frac{d \bar{z}}{d \bar{x}}\right)^2_{r=0} \frac{\partial^2 \phi}{\partial x^2} + \left(\frac{d^2 \bar{z}}{d \bar{x}^2}\right)_{r=0} \left(\frac{d \bar{z}}{d \bar{x}}\right)_{r=0} \frac{\partial \phi}{\partial x} + \left(\frac{d \bar{z}}{d \bar{x}}\right)_{r=0} \cos\theta \frac{\partial^2 \phi}{\partial x \partial r}$$

$$- \left(\frac{d \bar{z}}{d \bar{x}}\right)_{r=0} \frac{\sin\theta}{r} \frac{\partial^2 \phi}{\partial x \partial \theta} + \cos\theta \left(\frac{d \bar{z}}{d \bar{x}}\right)_{r=0} \frac{\partial^2 \phi}{\partial r \partial x} + \cos^2\theta \frac{\partial^2 \phi}{\partial r^2}$$

$$- \frac{\sin\theta \cos\theta}{r} \frac{\partial^2 \phi}{\partial r \partial \theta} + \frac{\sin\theta \cos\theta}{r^2} \frac{\partial \phi}{\partial \theta} - \frac{\sin\theta}{r} \left(\frac{d \bar{z}}{d \bar{x}}\right)_{r=0} \frac{\partial^2 \phi}{\partial \theta \partial x}$$

$$- \frac{\sin\theta \cos\theta}{r} \frac{\partial \phi}{\partial \theta} \tag{2-29}$$

Restricting this to small values of curvature, $\left(\frac{d^2 \bar{z}}{d \bar{x}^2}\right)$, yields:

$$\frac{\partial^2 \phi}{\partial \bar{z}^2} = \cos^2 \theta \frac{\partial^2 \phi}{\partial r^2} - \frac{2 \sin \theta \cos\theta}{r} \frac{\partial^2 \phi}{\partial r \, \partial\theta} + \frac{\sin^2 \theta}{r} \frac{\partial \phi}{\partial r}$$

$$+ \frac{\sin^2 \theta}{r^2} \frac{\partial^2 \phi}{\partial\theta^2} + \frac{2 \sin \theta \cos \theta}{r^2} \frac{\partial \phi}{\partial \theta} \tag{2-30}$$

Equations (2-21), (2-25), and (2-30) give the derivatives of the velocity potential in terms of the bent body coordinates. Substituting these equations into the equation of the velocity potential, equation (2-4) yields:

$$-\beta^2 \frac{\partial^2 \phi}{\partial x^2} + (\sin^2 \theta + \cos^2 \theta) \frac{\partial^2 \phi}{\partial r^2} + \frac{(\sin^2 \theta + \cos^2 \theta)}{r} \frac{\partial \phi}{\partial r}$$

$$\frac{(2 \sin \theta \cos \theta - 2 \sin \theta \cos \theta)}{r} \frac{\partial^2 \phi}{\partial r \partial\theta} + \frac{(\sin^2 \theta + \cos^2 \theta)}{r^2} \frac{\partial^2 \phi}{\partial\theta^2}$$

$$\frac{(2 \sin \theta \cos \theta - 2 \sin \theta \cos \theta)}{r} \frac{\partial \phi}{\partial \theta} = \beta^2 \frac{\partial \left(\frac{d^2 \bar{z}}{d \bar{x}^2}\right)_{r=0}}{\partial x} r \cos\theta \frac{\partial \phi}{\partial x} \tag{2-31}$$

Combining terms yields:

$$-\beta^2 \frac{\partial^2 \phi}{\partial x^2} + \frac{\partial^2 \phi}{\partial r^2} + \frac{1}{r} \frac{\partial \phi}{\partial r} + \frac{1}{r^2} \frac{\partial^2 \phi}{\partial\theta^2} = \beta^2 \frac{\partial \left(\frac{d^2 \bar{z}}{d x^2}\right)_{r=0}}{\partial x} r \cos \theta \frac{\partial \phi}{\partial x} \tag{2-32}$$

For small values of the derivatives of the curvature with respect to the x coordinate, this can be written:

$$-\beta^2 \frac{\partial^2 \phi}{\partial x^2} + \frac{\partial^2 \phi}{\partial r^2} + \frac{1}{r} \frac{\partial \phi}{\partial r} + \frac{1}{r^2} \frac{\partial^2 \phi}{\partial\theta^2} = 0 \tag{2-33}$$

This equation, written in bent body cylindrical coordinates, is of the same form as the equations of the velocity potential written in rigid body cylindrical coordinates. The First Order Method of developing solutions for this equation is described in references 4 and 5. It will be developed here for this equation which is written in flexible body coordinates.

The velocity components u, v, and w in the x, r, and $\theta$ directions are determined by the following equations:

$$u = V_\infty \cos\alpha + \frac{\partial\phi a}{\partial x} + \frac{\partial \phi c}{\partial x} \qquad (2\text{-}34)$$

$$v = V_\infty \sin\alpha \cos\theta + \frac{\partial\phi a}{\partial r} + \frac{\partial\phi c}{\partial r} \qquad (2\text{-}35)$$

$$w = -V_\infty \sin\alpha \sin\theta + \frac{1}{r} \frac{\partial\phi c}{\partial\theta} \qquad (2\text{-}36)$$

where $\phi_a$ is the axial flow disturbance potential and $\phi_c$ is the cross flow disturbance potential. The sum of these two potentials yields the total disturbance velocity potential, $\phi$.

The potentials must satisfy the boundary conditions at the surface of the body. The boundary conditions require that the flow at the surface be tangent to the body surface. This requirement is written:

$$\left(\frac{dr}{dx}\right)_R = \left(\frac{v}{u}\right)_R \qquad (2\text{-}37)$$

where R is the body radius at station x.

Subsuituting equations (2-34) and (2-35) yields:

$$\left(\frac{dr}{dx}\right)_R \quad \left(\frac{V_\infty \sin\alpha \cos\theta + \frac{\partial\phi a}{\partial r} + \frac{\partial\phi c}{\partial r}}{V_\infty \cos\alpha + \frac{\partial\phi a}{\partial x} + \frac{\partial\phi c}{\partial x}}\right)_R \qquad (2\text{-}38)$$

This equation can be written as

$$\left(\frac{dr}{dx} V\cos\alpha\right)_R + \left(\frac{dr}{dx}\frac{\partial\phi a}{\partial x}\right)_R + \left(\frac{dr}{dx}\frac{\partial\phi c}{\partial x}\right)_R = \left(V\sin\alpha\cos\theta\right)_R + \left(\frac{\partial\phi a}{\partial r}\right)_R + \left(\frac{\partial\phi c}{\partial r}\right)_R \qquad (2\text{-}39)$$

This equation is satisfied exactly if the two potentials satisfy the following equations:

$$\left(\frac{dr}{dx} V_\infty \cos\alpha\right)_R = \left(\frac{\partial\phi_a}{\partial r}\right)_R - \left(\frac{dr}{dx} \frac{\partial\phi_a}{\partial x}\right)_R \tag{2-40}$$

$$(V_\infty \sin\alpha)_R = \left(\frac{dr}{dx} \frac{1}{\cos\theta} \frac{\partial\phi_c}{\partial x}\right)_R - \left(\frac{1}{\cos\theta} \frac{\partial\phi_c}{\partial r}\right)_R \tag{2-41}$$

A solution of equation (2-33) that satisfies the axial flow boundary conditions as given in equation (2-40) is:

$$\phi_a(x, r) = \int_{\cosh^{-1}\frac{x}{\beta r}}^{0} f(x - \beta r \cosh z)\, dz \tag{2-42}$$

where f(0) = 0 for pointed bodies. The proof of this is given in appendix A.

The axial flow velocity perturbations in the axial and radial directions are obtained by taking the derivatives of equation (2-42):

$$\frac{\partial\phi_a}{\partial x} = \int_{\cosh^{-1}\frac{x}{\beta r}}^{0} f'(x - \beta r \cosh z)\, dz - \frac{f(0)}{\beta r\sqrt{\left(\frac{x}{\beta r}\right)^2 - 1}} \tag{2-43}$$

$$\frac{\partial\phi_a}{\partial r} = -\beta \int_{\cosh^{-1}\frac{x}{\beta r}}^{0} f'(x - \beta r \cosh z) \cosh z\, dz + \frac{f(0)\left(\frac{x}{\beta r}\right)}{r\sqrt{\frac{x}{\beta r}^{2} - 1}} \tag{2-44}$$

For pointed bodies, f is zero at $x - \beta r \cosh z = 0$. Thus, the last terms in equations (2-43) and (2-44) are zero. Let equations (2-42), (2-43), and (2-44) be written as series:

$$\phi a\,(x_n, r_n) = \sum_{i=2}^{n} \int_{\cosh^{-1}\psi_{n,\, i-1}}^{\cosh^{-1}\psi_{n,i}} f\,(x_n - \beta\, r_n \cosh z)\, dz \tag{2-45}$$

$$\left(\frac{\partial \phi a}{\partial x}\right)_n = \sum_{i=2}^{n} \int_{\cosh^{-1}\psi_{n,\, i-1}}^{\cosh^{-1}\psi_{n,i}} f'\,(x_n - \beta\, r_n \cosh z)\, dz \tag{2-46}$$

$$\left(\frac{\partial \phi a}{\partial r}\right)_n = -\beta \sum_{i=2}^{n} \int_{\cosh^{-1}\psi_{n,\, i-1}}^{\cosh^{-1}\psi_{n,i}} f'\,(x_n - \beta\, r_n \cosh z) \cosh z\, dz \tag{2-47}$$

where $x_n$, $r_n$ is a point on the surface of the body ($x_1$, $r_1$ is the body nose, $x_1 = 0$, $r_1 = 0$) and

$$\psi_{n,i} = \frac{x_n - (x_i - \beta\, r_i)}{\beta\, r_n} \tag{2-48}$$

For values of z such that

$$\cosh^{-1}\psi_{n,\, i-1} < z \leq \cosh^{-1}\psi_{n,i} \tag{2-49}$$

Let $f(x_n - \beta\, r_n \cosh z)$ be represented by

$$f\,(x_n - \beta\, r_n \cosh z) = a_i \left[(x_n - \beta\, r_n \cosh z) - (x_n - \beta\, r_n\, \psi_{n,i-1})\right] + \sum_{j=2}^{i-1} a_j \left[(x_n - \beta\, r_n\, \psi_{n,j}) - (x_n - \beta\, r_n\, \psi_{n,j-1})\right] \tag{2-50}$$

This can also be written:

$$f(x_n - \beta r_n \cosh z) = \beta r_n \left[ - a_i \cosh z + \sum_{j=2}^{i} (a_j - a_{j-1}) \psi_{n,j-1} \right] \tag{2-51}$$

where $a_1 = 0$. The derivative of equations (2-50) and (2-51) with respect to the argument $(x_n - \beta r_n \cosh z)$ is:

$$f'(x_n - \beta r_n \cosh z) = a_i \tag{2-52}$$

for values of z specified by equation (2-49). Thus equations (2-46) and (2-47) can be written:

$$\left(\frac{\partial \phi a}{\partial x}\right)_n = \sum_{i=2}^{n} a_i \left(\cosh^{-1} \psi_{n,i} - \cosh^{-1} \psi_{n,i-1}\right) \tag{2-53}$$

$$\left(\frac{\partial \phi a}{\partial r}\right)_n = - \beta \sum_{i=2}^{n} a_i \left(\sqrt{\psi^2_{n,i} - 1} - \sqrt{\psi^2_{n,i-1} - 1}\right) \tag{2-54}$$

Define $X_{n,i}$ and $Y_{n,i}$ as

$$X_{n,i} = \cosh^{-1}\psi_{n,i} - \cosh^{-1}\psi_{n,i-1} \tag{2-55}$$

$$Y_{n,i} = \sqrt{\psi^2_{n,i} - 1} - \sqrt{\psi^2_{n,i-1} - 1} \tag{2-56}$$

Substituting these expressions yields:

$$\left(\frac{\partial \phi a}{\partial x}\right)_n = \sum_{i=2}^{n} a_i X_{n,i} \tag{2-57}$$

$$\left(\frac{\partial \phi a}{\partial r}\right)_n = - \beta \sum_{i=2}^{n} a_i Y_{n,i} \tag{2-58}$$

To determine the coefficients, $a_i$, substitute equations (2-57) and (2-58) into equation (2-40).

$$\left(\frac{dr}{dx} V \cos\alpha\right)_n = -\beta \sum_{i=2}^{n} a_i \, Y_{n,i} - \left(\frac{dr}{dx}\right)_n \sum_{i=2}^{n} a_i \, X_{n,i} \tag{2-59}$$

$$a_n = \frac{-\left(\frac{dr}{dx} V \cos\alpha\right)_n - \sum_{i=2}^{n-1} a_i\left[\beta Y_{n,i} + \left(\frac{dr}{dx}\right)_n X_{n,i}\right]}{\beta Y_{n,n} + \left(\frac{dr}{dx}\right)_n X_{n,n}} \tag{2-60}$$

The axial flow perturbation velocities can be determined from equations (2-57) and (2-58) from the coefficients determined by equation (2-60).

A solution of equation (2-33) that satisfies the cross flow boundary conditions is:

$$\phi_c(x, r, \theta) = -\cos\theta\beta \int_{\cosh^{-1}\frac{x}{\beta r}}^{o} m(x - \beta r \cosh z) \cosh z \, dz \tag{2-61}$$

where m(0) is zero for pointed bodies. A proof that equation (2-61) is a solution of equation (2-33) is given in appendix B.

The cross flow velocity perturbation potentials in the axial, radial, and circumferential directions are obtained by taking the derivatives of equation (2-61):

$$\frac{\partial\phi_c}{\partial x} = -\cos\theta\beta \int_{\cosh^{-1}\frac{x}{\beta r}}^{o} m'(x - \beta r \cosh z)\cosh z \, dz + \frac{m(0)\cos\theta\left(\frac{x}{\beta r}\right)}{r\sqrt{\left(\frac{x}{\beta r}\right)^2 - 1}} \tag{2-62}$$

$$\frac{\partial\phi_c}{\partial x} = +\cos\theta\,\beta^2 \int_{\cosh^{-1}\frac{x}{\beta r}}^{o} m'(x - \beta r \cosh z)\cosh^2 z \, dz - \frac{m(0)\cos\theta\beta\left(\frac{x}{\beta r}\right)^2}{r\sqrt{\left(\frac{x}{\beta r}\right)^2 - 1}} \tag{2-63}$$

$$\frac{1}{r}\ \frac{\partial\phi\ c}{\partial\theta}\quad \frac{\sin\theta\beta}{r}\int_{\cosh^{-1}\frac{r}{\beta r}}^{0} m(x - \beta r \cosh z) \cosh z\, dz \tag{2-64}$$

For pointed bodies, m is zero at x - βr cosh z = 0. Thus the last terms in equations (2-62) and (2-63) are zero. Let equations (2-61), (2-62), (2-63), and (2-64) be written as series:

$$\phi_c(x_n, r_n, \theta) = -\cos\theta\beta \sum_{i=2}^{n} \int_{\cosh^{-1}\psi_{n,i-1}}^{\cosh^{-1}\psi_{n,i}} m(x_n - \beta r_n \cosh z) \cosh z\, dz \tag{2-65}$$

$$\left(\frac{\partial\phi\ c}{\partial\ x}\right)_n = -\cos\theta\beta \sum_{i=2}^{n} \int_{\cosh^{-1}\psi_{n,i-1}}^{\cosh^{-1}\psi_{n,i}} m'(x_n - \beta\ r_n \cosh z)\ \cosh z\, dz \tag{2-66}$$

$$\left(\frac{\partial\phi c}{\partial\ r}\right)_n = \cos\theta\beta^2 \sum_{i=2}^{n} \int_{-\cosh^{-1}\psi_{n,i-1}}^{\cosh^{-1}\psi_{n,i}} m'(x_n - \beta r_n \cosh z) \cosh^2 z\, dz \tag{2-67}$$

$$\frac{1}{r_n}\left(\frac{\partial\phi\ c}{\partial\theta}\right)_n = \frac{\sin\theta}{r_n}\ \beta\sum_{i=2}^{n} \int_{\cosh^{-1}\psi_{n,i=1}}^{\cosh^{-1}\psi_{n,i}} m(x_n - \beta\ r_n \cosh z) \cosh z\, dz \tag{2-68}$$

where $x_n$, $r_n$ is a point on the body surface ($x_1, r_1, \theta$ is the body nose, $x_1 = 0$, $r_1 = 0$) and $\psi_{r,i}$ is given by equation (2-48). For values of z such that

$$\cosh^{-1}\psi_{n,i-1} < z \leq \cosh^{-1}\psi_{n,i} \tag{2-69}$$

let $m(x_n - \beta r_n \cosh z)$ be represented by

$$m(x_n - \beta r_n \cosh z) = b_i \left[ (x_n - \beta r_n \cosh z) - (x_n - \beta r_n \psi_{n,i-1}) \right] \tag{2-70}$$
$$+ \sum_{j=2}^{i-1} b_j \left[ (x_n - \beta r_n \psi_{n,j}) - (x_n - \beta r_n \psi_{n,j-1}) \right]$$

This can also be written:

$$m(x_n - \beta r_n \cosh z) = \beta r_n \left[ - b_i \cosh z + \sum_{j=2}^{i} (b_j - b_{j-1}) \psi_{n,j-1} \right] \tag{2-71}$$

where $b_1 = 0$. The derivative of equations (2-70) and (2-71) with respect to the argument $(x_n - \beta r_n \cosh z)$ is:

$$m' (x_n - \beta r_n \cosh z) = b_i \tag{2-72}$$

for values of z specified by equation (2-69). Thus equations (2-66), (2-67), and (2-68) can be written:

$$\left(\frac{\partial \phi c}{\partial x}\right)_n = - \cos \theta \beta \sum_{i=2}^{n} b_i \left\{ \sqrt{\psi^2_{n,i} - 1} - \sqrt{\psi^2_{n,i-1} - 1} \right\} \tag{2-73}$$

$$\left(\frac{\partial \phi c}{\partial r}\right)_n = \frac{1}{2} \cos \theta \beta^2 \sum_{i=2}^{n} b_i \left\{ \cosh^{-1} \psi_{n,i} - \cosh^{-1} \psi_{n,i-1} \right. \tag{2-74}$$
$$\left. + \psi_{n,i} \sqrt{\psi^2_{n,i} - 1} - \psi_{n,i-1} \sqrt{\psi^2_{n,i-1} - 1} \right\}$$

$$\frac{1}{r_n} \left(\frac{\partial \phi c}{\partial \theta}\right)_n = \frac{1}{2} \sin \theta \beta^2 \sum_{i=2}^{n} \left\{ - b_i \left( \cosh^{-1} \psi_{n,i} - \cosh^{-1} \psi_{n,i-1} \right. \right. \tag{2-75}$$
$$\left. + \psi_{n,i} \sqrt{\psi^2_{n,1} - 1} - \psi_{n,i-1} \sqrt{\psi^2_{n,i-1} - 1} \right)$$
$$\left. + \left( 2 \sum_{j=2}^{i} (b_j - b_{j-1}) \psi_{n,j-1} \right) \left( \sqrt{\psi^2_{n,i} - 1} - \sqrt{\psi^2_{n,i-1} - 1} \right) \right\}$$

Defining $Z_{n,i}$ as

$$Z_{n,i} = \psi_{n,i}\sqrt{\psi^2_{n,i} - 1} - \psi_{n,i-1}\sqrt{\psi^2_{n,i-1} - 1} \qquad (2\text{-}76)$$

and substituting equations (2-55), (2-56), and (2-76) into equations (2-73), (2-74), and (2-75) yields:

$$\left(\frac{\partial \phi c}{\partial x}\right)_n = -\cos\theta\beta \sum_{i=2}^{n} b_i\, Y_{n,i} \qquad (2\text{-}77)$$

$$\left(\frac{\partial \phi\, c}{\partial r}\right)_n = \frac{1}{2}\cos\theta\,\beta^2 \sum_{i=2}^{n} b_i\,(X_{n,i} + Z_{n,i}) \qquad (2\text{-}78)$$

$$\frac{1}{r_n}\left(\frac{\partial \phi c}{\partial \theta}\right)_n = \frac{1}{2}\sin\theta\beta^2 \sum_{i=2}^{n}\left[2\left\{\sum_{j=2}^{i}(b_j - b_{j-1})\,\psi_{n,j-1}\right\}Y_{n,i} - b_i\left\{X_{n,i} + Z_{n,i}\right\}\right] \qquad (2\text{-}79)$$

To determine the coefficients, $b_i$, substitute equations (2-77) and (2-78) into equation (2-41):

$$2(V_\infty \sin\alpha)_n = -\beta\sum_{i=2}^{n} b_i \left\{2\left(\frac{d\,r}{d\,x}\right)_n Y_{n,i} + \beta\,(X_{n,i} + Z_{n,i})\right\} \qquad (2\text{-}80)$$

$$b_n = \frac{-2(V\sin\alpha)_n - \beta\displaystyle\sum_{i=2}^{n-1} b_i\left\{2\left(\frac{d\,r}{d\,x}\right)_n Y_{n,i} + \beta\,(X_{n,i} + Z_{n,i})\right\}}{\beta\left\{2\left(\frac{d\,r}{d\,x}\right)_n Y_{n,n} + \beta\,(X_{n,n} + Z_{n,n})\right\}} \qquad (2\text{-}81)$$

Thus the cross flow disturbance components can be determined from equations (2-77), (2-78), and (2-79) using the coefficients from equation (2-81).

The flow velocity at station n is determined by equations (2-34), (2-35), and (2-36):

$$u_n = V_\infty \cos \alpha_n + \left(\frac{\partial \phi a}{\partial x}\right)_n + \left(\frac{\partial \phi c}{\partial x}\right)_n \tag{2-82}$$

$$v_n = \left(\frac{\partial \phi a}{\partial r}\right)_n + \left(\frac{\partial \phi c}{\partial r}\right)_n \tag{2-83}$$

$$w_n = - V_\infty \sin \alpha_n \sin \theta + \frac{1}{r_n} \left(\frac{\partial \phi c}{\partial \theta}\right)_n \tag{2-84}$$

These velocity components can be determined from the perturbations given by equations (2-57), (2-58), (2-77), (2-78), and (2-79).

The forebody axial force at station n is given by:

$$A_n = \left[\left(\frac{r_{n+1} \; r_n}{2}\right)^2 - \left(\frac{r_n - r_{n-1}}{2}\right)^2\right] q \int_0^\pi C_{pn}(\theta) d_\theta \tag{2-85}$$

The total forebody axial force is given by:

$$A = \sum_{n=2}^{N=1} A_n \tag{2-86}$$

The local normal force per unit length at body station n is given by:

$$N'_n = -2 q r_n \int_0^\pi C_{pn}(\theta) \cos \theta \; d\theta \tag{2-87}$$

The total normal force is given by:

$$NF = \sum_{n=2}^{N-1} N'_n \left(\frac{x_{n+1} - x_{n-1}}{2}\right) \tag{2-88}$$

The pitching moment about the center of gravity is given by:

$$MF = \sum_{n=2}^{N-1} N'_n (L - LCG - x_n)\left(\frac{x_{n+1} - x_{n-1}}{2}\right) \tag{2-89}$$

The center of pressure, measured from the base, is given by:

$$LCP = LCG + \frac{MF}{NF} \tag{2-90}$$

The forebody axial force at a station, $A_n$, on the local normal force per unit length, $N'_n$, is determined by the pressure coefficient. The exact expression for the pressure coefficient is:

$$C_{pn} = \frac{2}{\gamma M_\infty{}^2}\left\{\left[1 + \frac{\gamma - 1}{2} M_\infty^2 \left(1 - \frac{u_n^2 + v_n^2 + w_n^2}{V_\infty{}^2}\right)\right]^{\frac{\gamma}{\gamma - 1}} - 1\right\} \tag{2-91}$$

The pressure coefficient is determined from the velocity components given by equations (2-82), (2-83), and (2-84).

These results, which are based on the First Order Method, should reduce to the results of the Slender Body Method of reference 3 when the slender body restrictions are imposed. It is shown in appendix C that the method developed in this study does reduce to Dahm's method with these restrictions.

A flow diagram describing the numerical analysis of the method developed here and the computer program of this numerical analysis is given in appendix D. This appendix also includes a description of the input data required for the program.

In order to check the validity of the program, calculations were made of the normal force on a rigid cone with a half-angle of 10 degrees and a base diameter of 3.52 ft. These computations were made with a dynamic pressure of 760 lb/ft$^2$ and an angle-of-attack of 0.1 radian. They compared with the known results of the Slender Body Method and with known results of exact calculations. This comparison is shown in figure (2-2). The agreement between the computer program of the study and the exact solution is quite good. A similar comparison is shown by Van Dyke in reference 5 between the First Order Method and exact results.

Computations were also made of the aerodynamic characteristics of the rigid Saturn V vehicle in order to compare the results of the program with wind tunnel results. Figure (2-3) shows the computed pressure coefficient along the rigid Saturn V vehicle at zero angle-of-attack and at a Mach number of 2.0. Also shown are wind tunnel results from reference 6.

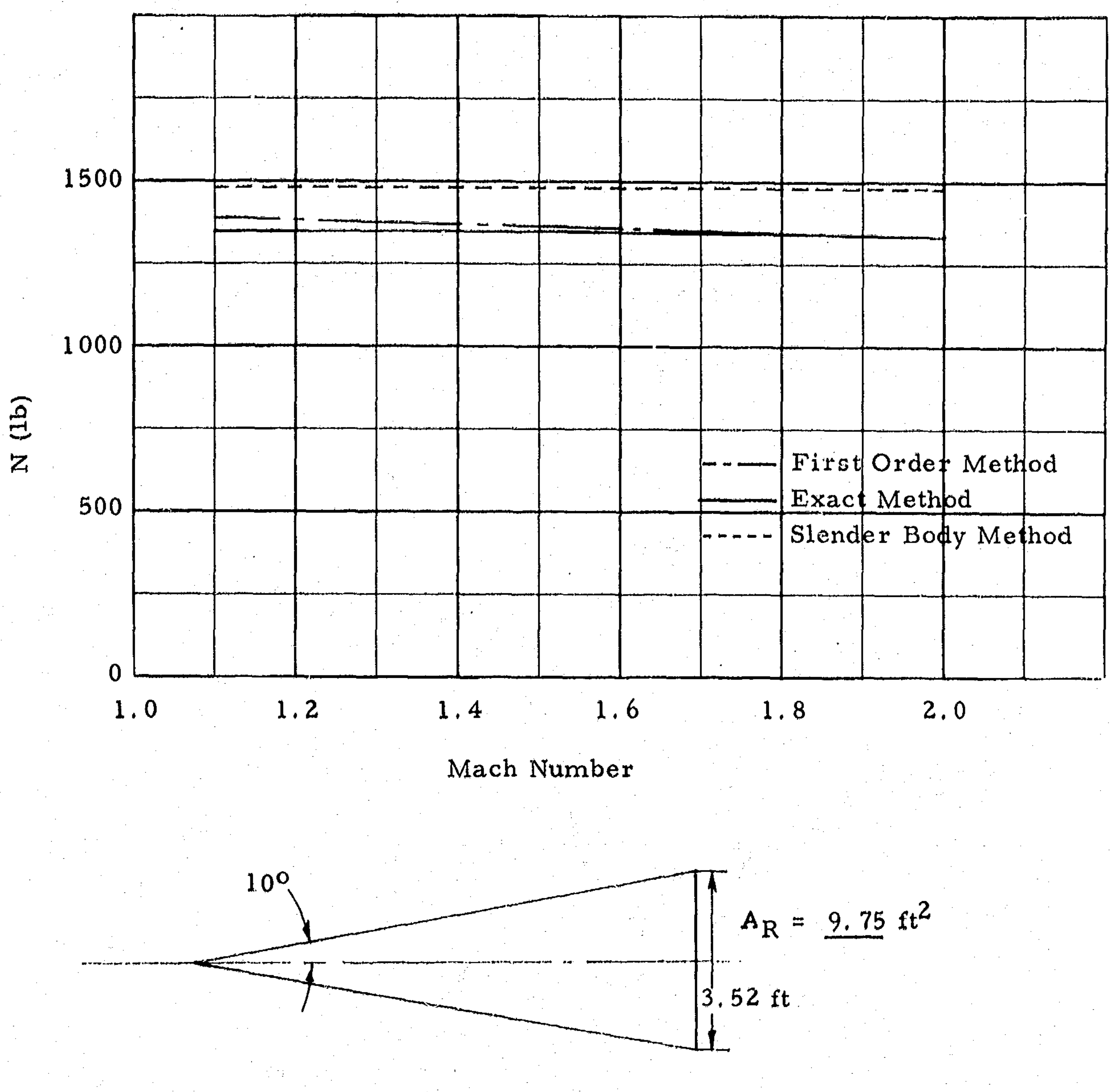


Figure 2-2. The First Order Method Applied to a Rigid $10^o$ Half-Angle Cone at $\alpha = 0.1$ rad

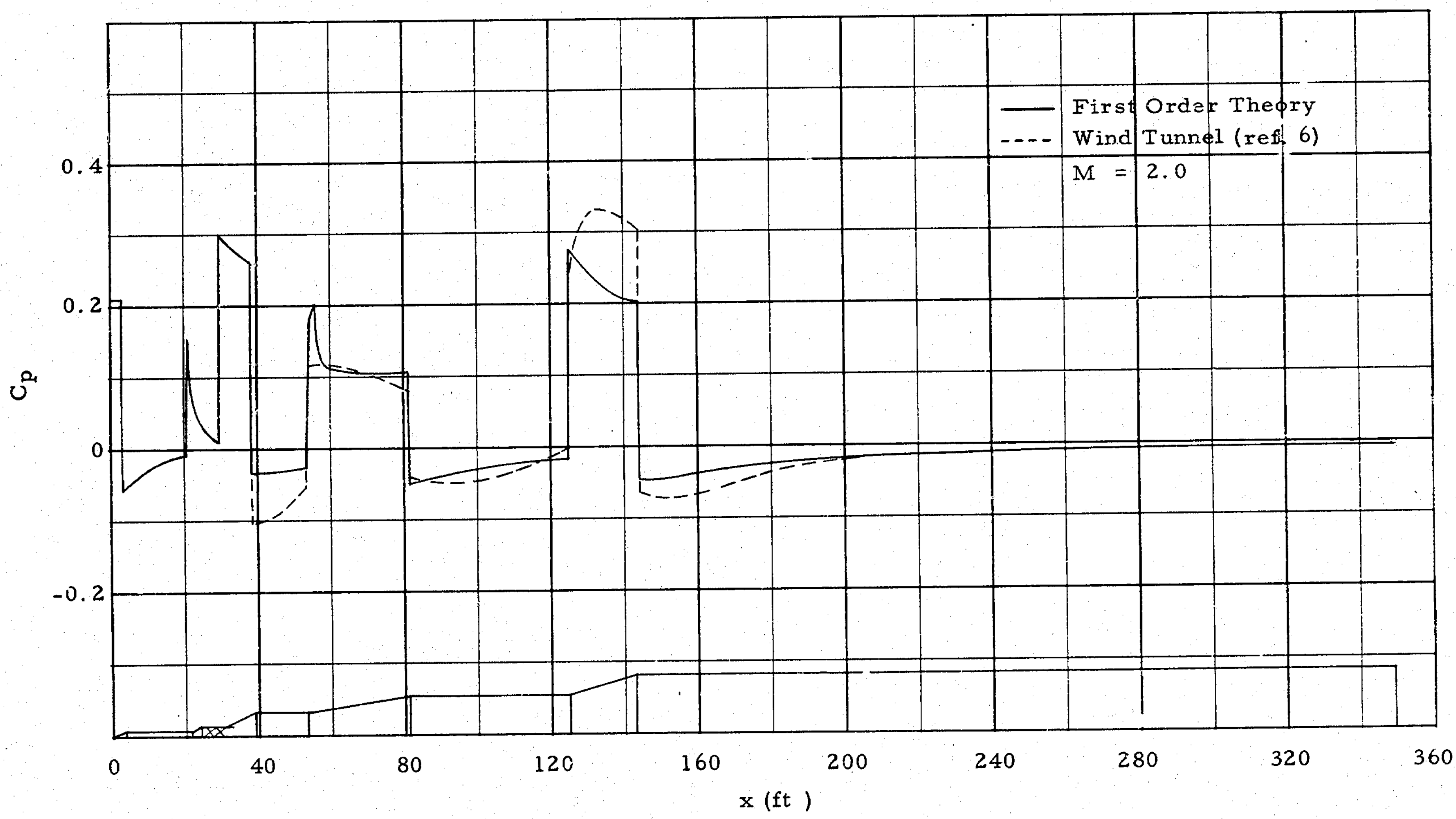


Figure 2-3. The First Order Method Applied to the Rigid Saturn V Vehicle at $\alpha = 0$

As stated in the introduction of reference 6, the discrepancies between theory and experiment are largely due to the flow separations that are observed in wind tunnel tests but are, in general, not accounted for in aerodynamic calculations. Figure (2-4) shows the local normal force distribution of the rigid Saturn V vehicle (without fins) at 8 degrees angle-of-attack, Mach number of 1.7, and a dynamic pressure of 760 $lb/ft^2$. Also shown in this figure are wind tunnel results of reference 6. As in the previous case, the discrepancies between the calculations and experimental data are primarily due to flow separation.

In order to determine the general behavior of the First Order Method for Flexible Bodies, calculations were made for a body of simple geometry. A flexed cone, shown in figure (2-5), was selected for this purpose. The aerodynamic characteristics of this cone were computed with the program developed during this study. The aerodynamic characteristics of the forebody agree well with known results. The effects of flexing are shown on the afterbody. The forebody induces a turn into the stream which is straightened by the afterbody. This straightening produces a normal force on the afterbody that is opposite in direction to that acting on the forebody and is greater in magnitude than that on the forebody. If rigid body aerodynamic derivatives with respect to angle-of-attack multiplied by the local angle-of-attack were used to determine the aerodynamic forces acting on the flexed body (which is the usual procedure), the computed normal force on the afterbody would be zero and the total body normal force would be that generated by the forebody. Thus the method derived in this study provides not only greater computing accuracy in determining the aerodynamic characteristics of flexible bodies but it also describes phenomena that have been generally ignored.

The First Order Method for Flexible Bodies developed in this section was then used to compute the aerodynamic characteristics of the rigid and flexed Saturn V vehicle. All these calculations were made at a Mach number of 1.70 and at a dynamic pressure of 760 $lb/ft^2$. In these calculations, an axially symmetric shroud was added to the Saturn V body to generate the local normal force that, in reality, is generated by the vehicle fin-shroud combination. This shroud is shown in figure (2-6). A theoretical justification for this method of simulating fins is given in references 3 and 7.

Local normal force calculations were made for a flexed Saturn V vehicle whose nose was at an angle-of-attack of 9.72 degrees and whose gimbal station was at an angle-of-attack of 8 degrees. The intermediate angles-of-attack may be determined from the deflection polynomial given in figure (2-7). The results of these calculations and rigid body calculations at 8 degrees angle-of-attack are compared in this figure. The effects of the flexed body can be seen as the discrepancies between the two curves.

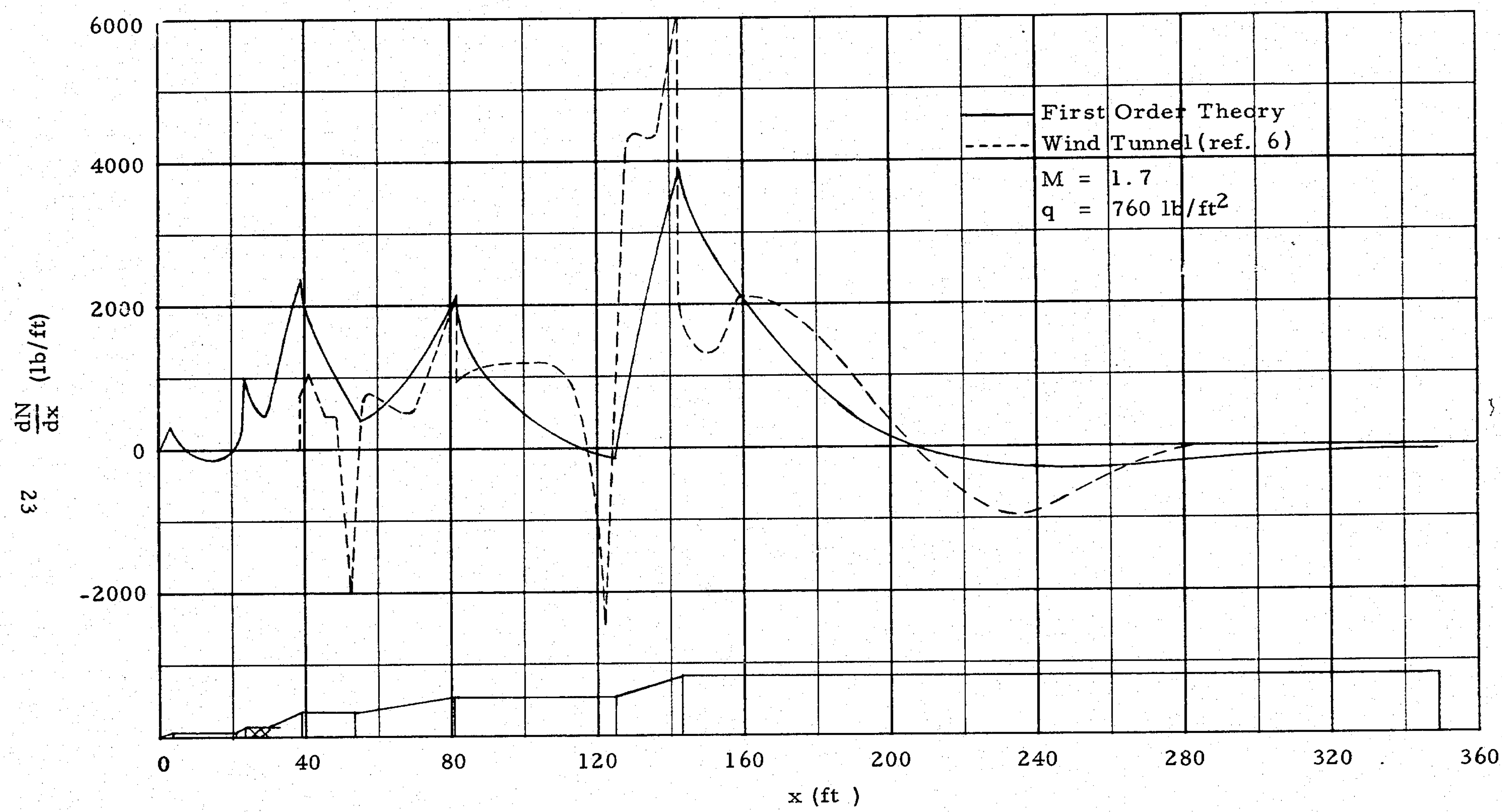


Figure 2-4. The First Order Method Applied to the Rigid Saturn V Vehicle without Fins at $\alpha = 0.1$ rad

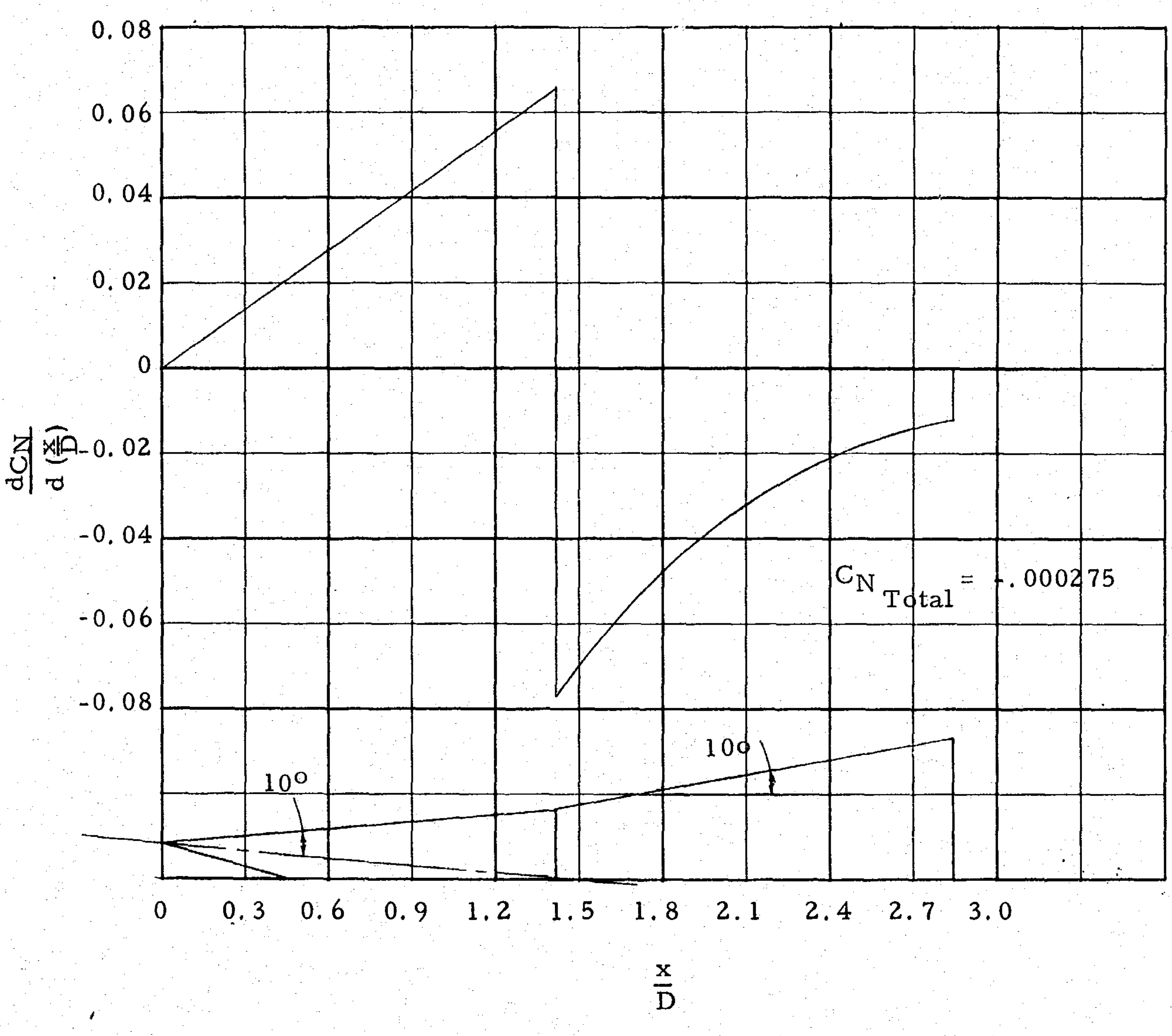


Figure 2-5. The First Order Method Applied to a Flexed Cone

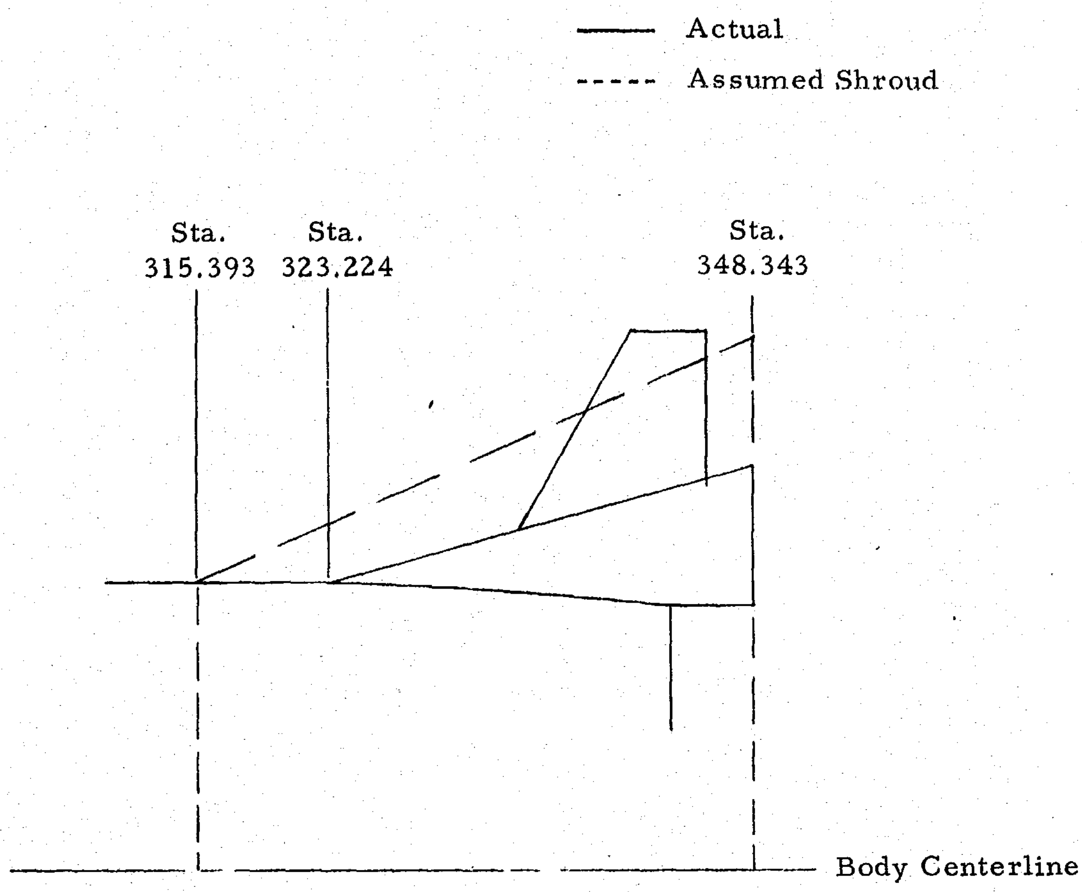


Figure 2-6. Frustum Simulation of the Saturn V Fin-Shroud Combination

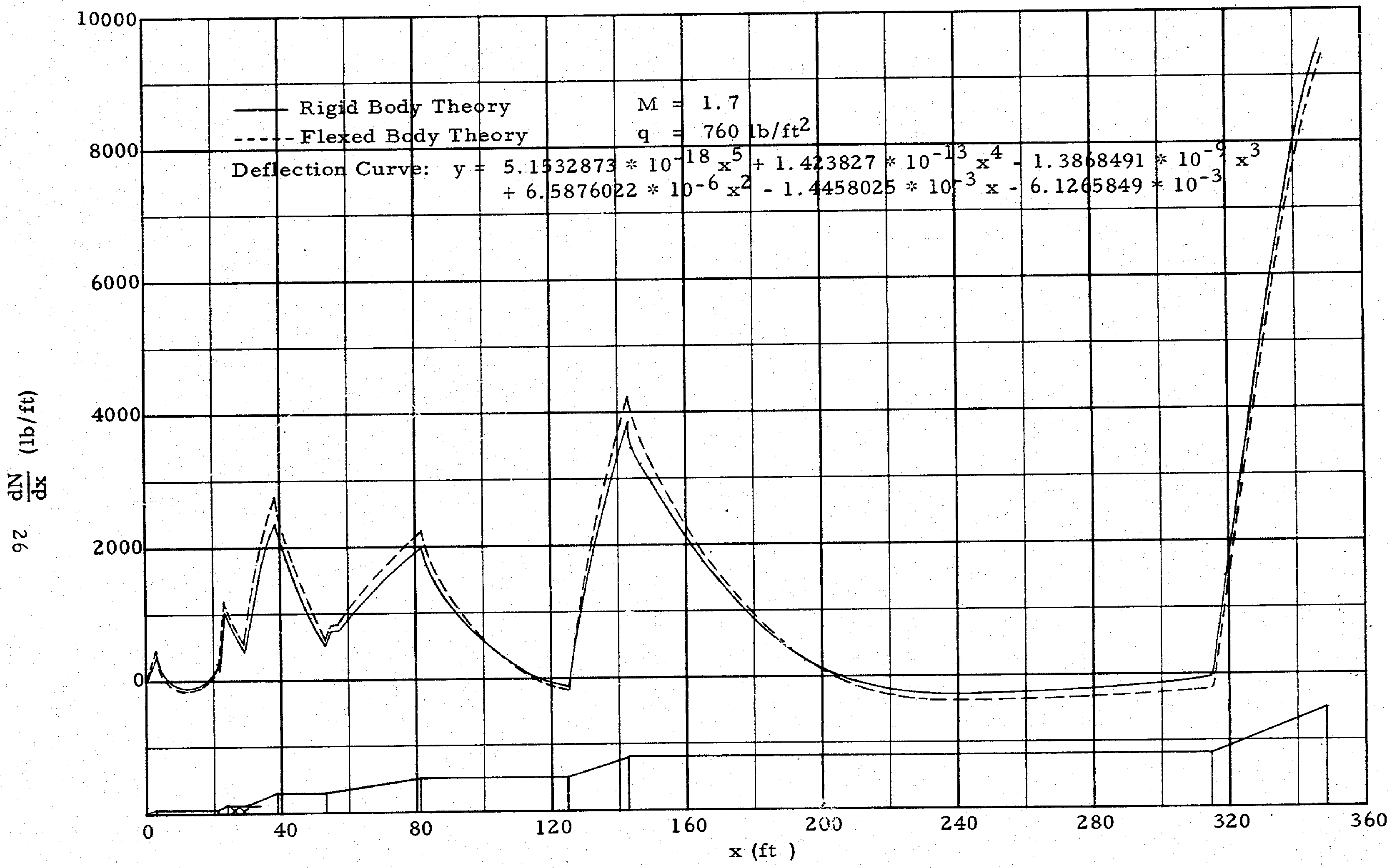


Figure 2-7. The First Order Method Applied to the Flexible Saturn V Vehicle as the Angle-of-Attack Varies from $\alpha = 9.72^{\circ}$ to $\alpha = 8^{\circ}$

The local normal force distribution of the rigid Saturn V vehicle at an angle-of-attack of 0.1 radian is given in figure (2-8). The normal force for this condition is $2.783 \times 10^5$ lb and the pitching moment about the center of gravity is $1.261 \times 10^8$ ft lb. Figures (2-9) and (2-10) show the local normal force distribution determined by the First Order Method for Flexible Bodies of the Saturn V flexed as shown in figures (3-8) and (3-9) respectively. The normal forces for these deflections are $-1.490 \times 10^5$ and $2.721 \times 10^3$ lb and the pitching moments are $1.900 \times 10^7$ and $-2.954 \times 10^5$ ft lb respectively.

For purposes of comparison, flexible body calculations were also made using the rigid body local normal force derivatives with respect to rigid body angle-of-attack multiplied by the local angle-of-attack at each body station. These calculations were made at a Mach number of 1.70 and a dynamic pressure of 760 lb/ft$^2$. Figure (2-11) shows the results of these calculations made for the vehicle deflected as shown in figure (3-10). Figure (2-12) shows the results for the vehicle deflected as shown in figure (3-11). The normal forces are $2.647 \times 10^4$ lb and $5.477 \times 10^2$ lb respectively. The pitching moments are $1.981 \times 10^7$ ft lb and $-3.243 \times 10^5$ ft lb respectively.

The deflection curves shown in figures (3-8) and (3-10) are almost identical as are those shown in figures (3-9) and (3-11). However, there is a considerable variation between the local normal force distribution shown in figures (2-9) and (2-11). Differences are also shown between the data in figures (2-10) and (2-12). There are also differences between the resultant body normal forces that correspond to the two deflections. Thus there is a significant difference in the local normal force distribution and the total body normal force computed by the First Order Method and that computed by modifying rigid body data to account for local angle-of-attack. However the pitching moment about the center of gravity of the Saturn V vehicle at a Mach number of 1.70 computed by both methods is almost identical. Considering the differences in the local normal force distribution, this is considered by the authors to be a coincidence.

In the following section, it is shown that the data in figures (2-9) and (2-11) can be used to determine the incremental aerodynamic loading caused by bending which is due to aerodynamic forces. The data in figures (2-10) and (2-12) can be used to determine the incremental aerodynamic loading caused by bending due to the normal acceleration of the vehicle.

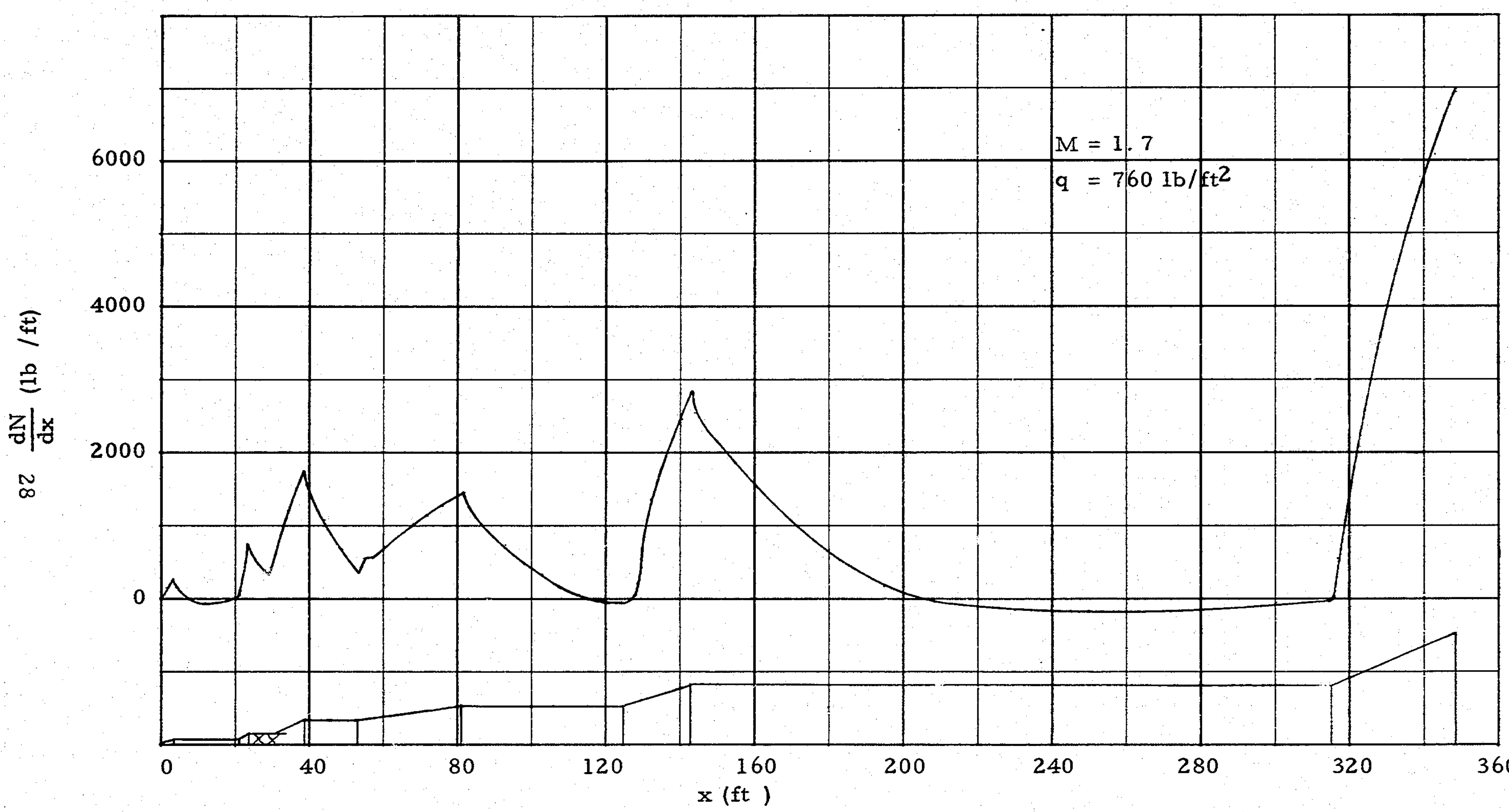


Figure 2-8. The First Order Method Applied to the Rigid Saturn V Vehicle at $\alpha = 0.1$ rad

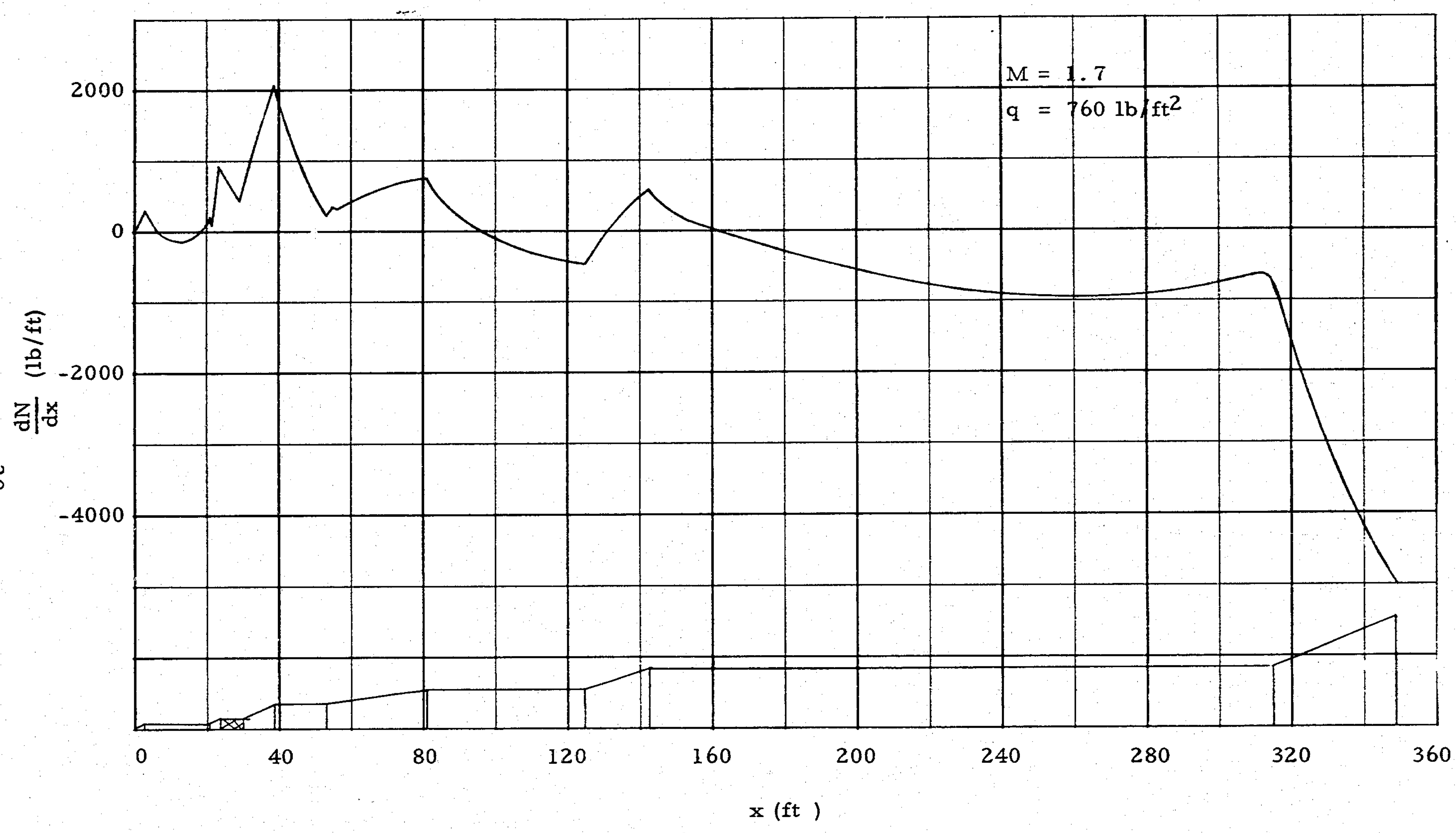


Figure 2-9. The First Order Method Applied to the Flexible Saturn V Vehicle with the Deflection Shown in Figure (3-8)

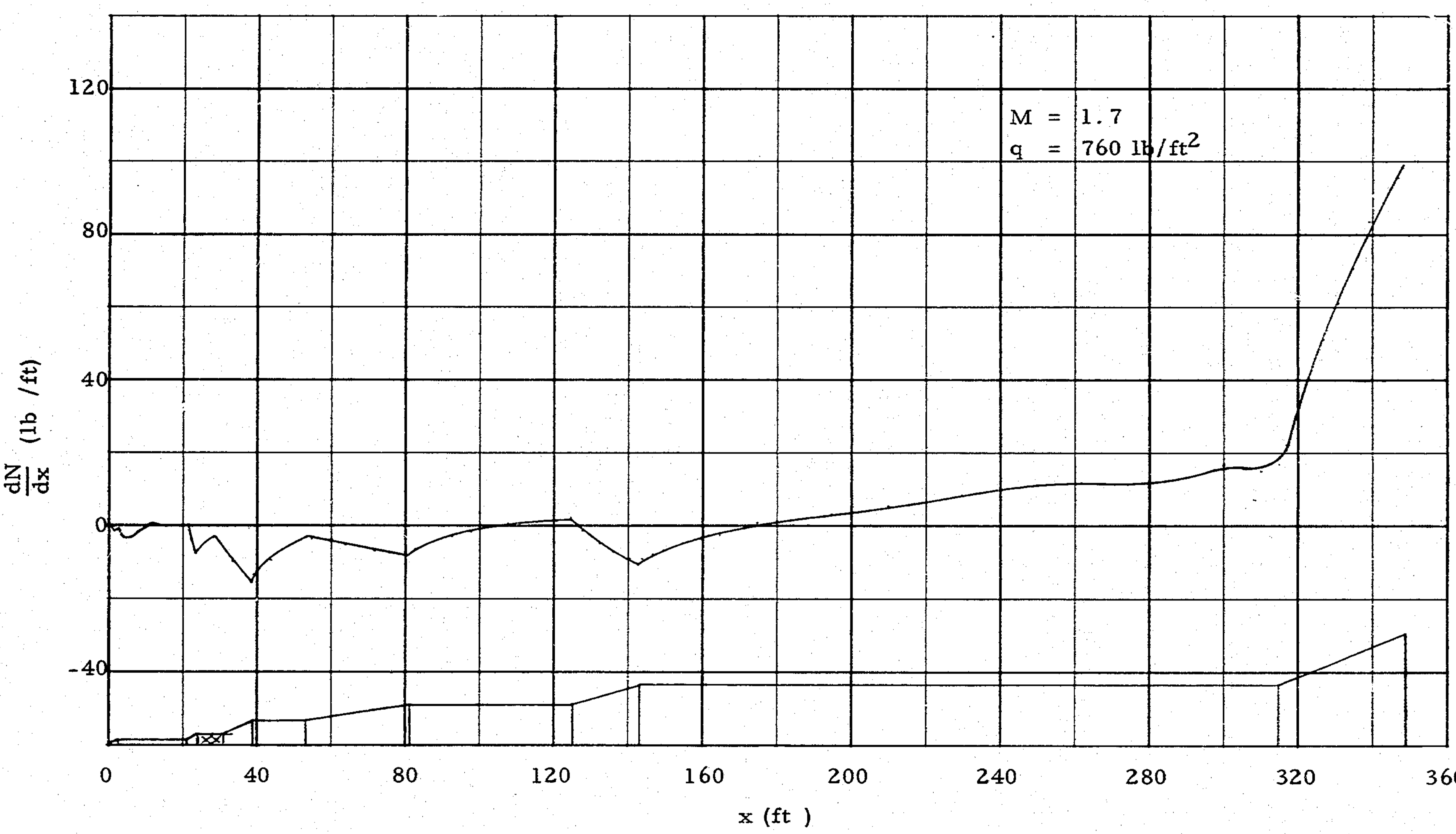


Figure 2-10. The First Order Method Applied to the Flexible Saturn V Vehicle with the Deflection Shown in Figure (3-9)

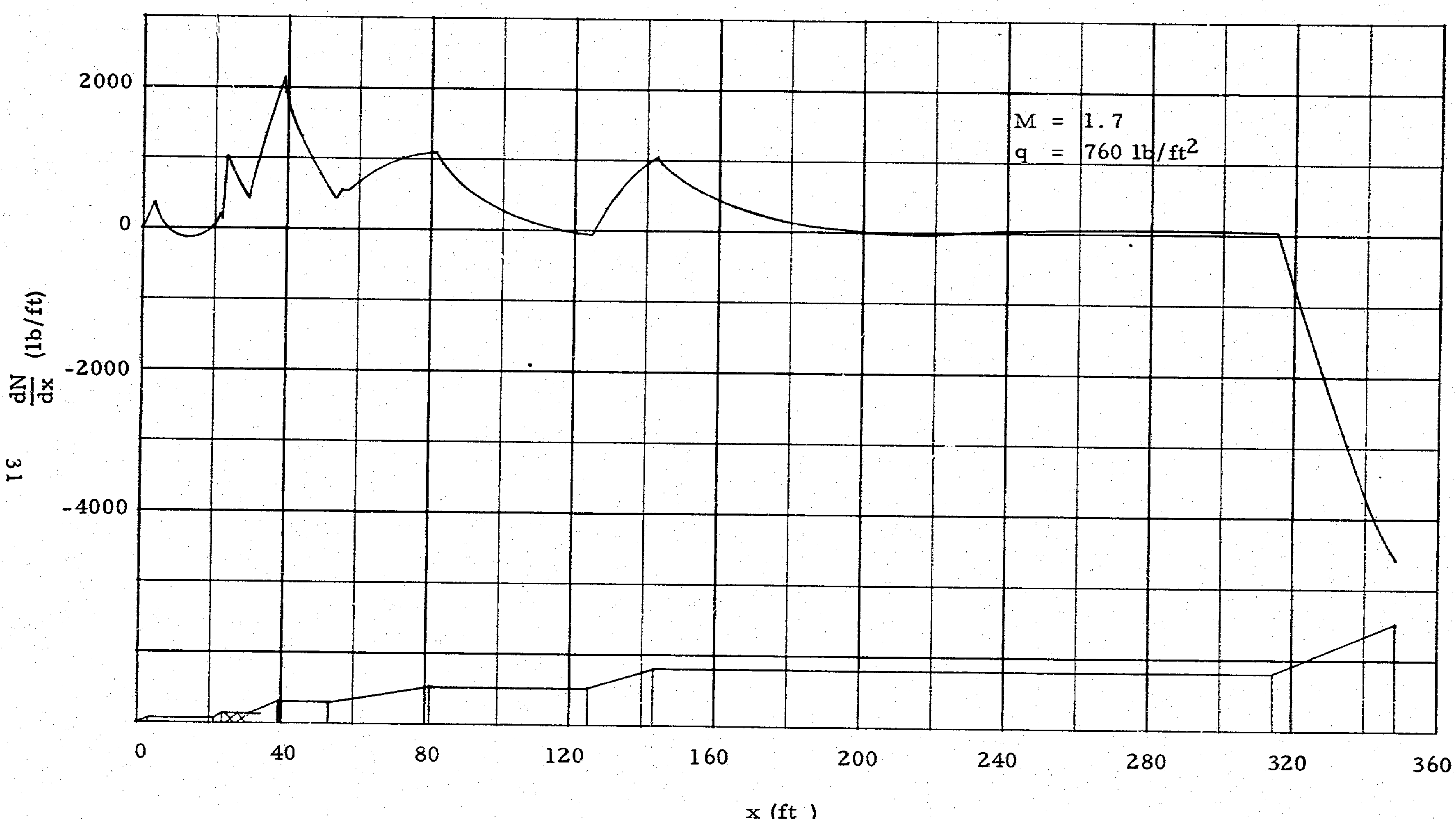


Figure 2-11. Local Normal Force Distribution Determined from the Rigid Body Data Multiplied by the Local Angle-of-Attack of the Flexible Saturn V Vehicle with the Deflection Shown in Figure (3-10)

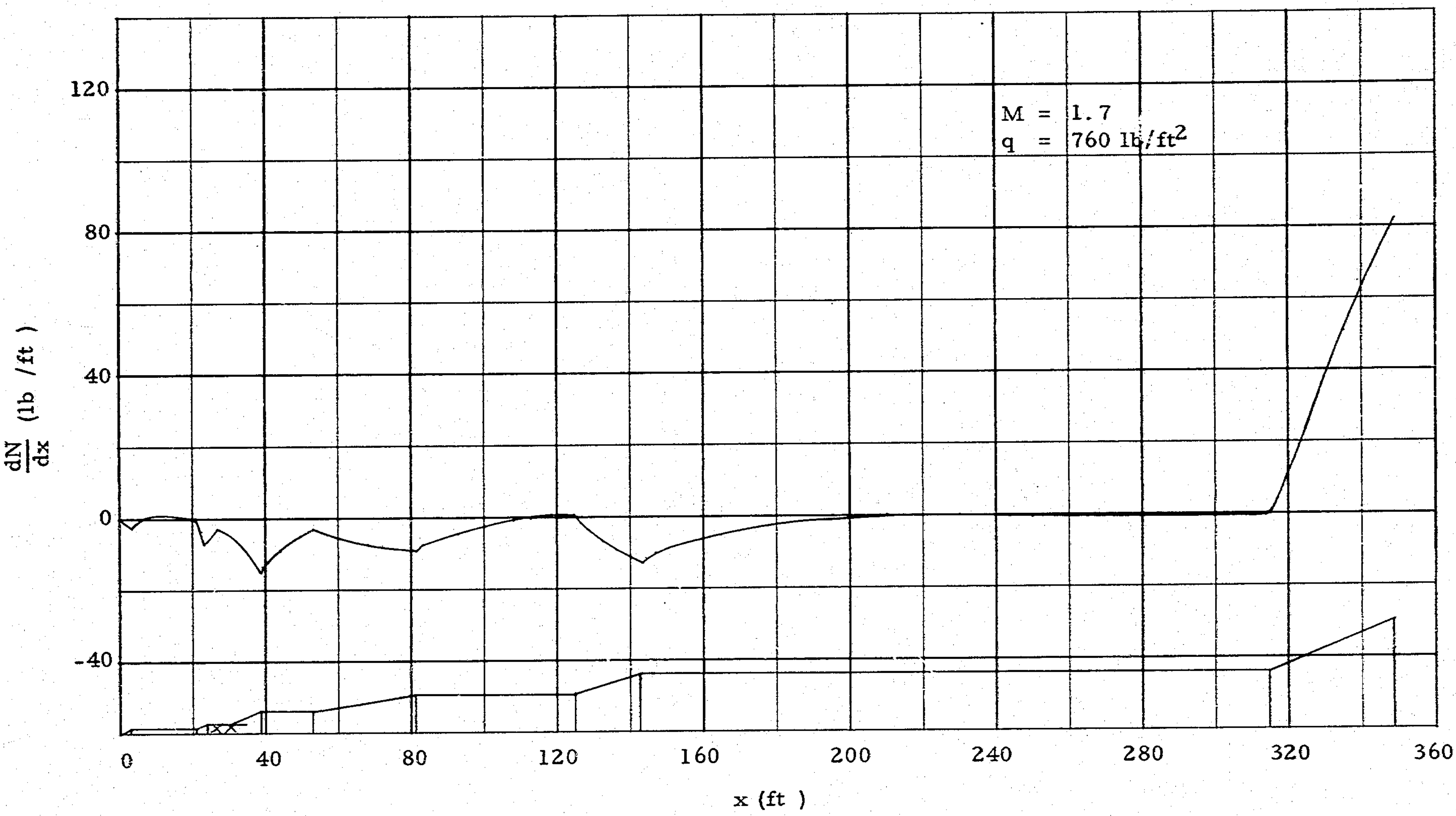


Figure 2-12. Local Normal Force Distribution Determined from Rigid Body Data Multiplied by the Local Angle-of-Attack of the Flexible Saturn V Vehicle Shown in Figure (3-11)

## III. STRUCTURAL FLEXING RESPONSE OF A VEHICLE TO AERODYNAMIC FORCES

The rigid body aerodynamic loads and the D'Alembert, or inertial, loads due to the normal acceleration of the vehicle cause the vehicle to flex. This flexing generates incremental aerodynamic loads due to the aerodynamic forces and incremental aerodynamic loads due to the normal acceleration. In the previous section a method was derived that facilitates the calculation of these incremental loads. In this section a method of calculating the vehicle flexing that is due to this loading is developed. An iterative procedure between these two analyses is described that determines the resultant incremental aerodynamic loads and the resultant deformation of the vehicle.

The analysis that follows is applicable to cases where the linear accelerations due to the rotational accelerations of the vehicle are negligible compared to the normal acceleration of the center of gravity of the vehicle. It is further restricted to cases where static beam theory, modified to include D'Alembert forces, is valid.

The following derivation is the first iteration. In this iteration, the vehicle flexing is caused by the rigid body aerodynamic forces and the D'Alembert forces. The incremental aerodynamic forces are zero. The forces acting on the vehicle are illustrated in figure (3-1). The structural bending moment acting on the vehicle is:

$$M_1(x) = \int_0^x (N_r' - \ddot{w}\, m')(x - \varepsilon)\, d\varepsilon \tag{3-1}$$

where $M_1(0) = 0$ and $M_1(L) = 0$. Since, for small angles, the local normal force of a rigid body is a linear function of angle-of-attack, this equation can be written:

$$M_1(x) = \alpha_r \int_0^x \frac{\partial N_r'}{\partial \alpha_r} (x - \varepsilon)\, d\varepsilon - \ddot{w} \int_0^x m' (x - \varepsilon)\, d\varepsilon \tag{3-2}$$

Thus the structural bending moment for small angles is a simple linear function of rigid body angle-of-attack and normal acceleration. Consider

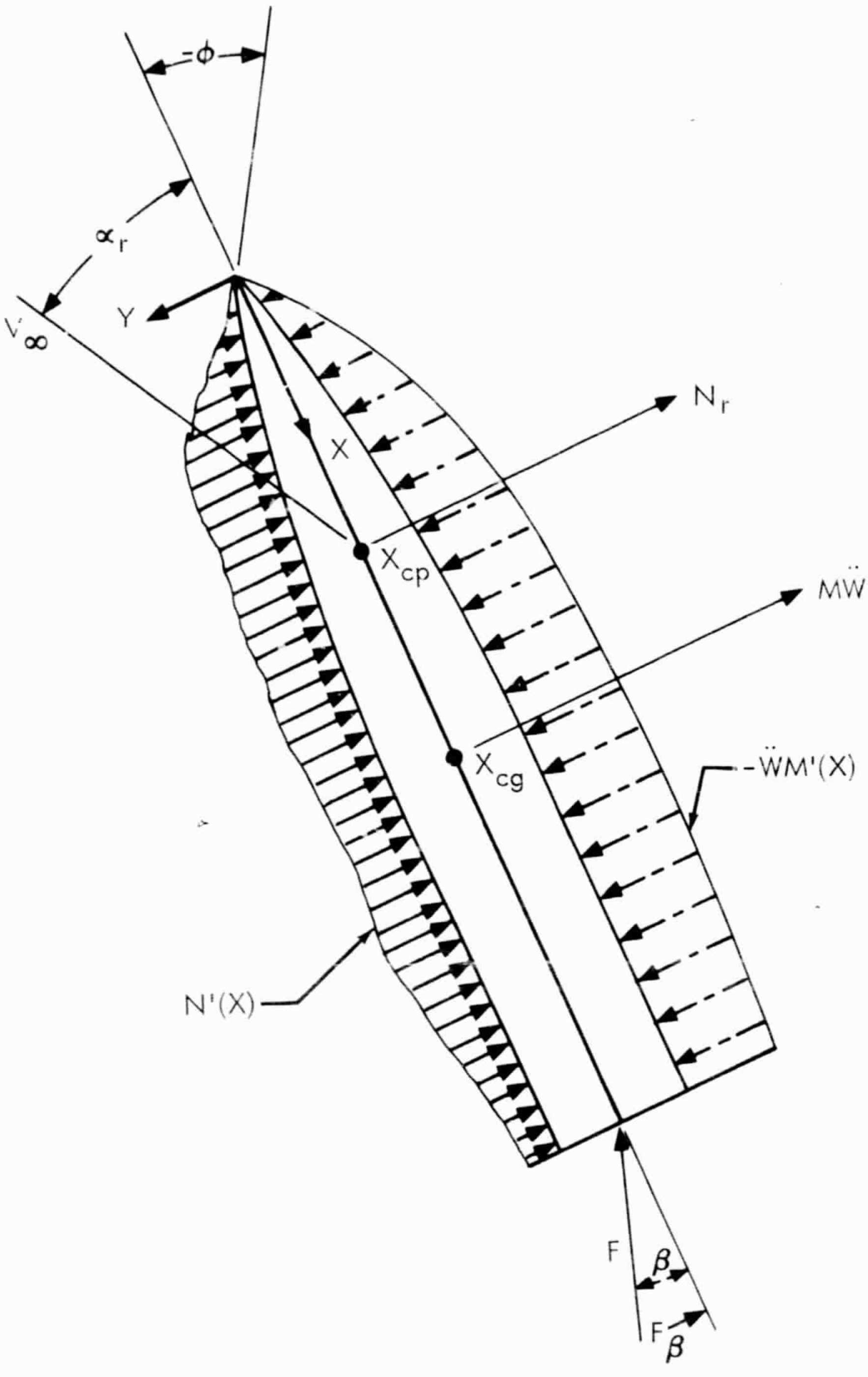


Figure 3-1. Forces Acting on a Rigid Body

the loading and coordinate system of figure (3-2). From the mechanics of structures, the flexing of the vehicle is determined by

$$\frac{d^2 y_1}{dx^2} = - \frac{M_1 (x)}{E I (x)} \tag{3-3}$$

Substituting equation (3-2) into equation (3-3)

$$\frac{d^2 y_1}{dx^2} = - \alpha_r \frac{1}{EI} \int_0^x \frac{\partial N_r'}{\partial \alpha_r} (x - \varepsilon) \, d\varepsilon + \ddot{w} \frac{1}{EI} \int_0^x m' (x - \varepsilon) d\varepsilon \tag{3-4}$$

Let

$$\bar{\bar{A}}_1 (x) = - \frac{1}{EI} \int_0^x \frac{\partial N_r'}{\partial \alpha_r} (x - \varepsilon) \, d\varepsilon \tag{3-5}$$

$$\bar{\bar{B}}_1 (x) = + \frac{1}{EI} \int_0^x m' (x - \varepsilon) \, d\varepsilon \tag{3-6}$$

where $\bar{\bar{A}}_1 (0) = 0$, $\bar{\bar{B}}_1 (0) = 0$. Then equation (3-4) can be written:

$$\frac{d^2 y_1}{dx^2} = \alpha_r \bar{\bar{A}}_1 (x) + \ddot{w} \bar{\bar{B}}_1 (x) \tag{3-7}$$

Integrating yields the following expansion for the body slopes:

$$\frac{dy_1}{dx} = \alpha_r \int_0^x \bar{\bar{A}}_1 (\varepsilon) \, d\varepsilon + \ddot{w} \int_0^x \bar{\bar{B}}_1 (\varepsilon) \, d\varepsilon \tag{3-8}$$

Let

$$\int_0^x \bar{\bar{A}}_1 (\varepsilon) \, d\varepsilon = \overline{A_1} (x) + G_{A_1} \tag{3-9}$$

$$\int_0^x \bar{\bar{B}}_1 (\varepsilon) \, d\varepsilon = \overline{B_1} (x) + G_{B_1} \tag{3-10}$$

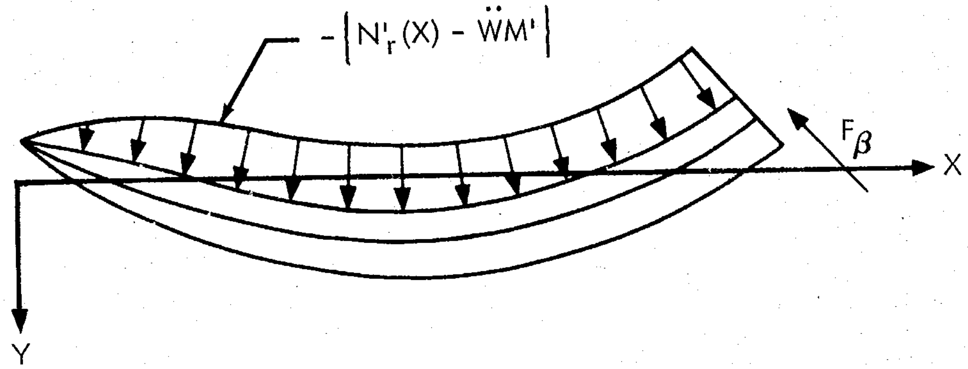


Figure 3-2. Flexible Beam Loading

where $\overline{A_1}(0) = 0$ and $\overline{B_1}(0) = 0$. Substituting yields:

$$\frac{dy_1}{dx} = \alpha_r \left\{ \overline{A_1}(x) + G_{A1} \right\} + \ddot{w} \left\{ \overline{B_1}(x) + G_{B1} \right\} \tag{3-11}$$

The displacements are determined by integrating this equation:

$$y_1 = \alpha_r \left\{ \int_0^x \overline{A_1}(\varepsilon)\, d\varepsilon + x\, G_{A1} \right\} + \ddot{w} \left\{ \int_0^x \overline{B_1}(\varepsilon)\, d\varepsilon + x\, G_{B_2} \right\} \tag{3-12}$$

Let

$$\int_0^x \overline{A}(\varepsilon)\, d\varepsilon = A_1(x) + H_{A1} \tag{3-13}$$

$$\int_0^x \overline{B}(\varepsilon)\, d\varepsilon = B_1(x) + H_{B1} \tag{3-14}$$

where $A_1(0) = 0$ and $B_1(0) = 0$. Equation (3-12) can be written:

$$y_1 = \alpha_r \left\{ A_1(x) + x\, G_{A1} + H_{A1} \right\} + \ddot{w} \left\{ B_1(x) + x\, G_{B1} + H_{B1} \right\} \tag{3-15}$$

The displacement and slope of the flexing vehicle is linear in terms of the rigid body angle-of-attack and normal vehicle acceleration. The first terms in equations (3-11) and (3-15) give the flexing caused by the rigid body aerodynamic forces and the second terms yield the flexing generated by the normal acceleration. The terms G and H are integration constants that position the body with respect to the rigid body coordinate system of figure (3-2). These constants are evaluated by the requirement that the total body mass not translate or rotate with respect to the rigid body coordinate system. The translational and rotational requirements for the flexing caused by the rigid body aerodynamic forces are:

$$0 = \int_0^L m' \left\{ A_1(x) + x\, G_{A1} + H_{A1} \right\} dx \tag{3-16}$$

$$0 = \int_0^L m' \left\{ A_1(x) + x\, G_{A1} + H_{A1} \right\} x\, dx \tag{3-17}$$

The requirements for the flexing caused by the D'Alembert forces are:

$$0 = \int_0^L m' \left\{ B_1(x) + x\, G_{B_1} + H_{B_1} \right\} dx \tag{3-18}$$

$$0 = \int_0^L m' \left\{ B_1(x) + x\, G_{B_1} + H_{B_1} \right\} x\, dx \tag{3-19}$$

Consider the following definitions:

$$IA_1 = \int_0^L m' A_1(x)\, dx \tag{3-20}$$

$$IAX_1 = \int_0^L m' A_1(x)\, x\, dx \tag{3-21}$$

$$IB_1 = \int_0^L m' B_1(x)\, dx \tag{3-22}$$

$$IBX_1 = \int_0^L m' B_1(x)\, x\, dx \tag{3-23}$$

$$IM_1 = \int_0^L m'\, dx \tag{3-24}$$

$$IML_1 = \int_0^L m'\, x\, dx \tag{3-25}$$

$$IMLL_1 = \int_0^L m'\, x^2\, dx \tag{3-26}$$

Substituting these equations into equations (3-16), (3-17), (3-18), and (3-19) yields:

$$G_{A_1}\, IML_1 + H_{A_1}\, IM_1 = -IA_1 \tag{3-27}$$

$$G_{A_1}\, IMLL_1 + H_{A_1}\, IML_1 = -IAX_1 \tag{3-28}$$

$$G_{B_1}\, IML_1 + H_{B_1}\, IM_1 = -IB_1 \tag{3-29}$$

$$G_{B_1}\, IMLL_1 + H_{B_1}\, IML_1 = -IBX_1 \tag{3-30}$$

Solving these equations for the integration constants yields:

$$G_{A1} = \frac{IAX_1\ IM_1 - IA_1\ IML_1}{IML_1^{\ 2} - IM_1\ IMLL_1} \tag{3-31}$$

$$H_{A1} = \frac{IA_1\ IMLL_1 - IAX_1\ IML_1}{IML_1^{\ 2} - IM_1\ IMLL_1} \tag{3-32}$$

$$G_{B1} = \frac{IBX_1\ IM_1 - IB_1\ IML_1}{IML_1^{\ 2} - IM_1\ IMLL_1} \tag{3-33}$$

$$H_{B1} = \frac{IB_1\ IMLL_1 - IBX_1\ IML_1}{IML_1^{\ 2} - IM_1\ IMLL_1} \tag{3-34}$$

Consider the following definitions:

$$\overline{P}_1(x) = \overline{A}_1(x) + G_{A1} \tag{3-35}$$

$$\overline{Q}_1(x) = \overline{B}_1(x) + G_{B1} \tag{3-36}$$

$$P_1(x) = A_1(x) + x\ G_{A1} + H_{A1} \tag{3-37}$$

$$Q_1(x) = B_1(x) + x\ G_{B1} + H_{B1} \tag{3-38}$$

Substituting equation (3-7) into equation (3-3), rewriting equation (3-7), and substituting equations (3-35), (3-36), (3-37), and (3-8) into equations (3-11) and (3-15) yields:

$$M_1 = -\ \alpha_r\ EI(x)\ \overset{=}{A}_1(x) - \ddot{w}\ EI(x)\ \overset{=}{B}_1(x) \tag{3-39}$$

$$\frac{d^2 y_1}{dx^2} = \alpha_r\ \overset{=}{A}_1(x) + \ddot{w}\ \overset{=}{B}_1(x) \tag{3-7}$$

$$\frac{dy_1}{dx} = \alpha_r\ \overline{P}_1(x) + \ddot{w}\ \overline{Q}_1(x) \tag{3-40}$$

$$y_1 = \alpha_r\ P_1(x) + \ddot{w}\ Q_1(x) \tag{3-41}$$

From figures (3-1) and (3-2), the local angle-of-attack along the vehicle for the first iteration is:

$$\alpha_1 (x) = \alpha_r + \frac{d y_1}{dx} \tag{3-42}$$

Substituting equation (3-39) yields the following expression for the first iteration angle-of-attack distribution along the body:

$$\alpha_1 (x) = \alpha_r + \alpha_r \overline{P}_1 (x) + \ddot{w} \overline{Q} (x) \tag{3-43}$$

For selected values of rigid body angle-of-attack and normal acceleration, the local normal force for the flexed vehicle can be computed by the flexible body aerodynamic method of the previous section. However, a more general representation is required that is valid over a wide range of rigid body angles-of-attack and normal accelerations. This general representation is obtained by observing in equation (3-43) that the local angle-of-attack distribution is determined by the summation of the curves, or terms. Because of the linearity of the aerodynamic equations, the local normal force can be described as the sum of three terms, each one being generated by a term in the equation of the local angle-of-attack distribution. This yields the following equation:

$$N_1' (x) = \frac{\partial N_r' (x)}{\partial \alpha_r} \alpha_r + \frac{\partial N_1' (x)}{\partial \alpha_r} \alpha_r + \frac{\partial N_1' (x)}{\partial \ddot{w}} \ddot{w} \tag{3-44}$$

The term $\frac{\partial N_r (x)}{\partial \alpha_r}$ is the rigid body local normal force derivative with respect to the rigid angle-of-attack. The term $\frac{\partial N_1' (x)}{\partial \alpha_r}$ is the first iteration of the incremental normal force derivative with respect to the rigid body angle-of-attack caused by the flexing (or local angle-of-attack distribution) that is due to aerodynamic forces. It is determined by the flexible body aerodynamic analysis of the previous section using $\overline{P}_1(x)$ as the local angle-of-attack distribution. $\frac{\partial N_1}{\partial \ddot{w}}$ is the first iteration of the incremental local normal force derivative with respect to normal acceleration caused by the flexing that is due to the normal acceleration. It is also determined by the flexible body aerodynamic program. In this incidence, the local angle-of-attack distribution is given by $\overline{Q}_1 (x)$.

Digressing briefly, a physical interpretation will be made of the terms in equation (3-44). Consider figure (3-3). Illustration A shows a rigid model placed at a positive angle-of-attack in a wind tunnel and held motionless. The local normal force distribution acting on this model is given by $\frac{\partial N_r}{\partial \alpha_r} \alpha_r$ In illustration B, a flexible model (suspended at the base) is placed in a wind tunnel and also held motionless. The rigid body centerline is positioned with respect to the flexed body by the requirements of translational and rotational mass distribution. The rigid body angle-of-attack, $\alpha_r$, is determined by the

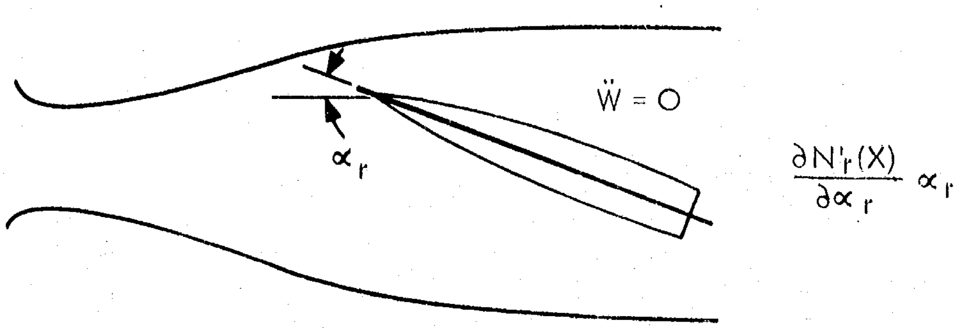


A. RIGID BODY LOADS

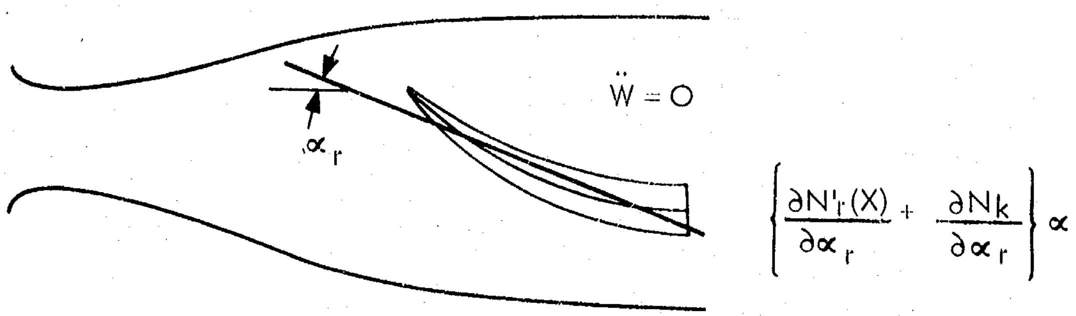


B. INCREMENTAL LOADS DUE TO AERODYNAMIC FORCES

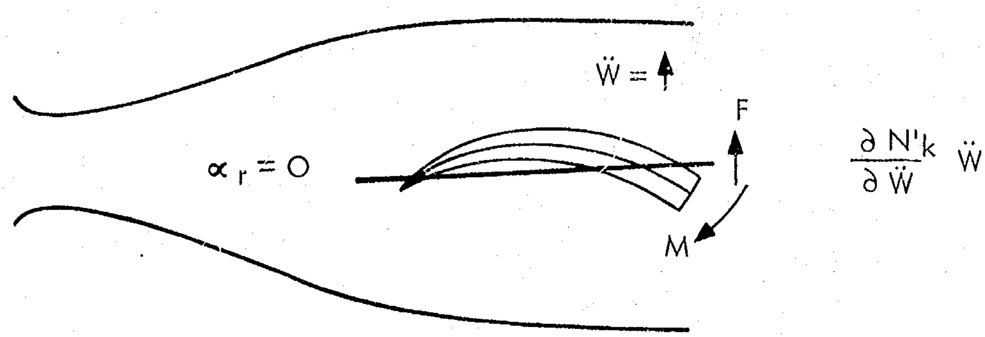


C. INCREMENTAL LOADS DUE TO ACCELERATION

Figure 3-3. Illustration of the Incremental Aerodynamic Loads Caused by Flexing angle this axis makes with the flow stream. The local normal force distribution is given by $\left\{\frac{\partial N_r'}{\partial \alpha_r} + \frac{\partial N_k'}{\partial \alpha_r}\right\} \alpha_r$ where k is a sufficiently large iteration. In illustration C, a flexible model (suspended at the base) is placed in a wind tunnel and oscillated up and down with the rigid centerline held horizontal. The condition shown is when the model is motionless at the lower extremity of its cycle. Here it is at zero angle-of-attack and has a positive acceleration. The local normal force distribution is given by $\frac{\partial N_k'}{\partial \ddot{w}} \ddot{w}$ where k is a sufficiently large iteration.

Returning to the first iteration, the body normal force and pitching moment about the center of gravity can be obtained from equation (3-44). Consider the following definitions:

$$\frac{\partial N_r}{\partial \alpha_r} = \int_0^L \frac{\partial N_r'}{\partial \alpha_r} \, dx \tag{3-45}$$

$$\frac{\partial N_1}{\partial \alpha_r} = \int_0^L \frac{\partial N_1'}{\partial \alpha_r} \, dx \tag{3-46}$$

$$\frac{\partial N_1}{\partial \ddot{w}} = \int_0^L \frac{\partial N_1'}{\partial \ddot{w}} \, dx \tag{3-47}$$

$$\frac{\partial MA_r}{\partial \alpha_r} = \int_0^L \frac{\partial N_r'}{\partial \alpha_r} (x_{cg} - x) \, dx \tag{3-48}$$

$$\frac{\partial MA_1}{\partial \alpha_r} = \int_0^L \frac{\partial N_1'}{\partial \alpha_r} (x_{cg} - x) \, dx \tag{3-49}$$

$$\frac{\partial MA_1}{\partial \ddot{w}} = \int_0^L \frac{\partial N_1'}{\partial \ddot{w}} (x_{cg} - x) \, dx \tag{3-50}$$

Then the first iteration of the body normal force can be written:

$$N_1 = \left(\frac{\partial N_r}{\partial \alpha_r} + \frac{\partial N_1}{\partial \alpha_r}\right) \alpha_r + \frac{\partial N_1}{\partial \ddot{w}} \ddot{w} \tag{3-51}$$

and the first iteration of the pitching moment about the center of gravity can be written:

$$MA_1 = \left(\frac{\partial MA_r}{\partial \alpha_r} + \frac{\partial MA_1}{\partial \alpha_r}\right) \alpha_r + \frac{\partial MA_1}{\partial \ddot{w}} \ddot{w} \qquad (3\text{-}52)$$

After completing this first iteration, the second must be performed, then the third, etc. The following is a derivation of the $k^{th}$ iteration of determining the flexible body aerodynamic characteristics and displacements once the $k - 1^{th}$ iteration has been carried out. The procedure is identical to the first iteration except that the incremental aerodynamic loads obtained in the $k - 1^{th}$ iteration are used in developing the relations of the $k^{th}$ iteration. Actually the first iteration can be considered a special case of the general $k^{th}$ iteration where the incremental loads for the $k = 0$ case are all zero.

For the $k^{th}$ iteration, the expression that determines the structural bending is:

$$M_k(x) = \alpha_r \int_0^x \left(\frac{\partial N_k'}{\partial \alpha_r} + \frac{\partial N_{k-1}'}{\partial \alpha_r}\right)(x-\varepsilon)\, d\varepsilon - \ddot{w} \int_0^x \left(m' - \frac{\partial N_{k-1}'}{\partial \ddot{w}}\right)$$

$$(x-\varepsilon)\, d\varepsilon \qquad (3\text{-}53)$$

As in equation (3-7), the second derivative of the flexible body displacement is:

$$\frac{d^2 y_k}{dx^2} = \alpha_r \overset{=}{A}_k(x) + \ddot{w} \overset{=}{B}_k(x) \qquad (3\text{-}54)$$

where

$$\overset{=}{A}_k(x) = -\frac{1}{EI} \int_0^x \left(\frac{\partial N_r}{\partial \alpha_r} + \frac{\partial N_{k-1}'}{\partial \alpha_r}\right)(x-\varepsilon)\, d\varepsilon \qquad (3\text{-}55)$$

$$\overset{=}{B}_k(x) = \frac{1}{EI} \int_0^x \left(m' - \frac{\partial N_{k-1}'}{\partial \ddot{w}}\right)(x-\varepsilon)\, d\varepsilon \qquad (3\text{-}56)$$

where $\overset{=}{A}_k(0) = 0$ and $\overset{=}{B}_k(0) = 0$. The vehicle slope is given by:

$$\frac{dy_k}{dx} = \alpha_r \left\{\overline{A}_k(x) + GA_k\right\} + \ddot{w} \left\{\overline{B}_k(x) + GB_k\right\} \qquad (3\text{-}57)$$

where

$$\bar{A}_k(x) = \int_0^x \bar{\bar{A}}_k(\varepsilon)\, d\varepsilon - G_{A_k} \qquad (3\text{-}58)$$

$$\bar{B}_k(x) = \int_0^x \bar{\bar{B}}_k(\varepsilon)\, d\varepsilon - G_{B_k} \qquad (3\text{-}59)$$

and $\bar{A}_k(0) = 0$ and $\bar{B}_k(0) = 0$. As in equation (3-15) the vehicle displacement is given by:

$$y_k = \alpha_r \left\{ A_k(x) + x\, G_{A_k} + H_{A_k} \right\} + \ddot{w} \left\{ B_k(x) + x\, G_{B_k} + H_{B_k} \right\} \qquad (3\text{-}60)$$

where

$$A_k(x) = \int_0^x \bar{A}_k(\varepsilon)\, d\varepsilon - H_{A_k} \qquad (3\text{-}61)$$

$$B_k(x) = \int_0^x \bar{B}_k(\varepsilon)\, d\varepsilon - H_{B_k} \qquad (3\text{-}62)$$

and $A_k(0) = 0$ and $B_k(0) = 0$. From the mass translation and rotation requirement:

$$G_{A_k} = \frac{IAX_k\, IM_k - IA_k\, IML_k}{IML_k^2 - IM_k\, IMLL_k} \qquad (3\text{-}63)$$

$$H_{A_k} = \frac{IA_k\, IMLL_k - IAX_k\, IML_k}{IML_k^2 - IM_k\, IMLL_k} \qquad (3\text{-}64)$$

$$G_{B_k} = \frac{IBX_k\, IM_k - IB_k\, IML_k}{IML_k^2 - IM_k\, IMLL_k} \qquad (3\text{-}65)$$

$$H_{B_k} = \frac{IB_k\, IMLL_k - IBX_k\, IML_k}{IML_k^2 - IM_k\, IMLL_k} \qquad (3\text{-}66)$$

where

$$IA_k = \int_0^L m'\, A_k(x)\, dx \qquad (3\text{-}67)$$

$$IAX_k = \int_0^L m' A_k(x)\, x\, dx \tag{3-68}$$

$$IB_k = \int_0^L m' B_k(x)\, dx \tag{3-69}$$

$$IBX_k = \int_0^L m' B_k(x)\, x\, dx \tag{3-70}$$

$$IM_k = \int_0^L m'\, dx \tag{3-71}$$

$$IML_k = \int_0^L m'\, x\, dx \tag{3-72}$$

$$IMLL_k = \int_0^L m'\, x^2\, dx \tag{3-73}$$

Let

$$\overline{P}_k(x) = \overline{A}_k(x) + G_{A_k} \tag{3-74}$$

$$\overline{Q}_k(x) = \overline{B}_k(x) + G_{B_k} \tag{3-75}$$

$$P_k(x) = A_k(x) + x\, G_{A_k} + H_{A_k} \tag{3-76}$$

$$Q_k(x) = B_k(x) + x\, G_{B_k} + H_{B_k} \tag{3-77}$$

Substituting equation (3-54) into equation (3-3), rewriting equation (3-54), and substituting equations (3-74), (3-75); (3-76), and (3-77) into equations (3-57) and (3-60) yields:

$$M_k = -\alpha_r\, EI(x)\, \overset{=}{A}_k(x) - \ddot{w}\, EI(x)\, \overset{=}{B}_k(x) \tag{3-78}$$

$$\frac{d^2 y_k}{dx^2} = \alpha_r\, \overset{=}{A}_k(x) + \ddot{w}\, \overset{=}{B}_k(x) \tag{3-54}$$

$$\frac{dy_k}{dx} = \alpha_r\, \overline{P}_k(x) + \ddot{w}\, \overline{Q}_k(x) \tag{3-79}$$

$$y_k = \alpha_r P_k(x) + \ddot{w}\; Q_k(x) \tag{3-80}$$

The local angle-of-attack along the vehicle of the k[th] iteration is:

$$\alpha_k(x) = \alpha_r + \frac{d\,y_k}{dx} \tag{3-81}$$

Substituting equation (3-77) yields:

$$\alpha_k(x) = \alpha_r + \alpha_r \bar{P}_k(x) + \ddot{w}\,\bar{Q}_k(x) \tag{3-82}$$

The local normal force of this iteration is:

$$N'_k(x) = \frac{\partial N'_r(x)}{\partial \alpha_r}\,\alpha_r + \frac{\partial N'_k(x)}{\partial \alpha_r}\,\alpha_r + \frac{\partial N'_k(x)}{\partial \ddot{w}}\,\ddot{w} \tag{3-83}$$

Here $\frac{\partial N'_r(x)}{\partial \alpha_r}$ is the rigid body local normal force derivative with respect to the rigid angle-of-attack. $\frac{\partial N'_k(x)}{\partial \alpha_r}$ is the k[th] iteration of the incremental local normal force derivative with respect to the rigid body angle-of-attack caused by flexing that is due to aerodynamic forces. It is determined by the flexible body aerodynamic program, using $\bar{P}_k(x)$ as the angle-of-attack distribution. $\frac{\partial N'_k(x)}{\partial \ddot{w}}$ is the second iteration of the incremental local normal force derivative with respect to normal acceleration caused by flexing that is due to acceleration. It is also determined by the aerodynamic program of the previous section, using $\bar{Q}_k(x)$ as the angle-of-attack.

The k[th] iteration of the body normal force and pitching moment about the center of gravity can be obtained from equation (3-83). Consider the following definitions:

$$\frac{\partial N_r}{\partial \alpha_r} = \int_0^L \frac{\partial N'_r}{\partial \alpha_r}\, dx \tag{3-84}$$

$$\frac{\partial N'_k}{\partial \alpha_r} = \int_0^L \frac{\partial N'_k}{\partial \alpha_r}\, dx \tag{3-85}$$

$$\frac{\partial N'_k}{\partial \ddot{w}} = \int_0^L \frac{\partial N'_k}{\partial \ddot{w}}\, dx \tag{3-86}$$

$$\frac{\partial MA_r}{\partial \alpha_r} = \int_0^L \frac{\partial N_r'}{\partial \alpha_r} (x_{cg} - x)\, dx \qquad (3\text{-}87)$$

$$\frac{\partial MA_k}{\partial \alpha_r} = \int_0^L \frac{\partial N_k'}{\partial \alpha_r} (x_{cg} - x)\, dx \qquad (3\text{-}88)$$

$$\frac{\partial MA_k}{\partial \ddot{w}} = \int_0^L \frac{\partial N_k'}{\partial \ddot{w}} (x_{cg} - x)\, dx \qquad (3\text{-}89)$$

Then the $k^{th}$ iteration of the body normal force is:

$$N_k = \left( \frac{\partial N_r}{\partial \alpha_r} + \frac{\partial N_k}{\partial \alpha_r} \right) \alpha_r + \frac{\partial N_k}{\partial \ddot{w}} \ddot{w} \qquad (3\text{-}90)$$

and the $k^{th}$ iteration of pitching moment is:

$$MA_k = \left( \frac{\partial MA_r}{\partial \alpha_r} + \frac{\partial MA_k}{\partial \alpha_r} \right) \alpha_r + \frac{\partial MA_k}{\partial \ddot{w}} \ddot{w} \qquad (3\text{-}91)$$

A numerical analysis was made of the $k^{th}$ iteration and a flow diagram was prepared. The flow diagram is given in appendix E along with a listing of the computer program. Instructions for loading the inputs to the program and sample inputs and outputs are included.

Calculations were made to determine the parameters in the slope and deflection equations of the Saturn V vehicle at maximum dynamic pressure. This dynamic pressure is 760 lbs/ft$^2$ and the Mach number is 1.70. The mass distribution and bending stiffness are given in figures (3-4) and (3-5). In the first iteration, the rigid body local normal force derivatives were obtained from figure (2-8). These are the necessary parameters of the first iteration. The iteration procedure was then carried out the second and third time. The process converges rapidly and the third iteration appears to provide sufficient accuracy for the purpose of this study. The vehicle slope and deflection parameters $\overline{P}_3(x)$, $\overline{Q}_3(x)$, $P_3(x)$, and $Q_3(x)$ of the third iteration are given in figures (3-6), (3-7), (3-8), and (3-9). The incremental aerodynamic force distributions, determined by the First Order Method for Flexible Bodies, that correspond to these flexing configurations are given in figures (2-9) and (2-10).

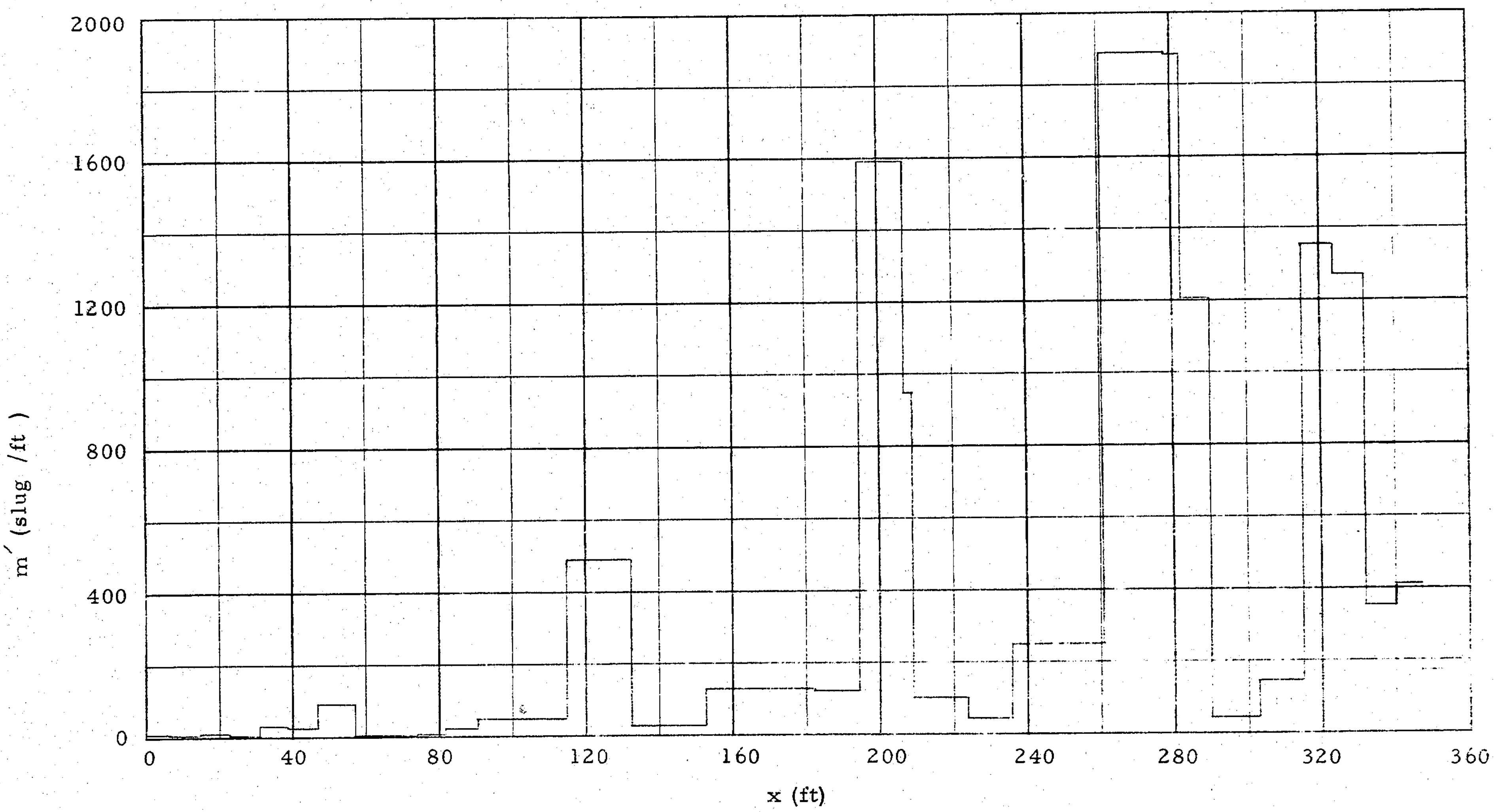


Figure 3-4. Saturn V Mass Distribution at Time
t = 79 sec

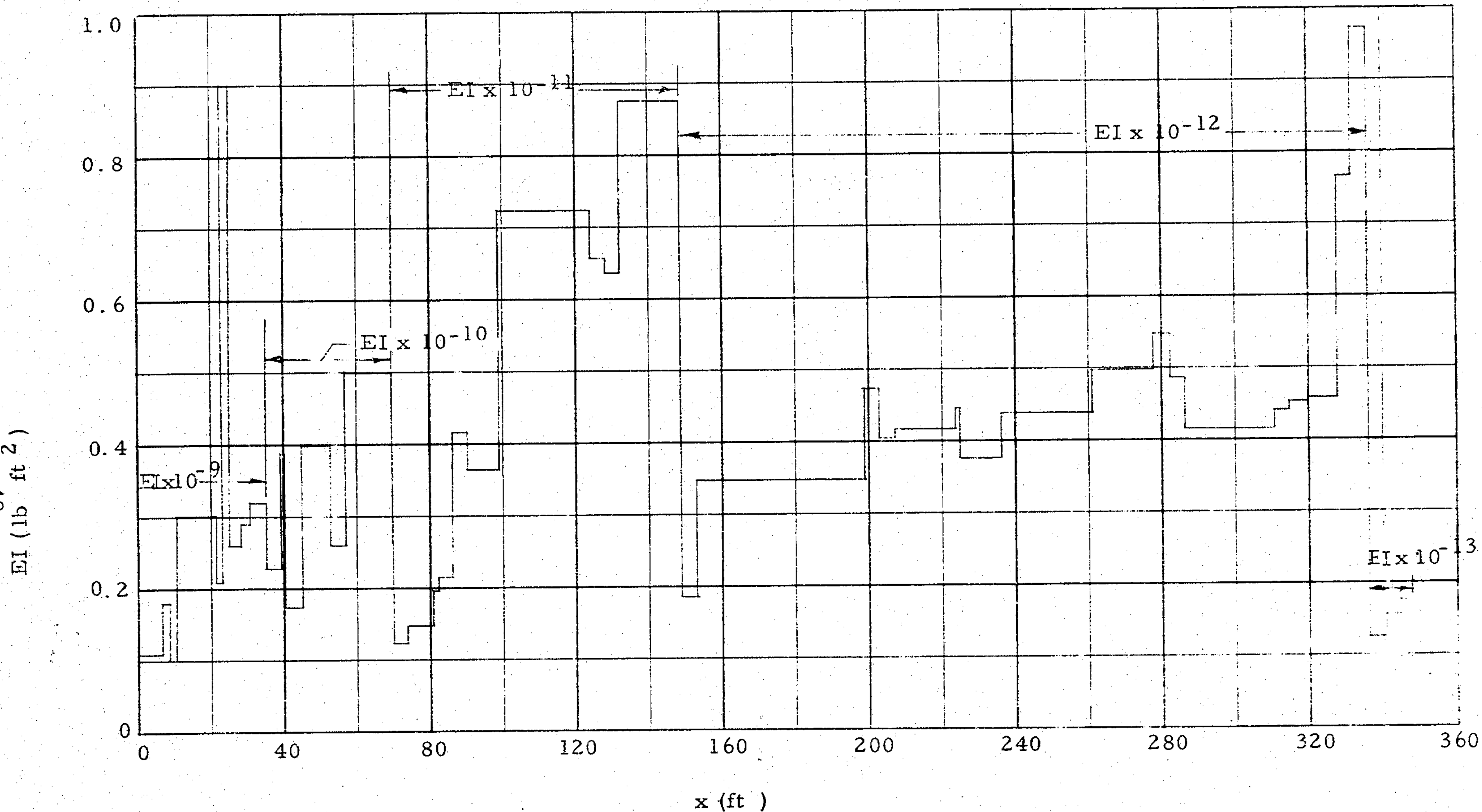


Figure 3-5. Saturn V Stiffness Distribution

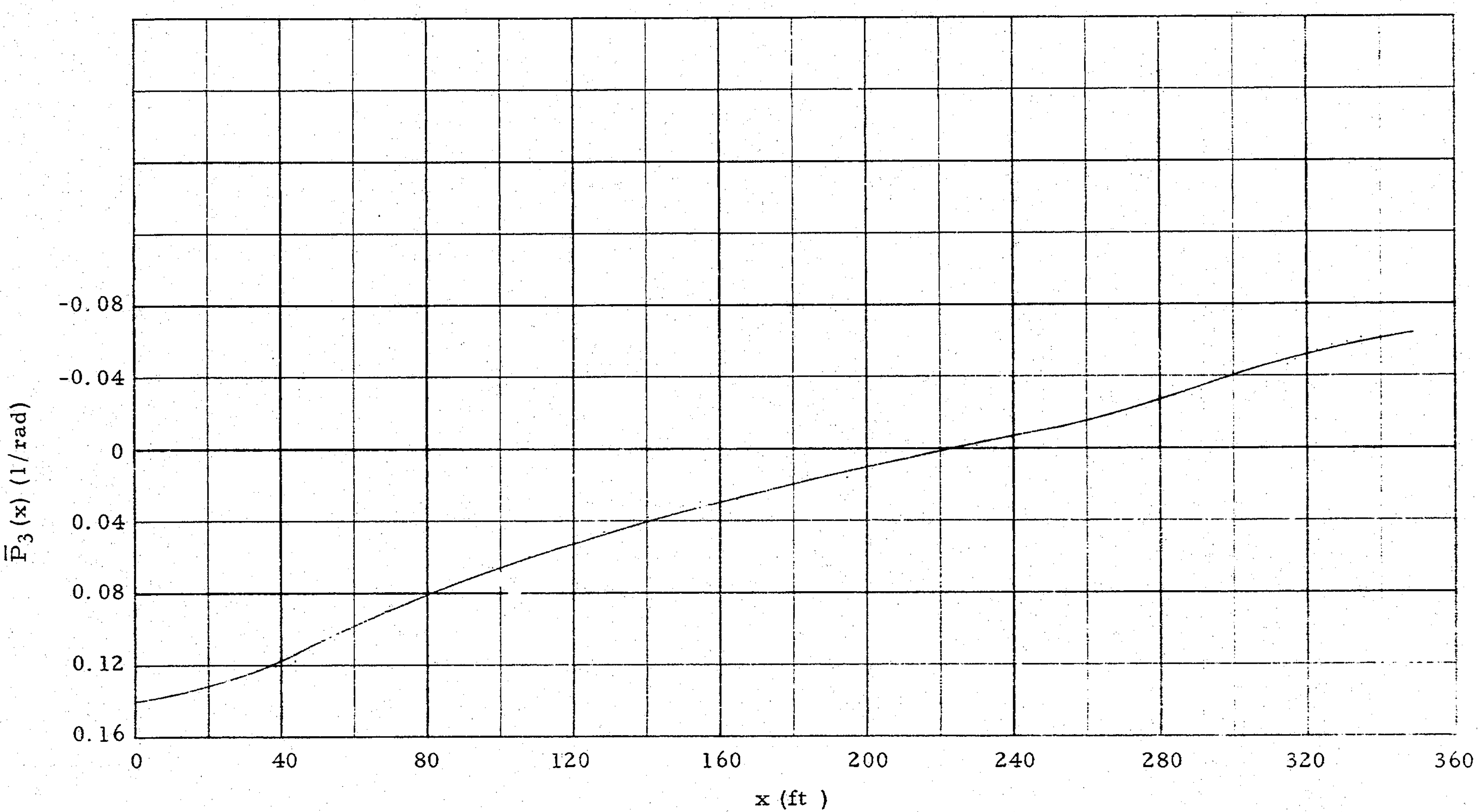


Figure 3-6. Saturn V Incremental Slope Derivative with Respect to $\alpha_r$

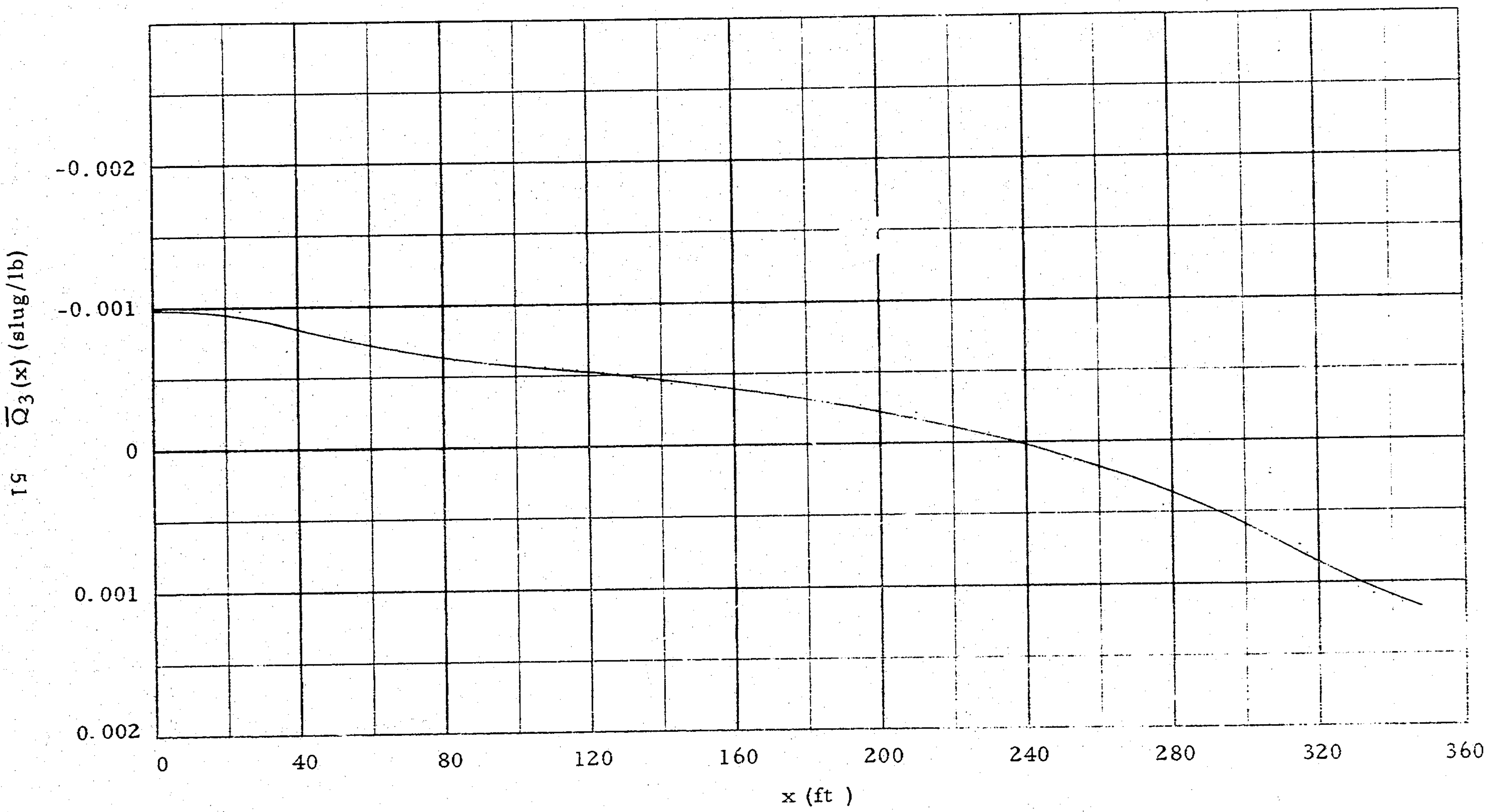


Figure 3-7. Saturn V Incremental Slope Derivative with Respect to $\ddot{w}$

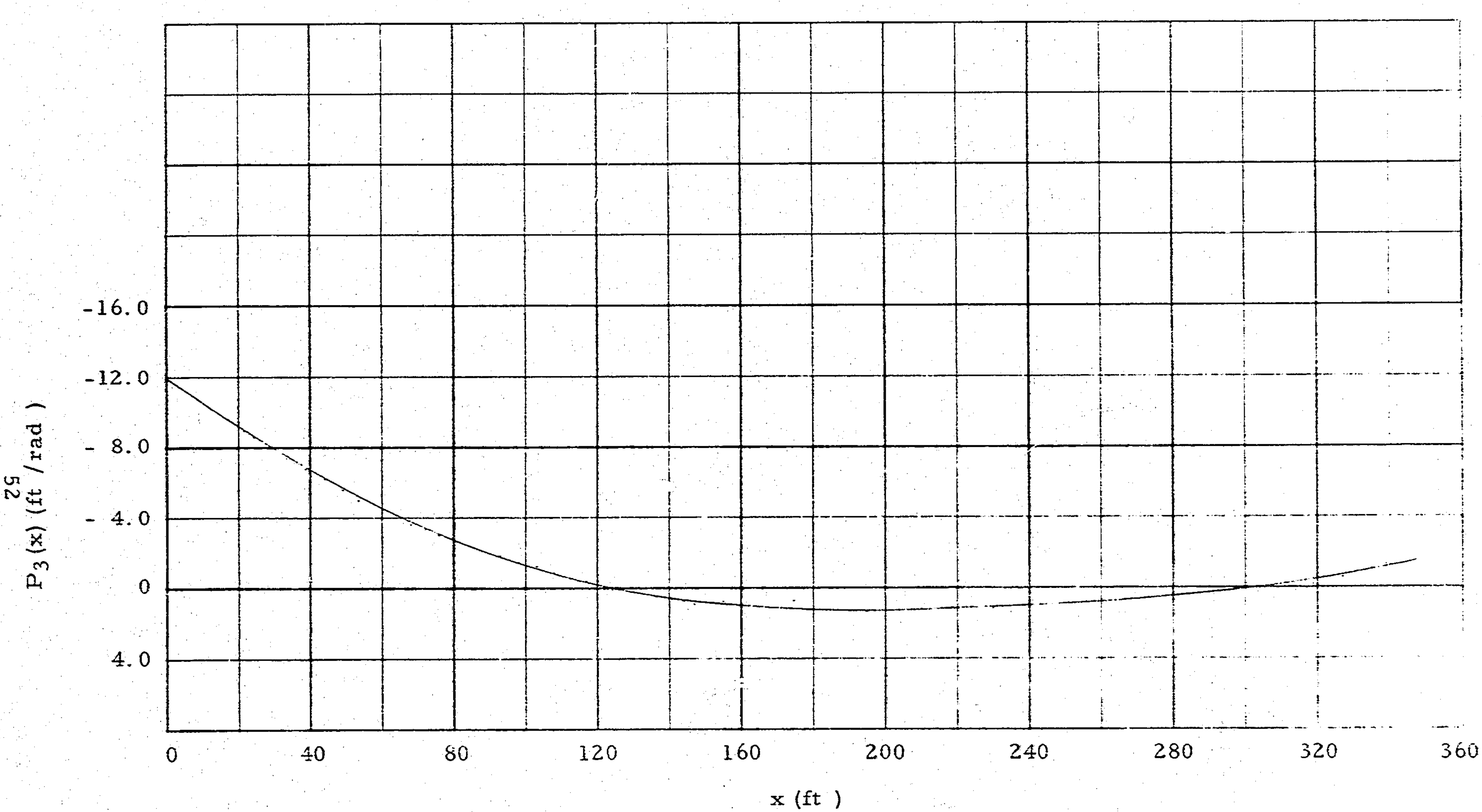


Figure 3-8. Saturn V Incremental Displacement Derivative with Respect to $\alpha_r$

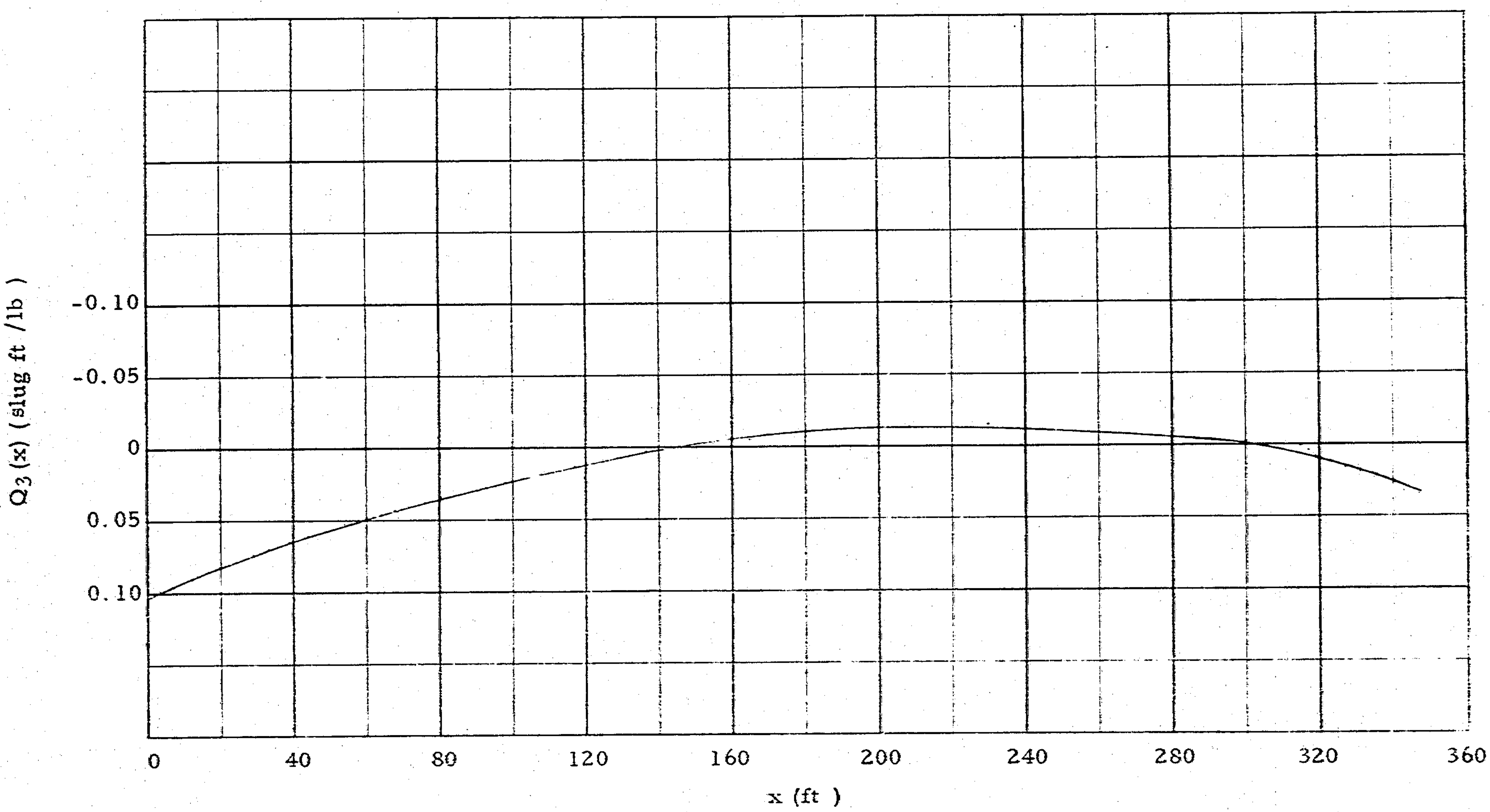


Figure 3-9. Saturn V Incremental Displacement Derivative with Respect to $\ddot{w}$

The rigid body normal force derivative with respect to the rigid body angle-of-attack, $\frac{\partial Nr}{\partial \alpha r}$, is $2.783 \times 10^6$ lbs/rad; and the rigid body pitching moment derivative with respect to the rigid body angle-of-attack, $\frac{\partial MAr}{\partial \alpha r}$, is $1.261 \times 10^8$ ft lb/rad. The third iteration of the incremental force derivative (determined by the flexible body methods of Section II) with respect to the rigid body angle-of-attack that is caused by bending due to the aerodynamic loading, $\frac{\partial N_3}{\partial \alpha r}$, is $-1.49 \times 10^5$ lb/rad. The corresponding pitching moment derivative, $\frac{\partial MA_3}{\partial \alpha r}$, is $1.90 \times 10^7$ ft lb/rad. The third iteration of the incremental normal force derivative with respect to the normal acceleration of the vehicle that is caused by bending due to the normal accelerations, $\frac{\partial N_3}{\partial \dot{w}}$, is $2.72 \times 10^3$ lb sec$^2$/ft. The corresponding pitching moment derivative, $\frac{MA_3}{\partial \dot{w}}$, is $-2.95 \times 10^5$ lb sec$^2$.

For purposes of comparison, aeroelastic calculations were made of the Saturn V vehicle using the rigid body local normal force derivatives multiplied by the local angle-of-attack to simulate the flexible body aerodynamic forces. For the third iteration, this resulted in local normal force distributions shown in figures (2-11) and (2-12) which correspond to the deflections shown in figures (3-10) and (3-11).

This third iteration of the incremental normal force derivative (determined by modifying the rigid body data to account for the local angle-of-attack distribution) with respect to the rigid body angle-of-attack that is caused by bending due to the aerodynamic loading, $\frac{\partial N_3}{\partial \alpha r}$, is $2.68 \times 10^4$ lb/rad. The corresponding incremental pitching moment derivative, $\frac{\partial MA_3}{\partial \alpha r}$, is $1.993 \times 10^7$ ft lb/rad. The incremental normal force derivative with respect to the normal acceleration of the vehicle that is caused by bending due to the normal acceleration was also determined using modified rigid body data. This resulted in a value of $5.46 \times 10^2$ lb sec$^2$/ft for $\frac{\partial N_3}{\partial \dot{w}}$. The corresponding pitching moment derivative, $\frac{\partial M_3}{\partial \dot{w}}$, is $-3.25 \times 10^5$ lb sec$^2$.

The aerodynamic characteristics of a flexible body as well as the body flexing itself are seen to be functions of normal vehicle acceleration as well as the rigid body angle-of-attack. Thus, in order to assess the full significance of the flexible body aerodynamic methods of section II, the dynamics of the vehicle must be analyzed. This dynamic analysis will be performed in section IV.

However, some indication of the significance of the flexible body local normal force distribution determined by the First Order Method of this report, as compared with the use of the rigid body local normal force derivatives multiplied by the local angles-of-attack, can be determined from static considerations.

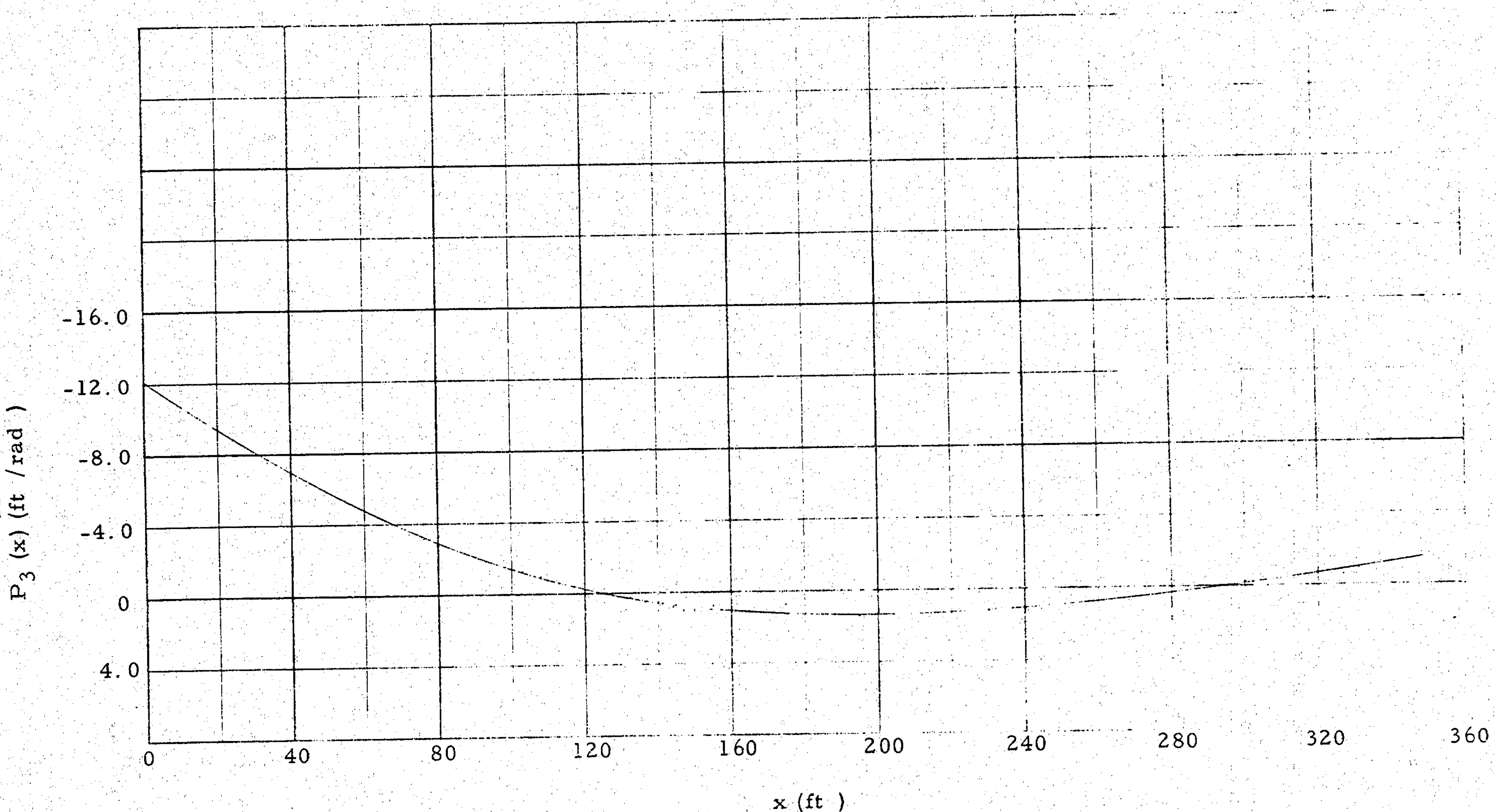


Figure 3-10. Saturn V Incremental Displacement Derivative with Respect to $\alpha_r$ Using Rigid Body Aerodynamic Terms Modified by the Local Angle-of-Attack

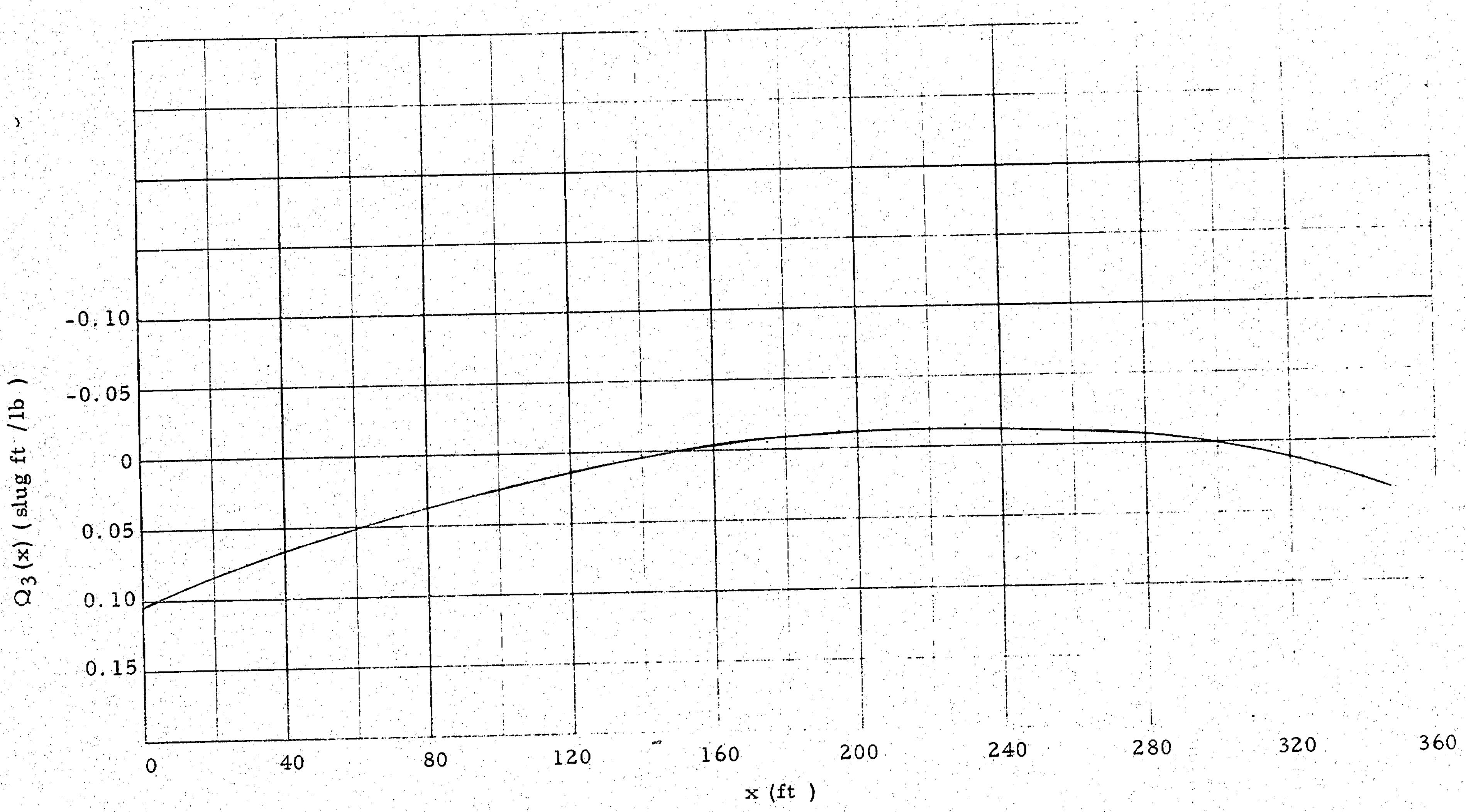


Figure 3-11. Saturn V Incremental Displacement Derivative with Respect to $\ddot{w}$ Using Rigid Body Aerodynamic Terms Modified by the Local Angle-of-Attack

Consider that the normal acceleration of the vehicle is zero. This case is demonstrated in figure (3-2), illustration B. The effects of body flexing are exaggerated in this case since the terms that are multiplied by the rigid body angle-of-attack are generally of opposite signs to those multiplied by the normal acceleration. And, in general, the rigid body angle-of-attack will have the same sign as the vehicle normal acceleration. The effects of flexible body aerodynamics with zero normal acceleration can then be considered an upper limit on the values that will be encountered in flight.

Consider equations (3-82), (3-90), and (3-91) for the third iteration with $\ddot{w} = 0$ and the vehicle at the maximum dynamic pressure.

$$\alpha_3(0) = \left\{1 + \overline{P}_3\ (0)\right\} \alpha_r \tag{3-92}$$

$$N_3 = \left\{\frac{\partial N_r}{\partial \alpha_r} + \frac{\partial N_3}{\partial \alpha_r}\right\} \alpha_r \tag{3-93}$$

$$MA_3 = \left\{\frac{\partial MA_r}{\partial \alpha_r} + \frac{\partial MA_3}{\partial \alpha_r}\right\} \alpha_r \tag{3-94}$$

Consider equation (3-93). Using flexible body aerodynamics yields $\overline{P}_3(0) = 0.137$. Thus, the incremental loading caused by bending due to the aerodynamic forces increases the angle-of-attack at the nose 13.7%. Using modified rigid body aerodynamics yields $\overline{P}_3(0) = 0.139$. This results in an increase in the angle-of-attack at the nose of 13.9%.

Consider equation (3-93). Flexible body aerodynamics yields $\frac{\partial N_3}{\partial \alpha_r} = -1.49\text{x}10^5$ lb/rad, which results in a decrease in the body normal force of 5.4%. Modified rigid body aerodynamics yields $\frac{\partial N_3}{\partial \alpha_r} = 2.68\text{x}10^4$ lb/rad, which increases the vehicle normal force 1.0%.

Flexible body aerodynamics yields $\frac{\partial MA_3}{\partial \alpha_r} = 1.90\text{x}10^7$ ft lb/rad. From equation (3-94), the incremental pitching moment caused by bending due to aerodynamic forces results in an increase in the pitching moment of 15.1%. The modified rigid body data yields $\frac{\partial M_3}{\partial \alpha_r} = 1.99\text{x}10^7$ ft lb/rad. The corresponding increase of pitching moment is 15.8%. Considering the differences in the local normal force distribution between figures (2-9) and (2-11) and between figures (2-10) and (2-12), this close agreement for the incremental pitching moment determined by the two aerodynamic methods is considered fortuitous in the case of the Saturn V vehicle.

The flexible body aerodynamic data applied to equations (3-93) and (3-94) results in a forward shift in the center of pressure of approximately 0.30 calibers. The modified rigid body aerodynamic data results in a corresponding shift of 0.20 calibers.

## IV. INTEGRATED VEHICLE DYNAMICS

In order to fully assess the significance of the flexible body aerodynamic loads, determined by the iterative procedure described in sections II and III, it is necessary to perform a dynamic analysis of the vehicle. This is required because the normal acceleration of the vehicle is a factor in the incremental aerodynamic loading caused by body flexing.

A basic dynamic model of the vehicle used in this study is only valid at frequencies below the control frequency of the vehicle since filters are not included. The objective of this analysis is to illustrate how the effects of flexible body aerodynamics can be incorporated into a vehicle dynamic analysis and also to determine the significance of the flexible body aerodynamic analysis of section II compared with rigid body aerodynamic terms modified to account for variations in load angle-of-attack.

Frequency response functions will be determined for a vehicle where all motion takes place in the yaw plane. This is illustrated in figure (4-1). The angular momentum equation is:

$$I \ddot{\phi} = MA_k - (L - x_{cg}) F \left\{ \beta + \frac{dy}{dx} (L) \right\} \tag{4-1}$$

$$I \ddot{\phi} - MA_k + (L - x_{cg}) F \left\{ \beta + \frac{dy}{dx} (L) \right\} = 0 \tag{4-2}$$

The translational momentum equation is:

$$m\ddot{w} = N_k + F \left\{ \beta + \frac{dy}{dx} (L) \right\} \tag{4-3}$$

$$m\ddot{w} - N_k - F \left\{ \beta + \frac{dy}{dx} (L) \right\} = 0 \tag{4-4}$$

The control equation is:

$$\beta = a_o \left\{ \phi + \frac{dy}{dx} (\bar{x}) \right\} + a_1 \dot{\phi} \tag{4-5}$$

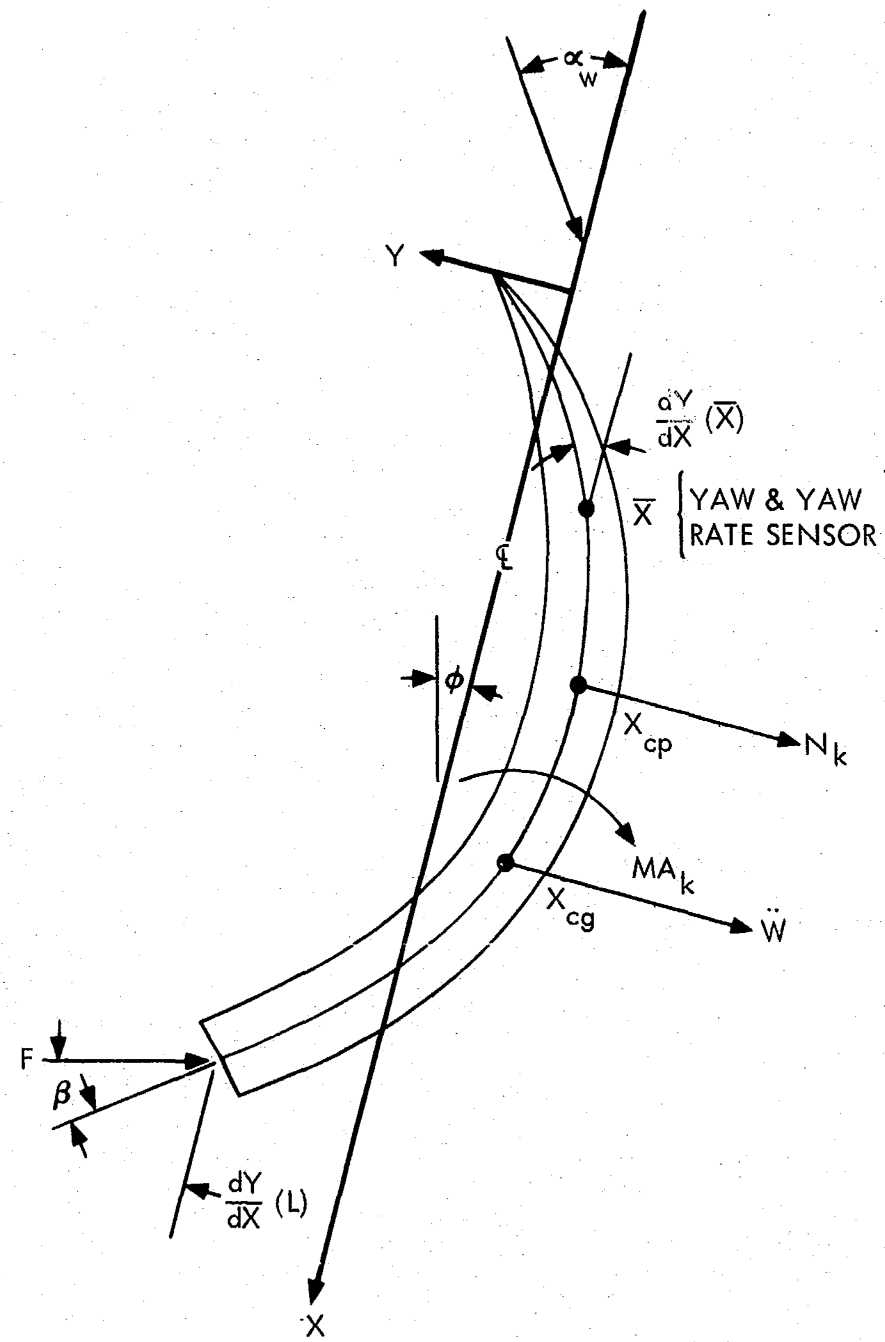


Figure 4-1. Yaw Plane Dynamics

Substituting equation (4-5) into equations (4-2) and (4-4) yields:

$$I\ddot{\phi} - MA_k + (L-x_{cg})\,F\left\{a_o\,\phi + a_o\frac{dy}{dx}(\bar{x}) + a_1\dot{\phi} + \frac{dy}{dx}(L)\right\} = 0 \qquad (4\text{-}6)$$

$$m\ddot{w} - N_k - F\left\{a_o\,\phi + a_o\frac{dy}{dx}(\bar{x}) + a_1\dot{\phi} + \frac{dy}{dx}(L)\right\} = 0 \qquad (4\text{-}7)$$

From equation (3-79)

$$\frac{dy}{dx}(\bar{x}) = \alpha_r\,\overline{P}_k(\bar{x}) + \ddot{w}\,\overline{Q}_k(\bar{x}) \qquad (4\text{-}8)$$

$$\frac{dy}{dx}(L) = \alpha_r\,\overline{P}_k(L) + \ddot{w}\,\overline{Q}_k(L) \qquad (4\text{-}9)$$

The rigid body angle-of-attack is determined by:

$$\alpha_r = \phi + \alpha_w - \dot{z}/V_\infty \qquad (4\text{-}10)$$

Substituting into equations (4-8) and (4-9) yields:

$$\frac{dy}{dx}(\bar{x}) = \phi\,\overline{P}_k(\bar{x}) + \ddot{w}\,\overline{Q}_k(\bar{x}) + (\alpha_w - \dot{z}/V_\infty)\,\overline{P}_k(\bar{x}) \qquad (4\text{-}11)$$

$$\frac{dy}{dx}(L) = \phi\,\overline{P}_k(L) + \ddot{w}\,\overline{Q}_k(L) + (\alpha_w - \dot{z}/V_\infty)\,\overline{P}_k(L) \qquad (4\text{-}12)$$

Repeating equations (3-90) and (3-91):

$$N_k = \alpha_r\left(\frac{\partial N_r}{\partial\alpha_r} + \frac{\partial N_k}{\partial\alpha_r}\right) + \ddot{w}\,\frac{\partial N_k}{\partial\ddot{w}} \qquad (3\text{-}90)$$

$$MA_k = \alpha_r\left(\frac{\partial MA_r}{\partial\alpha_r} + \frac{\partial MA_k}{\partial\alpha_r}\right) + \ddot{w}\,\frac{\partial MA_k}{\partial\ddot{w}} \qquad (3\text{-}91$$

Substituting equation (4-10) yields:

$$N_k = \phi\left(\frac{\partial N_r}{\partial\alpha_r} + \frac{\partial N_k}{\partial\alpha_r}\right) + \ddot{w}\,\frac{\partial N_k}{\partial\ddot{w}} + (\alpha_w - \dot{z}/V_\infty)\left(\frac{\partial N_r}{\partial\alpha_r} + \frac{\partial N_k}{\partial\alpha_r}\right) \qquad (4\text{-}13)$$

$$MA_k = \phi \left( \frac{\partial MA_r}{\partial \alpha_r} + \frac{\partial MA_k}{\partial \alpha_r} \right) + \ddot{w} \frac{\partial MA_k}{\partial \ddot{w}} + ( \alpha_W - \dot{z} / V_\infty )$$

$$\left( \frac{\partial MA_r}{\partial \alpha_r} + \frac{\partial MA_r}{\partial \alpha_r} \right) \tag{4-14}$$

Substituting equations (4-11), (4-12), (4-13), and (4-14) into equations (4-6) and (4-7) yields:

$$I \ddot{\phi} - \phi \left( \frac{\partial MA_r}{\partial \alpha_r} + \frac{\partial MA_k}{\partial \alpha_r} \right) - \ddot{w} \frac{\partial MA_k}{\partial \ddot{w}} - ( \alpha_W - \dot{z} / V_\infty ) \left( \frac{\partial MA_r}{\partial \alpha_r} + \frac{\partial MA_r}{\partial \alpha_r} \right)$$

$$+ (L - x_{cg}) F \left\{ a_o \phi + a_1 \dot{\phi} + (a_o \overline{P}_k (\bar{x}) + \overline{P}_k (L)) \phi + (a_o \overline{Q}_k (\bar{x}) + \overline{Q}_k (L)) \ddot{w} \right.$$

$$\left. + (a_o \overline{P}_k (\bar{x}) + \overline{P}_k (L)) ( \alpha_W - \dot{z} / V_\infty ) \right\} = 0 \tag{4-15}$$

$$M \ddot{w} - \phi \left( \frac{\partial N_r}{\partial \alpha_r} + \frac{\partial N_k}{\partial \alpha_r} \right) - \ddot{w} \frac{\partial N_k}{\partial \ddot{w}} - ( \alpha_W - \dot{z} / V_\infty ) \left( \frac{\partial N_r}{\partial \alpha_r} + \frac{\partial N_k}{\partial \alpha_r} \right)$$

$$- F \left\{ a_o \phi + a_1 \dot{\phi} + (a_o \overline{P}_k (\bar{x}) + \overline{P}_k (L)) \phi + (a_o \overline{Q}_k (\bar{x}) + \overline{Q}_k (L)) \ddot{w} \right.$$

$$\left. + (a_o \overline{P}_k (\bar{x}) + \overline{P}_k (L)) ( \alpha_W - \dot{z} / V_\infty ) \right\} = 0 \tag{4-16}$$

Collecting terms:

$$I \ddot{\phi} + (L - x_{cg}) F a_1 \dot{\phi} + \left\{ - \left( \frac{\partial MA_r}{\partial \alpha_r} + \frac{\partial MA_k}{\partial \alpha_r} \right) + (L - x_{cg}) F a_o + (L - x_{cg}) F \right.$$

$$\left. (a_o \overline{P}_k (\bar{x}) + \overline{P}_k (L)) \right\} \phi + \left\{ - \frac{\partial MA_k}{\partial \ddot{w}} + (L - x_{cg}) F (a_o \overline{Q}_k (\bar{x}) + \overline{Q}_k (L)) \right\} \ddot{w} =$$

$$- \left\{ - \left( \frac{\partial MA_r}{\partial \alpha_r} + \frac{\partial MA_r}{\partial \alpha r} \right) + (L - x_{cg}) F (a_o \overline{P}_k (\bar{x}) + \overline{P}_k (L)) \right\}$$

$$( \alpha_W - \dot{z} / V_\infty ) \tag{4-17}$$

$$F a_1 \dot{\phi} + \left\{ \left( \frac{\partial N_r}{\partial \alpha_r} + \frac{\partial N_k}{\partial \alpha_r} \right) + F a_o + F (a_o \overline{P}_k (\bar{x}) + \overline{P}_k (L)) \right\} \phi$$

$$+ \left\{ \frac{\partial N_k}{\partial \ddot{w}} - M + F (a_o \overline{Q} (\bar{x}) + \overline{Q}_k (L)) \right\} \ddot{w} =$$

$$- \left\{ \left( \frac{\partial N_r}{\partial \alpha_r} + \frac{\partial N_r}{\partial \alpha_r} \right) + F (a_o \overline{P}_k (\bar{x}) + \overline{P}_k (L)) \right\} ( \alpha_W - \dot{z} / V_\infty ) \tag{4-18}$$

Consider the following definitions:

$$\Delta x_2 = L - x_{cg} \tag{4-19}$$

$$S_1 = -\left(\frac{\partial MA_r}{\partial \alpha_r} + \frac{\partial MA_k}{\partial \alpha_r}\right) + (L - x_{cg})\, F\,(a_o(1 + \overline{P}_k(\bar{x})) + \overline{P}_k(L)) \tag{4-20}$$

$$S_2 = -\frac{\partial MA_k}{\partial \ddot{w}} + (L - x_{cg})\, F\,(a_o\, \overline{Q}_k(\bar{x}) + \overline{Q}_k(L)) \tag{4-21}$$

$$S_3 = -\left(\frac{\partial MA_r}{\partial \alpha_r} + \frac{\partial MA_r}{\partial \alpha_r}\right) + (L - x_{cg})\, F\,(a_o\, \overline{P}_k(\bar{x}) + \overline{P}_k(L)) \tag{4-22}$$

$$T_1 = \left(\frac{\partial N_r}{\partial \alpha_r} + \frac{\partial N_r}{\partial \alpha_r}\right) + F\,(a_o\,(1 + \overline{P}_k(\bar{x})) + \overline{P}_k(L)) \tag{4-23}$$

$$T_2 = \frac{\partial N_k}{\partial \ddot{w}} - M + F\,(a_o\, \overline{Q}_k(\bar{x}) + \overline{Q}_k(L)) \tag{4-24}$$

$$T_3 = \left(\frac{\partial N_r}{\partial \alpha_r} + \frac{\partial N_k}{\partial \alpha_r}\right) + F\,(a_o\, \overline{P}_k(\bar{x}) + \overline{P}_k(L)) \tag{4-25}$$

Substituting these expressions into equations (4-17) and (4-18) yields:

$$I\,\ddot{\phi} + a_1\,\Delta x_2\, F\,\dot{\phi} + S_1\,\phi + S_2\,\ddot{w} = -S_3\,(\alpha_w - \dot{z}/V_\infty) \tag{4-26}$$

$$a_1\, F\,\dot{\phi} + T_1\,\phi + T_2\,\ddot{w} = -T_3\,(\alpha_w - z/V_\infty) \tag{4-27}$$

or

$$T_2\, I\,\ddot{\phi} + a_1\, T_2\,\Delta x_2\, F\,\dot{\phi} + S_1\, T_2\,\phi + S_2\, T_2\,\ddot{w} = -S_3 T_2\,(\alpha_w - \dot{z}/V_\infty) \tag{4-28}$$

$$a_1\, S_2\, F\,\dot{\phi} + S_2\, T_1\,\phi + S_2\, T_2\,\ddot{w} = -S_2\, T_3\,(\alpha_w - \dot{z}/V_\infty) \tag{4-29}$$

Subtracting equation (4-29) from (4-28) yields:

$$T_2\, I\,\ddot{\phi} + a_1\, F\,(T_2\,\Delta x_2 - S_2)\,\dot{\phi} + (S_1\, T_2 - S_2\, T_1)\,\phi = \left(\frac{S_2\, T_3 - S_3\, T_2}{V_\infty}\right)$$

$$(V_w - \dot{z}) \tag{4-30}$$

where $\alpha_w = V_w/V_\infty$. Consider the following expressions:

$$V_w = V_{w0} + V_{w1} \sin w\, t \tag{4-31}$$

$$\phi = \phi_T + \phi_1 \sin \omega t + \phi_2 \cos \omega t \tag{4-32}$$

$$\dot{\phi} = \dot{\phi}_T + \omega \phi_1 \cos \omega t - w \phi_2 \sin \omega t \tag{4-33}$$

$$\ddot{\phi} = \ddot{\phi}_T - \omega^2 \phi_1 \sin \omega t - \omega^2 \phi_2 \cos \omega t \tag{4-34}$$

$$\ddot{w} = \ddot{w}_T + \ddot{w}_1 \sin w t + \ddot{w}_2 \cos w t \tag{4-35}$$

Substituting these equations into equation (4-30) yields:

$$T_2 I \ddot{\phi}_T + a_1 F (T_2 \Delta x_2 - S_2) \dot{\phi}_T + (S_1 T_2 - S_2 T_1) \phi_T = \left( \frac{S_2 T_3 - S_3 T_2}{V_\infty} \right) (V_{w0} - \dot{z}) \tag{4-36}$$

$$-T_2 I \omega^2 \phi_1 - a_1 F (T_2 \Delta x_2 - S_2) \omega \phi_2 + (S_1 T_2 - S_2 T_1) \phi_1 = \left( \frac{S_2 T_3 - S_3 T_2}{V_\infty} \right) V_{w_1} \tag{4-37}$$

$$-T_2 I \omega^2 \phi_2 + a_1 F (T_2 \Delta x_2 - S_2) \omega \phi_1 + (S_1 T_2 - S_2 T_1) \phi_2 = 0 \tag{4-38}$$

Let the transient solution be represented by:

$$\phi_T = R_1 e^{r_1 t} + R_2 e^{r_2 t} + R_3 \tag{4-39}$$

$$r_{1,2} = \frac{-a_1 F (T_2 \Delta x_2 - S_2) \pm \sqrt{a_1^2 F^2 (T_2 \Delta x_2 - S_2)^2 - 4 T_2 I (S_1 T_2 - S_2 T_1)}}{2 T_2 I} \tag{4-40}$$

$$R_3 = \left( \frac{S_2 T_3 - S_3 T_2}{V_\infty} \right) \left( \frac{V_{w0} - \dot{z}}{S_1 T_2 - S_2 T_1} \right) \tag{4-41}$$

$$R_1 = \frac{r_2 (\phi_T(0) - R_3) - \dot{\phi}_T(0)}{(r_2 - r_1)} \tag{4-42}$$

$$R_2 = \frac{-r_1 (\phi_T(0) - R_3) + \dot{\phi}_T(0)}{(r_2 - r_1)} \tag{4-43}$$

To determine the constants $\phi_1$ and $\phi_2$ in the steady state solution, rewrite equations (4-37) and (4-38):

$$(S_1 T_2 - S_2 T_1 - T_2 I \omega^2) \phi_1 - a_1 F (T_2 \Delta x_2 - S_2) \omega \phi_2 = \left( \frac{S_2 T_3 - S_3 T_2}{V_\infty} \right) V_{w1} \tag{4-44}$$

$$a_1 F (T_2 \Delta x_2 - S_2) \omega \phi_1 + (S_1 T_2 - S_2 T_1 - T_2 I \omega^2) \phi_2 = 0 \tag{4-45}$$

Solving these equations yields:

$$\frac{\phi_1}{V_{w1}} = \frac{1/V_\infty \; (S_2T_3 - S_3T_2)\,(S_1T_2 - S_2T_1 - T_2I\omega^2)}{(S_1T_2 - S_2T_1 - T_2I\omega^2)^2 + a_1^2F^2(T_2\,\Delta x_2 - S_2)^2\,\omega^2} \tag{4-46}$$

$$\frac{\phi_2}{V_{w1}} = \frac{-1/V_\infty \; (S_2T_3 - S_3T_2)\,a_1F(T_2\,\Delta x_2 - S_2)\,\omega}{(S_1T_2 - S_2T_1 - T_2I\omega^2)^2 + a_1^2F^2(T_2\,\Delta x_2 - S_2)^2\,\omega^2} \tag{4-47}$$

The absolute value of the frequency response function, $F_{\phi, v}(\omega)$, of wind velocity to rigid body pitch angle is:

$$\left|F_{\phi, v}(\omega)\right| = +\sqrt{\left(\frac{\phi_1}{V_{w1}}\right)^2 + \left(\frac{\phi_2}{V_{w1}}\right)^2} \tag{4-48}$$

and the corresponding phase angle is:

$$\theta_{\phi, v} = \tan^{-1}\left(\frac{-\phi_2/V_w}{\phi_2/V_w}\right) \tag{4-49}$$

The frequency response function of wind velocity to normal body acceleration will now be determined. Substituting equations (4-31), (4-32), (4-33), and (4-35) into equation (4-27) yields:

$$a_1F\,\dot{\phi}_T + T_1\,\phi_T + T_2\,\ddot{w}_T = \frac{-T_3}{V_\infty}\,(V_{w0} - \dot{z}) \tag{4-50}$$

$$-a_1F\,\omega\phi_2 + T_1\,\phi_1 + T_2\,\ddot{w}_1 = \frac{T_3}{V_\infty}\,V_{w1} \tag{4-51}$$

$$+a_1F\,\omega\phi_1 + T_1\,\phi_2 + T_2\,\ddot{w}_2 = 0 \tag{4-52}$$

This yields:

$$\ddot{w}_T = \frac{-a_1F}{T_2}\,\dot{\phi}_T\;\frac{-T_1}{T_2}\,\phi_T\;\frac{-T_3}{T_2V_\infty}\,(V_{w0} - \dot{z}) \tag{4-53}$$

$$\frac{\ddot{w}_1}{V_{w1}} = +\frac{a_1F\omega}{T_2}\,\frac{\phi_2}{V_{w1}} - \frac{T_1}{T_2}\,\frac{\phi_1}{V_{w1}} - \frac{T_3}{T_2\;V_\infty} \tag{4-54}$$

$$\frac{\ddot{w}2}{V_{w1}} = - \frac{a_1 F \omega}{T2} \frac{\phi_1}{V_{w1}} - \frac{T_1}{T2} \phi_2 \qquad (4\text{-}55)$$

Where $\phi_1 / V_{w1}$ and $\phi_2 / V_{w1}$ are determined by equations (4-46) and (4-47). The absolute value of the frequency response function, $F_{\ddot{w},v}(\omega)$, of wind velocity to normal vehicle acceleration is given by:

$$\left| F_{\ddot{w},v}(\omega) \right| = + \sqrt{\left(\frac{\ddot{w}1}{V_{w1}}\right)^2 + \left(\frac{\ddot{w}2}{V_{w1}}\right)^2} \qquad (4\text{-}56)$$

and the corresponding phase angle is:

$$\theta_{\ddot{w},v} = \tan^{-1} \left( \frac{-\ddot{w}2 / V_{w1}}{\ddot{w}1 / V_{w1}} \right) \qquad (4\text{-}57)$$

To determine the frequency response function of wind velocity to engine gimbal angle, substitute equation (4-11) into equation (4-5):

$$\beta = a_o \left\{ 1 + \overline{P}_k(\bar{x}) \right\} \phi + a_1 \dot{\phi} + a_o \overline{Q}_k(\bar{x}) \ddot{w} + a_o \overline{P}_k(\bar{x}) (\alpha_w - \dot{z} / V_\infty) \qquad (4\text{-}58)$$

Substituting equations (4-31), (4-32), (4-33), and (4-35) yields:

$$\beta_T = a_o \left\{ 1 + \overline{P}_k(\bar{x}) \right\} \phi_T + a_1 \dot{\phi}_T + a_o \overline{Q}_k(\bar{x}) \ddot{w}_T + a_o \overline{P}_k(\bar{x}) (V_{wo} - \dot{z})/V_\infty \qquad (4\text{-}59)$$

$$\frac{\beta_1}{V_{w1}} = a_o \left\{ 1 + \overline{P}_k(\bar{x}) \right\} \frac{\phi_1}{V_{w1}} - a_1 \omega \frac{\phi_2}{V_{w1}} + a_o \overline{Q}_k(\bar{x}) \frac{\ddot{w}1}{V_{w1}} + a_o \overline{P}_k(\bar{x}) / V_\infty \qquad (4\text{-}60)$$

$$\frac{\beta_2}{V_{w1}} = a_o \left\{ 1 + \overline{P}_k(\bar{x}) \right\} \frac{\phi_1}{V_{w1}} + a_1 \omega \frac{\phi_2}{V_{w1}} + a_o \overline{Q}_k(\bar{x}) \frac{\ddot{w}2}{V_{w1}} \qquad (4\text{-}61)$$

where

$$\beta = \beta_T + \beta_1 \sin wt + \beta_2 \cos wt \qquad (4\text{-}62)$$

The functions $\phi_1 / V_{w1}$, $\phi_2 / V_{w1}$, $\ddot{w}_1 / V_{w1}$, and $\ddot{w}_2 / V_{w1}$ are determined from equations (4-46), (4-47), (4-54), and (4-55). The absolute value of the frequency response function of wind velocity to engine gimbal angle is

$$\left| F_{\beta,v}(\omega) \right| = + \sqrt{\left(\frac{\beta_1}{V_{w1}}\right)^2 + \left(\frac{\beta_2}{V_{w1}}\right)^2} \qquad (4\text{-}63)$$

and its corresponding phase angle is:

$$\theta_{\beta, v} = \tan^{-1} \left( \frac{- \beta_2 / V_{w1}}{\beta_1 / V_{w1}} \right) \qquad (4-64)$$

A numerical analysis was made of equations derived in this section. This analysis and a listing of the computer program made from the numerical analysis is given in appendix F. Sample inputs and outputs are also included in this appendix.

Saturn V dynamic calculations were made in the low frequency range at maximum dynamic pressure. These calculations were made using only rigid body aerodynamic data and they were also made using this data and the incremental data caused by bending. This flexible body data was obtained from the First Order Method for Flexible Bodies. The absolute value of the wind velocity to yaw angle frequency response function at $\omega = 0$, $|F_{\phi, v}(0)|$, obtained from rigid body data was $5.71 \times 10^{-4}$ rad sec/ft. Using the data from the First Order Method for Flexible Bodies yields $|F_{\phi, v}(0)| = 7.18 \times 10^{-4}$ rad sec/ft. This is an increase of 17.8%. The absolute values of those frequency response functions at $\omega = 0.2$ rad/sec is essentially unchanged. However, the phase lag for the rigid body aerodynamic case is 0.55 rad; and, for the flexible body aerodynamic case, it is 0.62 rad.

The rigid body aerodynamic data yields 3.20 sec for the absolute value of wind velocity to normal vehicle acceleration frequency response function, $|F_{\ddot{w}, v}(0)|$, at $\omega = 0$. Including the flexible body data yields $|F_{\ddot{w}, v}(0)| = 3.63$ sec. This is an increase of 0.13%. These absolute values are virtually unchanged at $\omega = 0.2$ rad/sec. The rigid body data yields a phase lag at this frequency of 0.27 rad. The flexible body aerodynamic data results in a corresponding phase lag of 0.34 rad.

An absolute value of the frequency response function of wind velocity to engine gimbal angle at $\omega = 0$, $|F_{\beta, v}(0)|$, of $4.91 \times 10^{-4}$ rad sec/ft was computed using rigid body aerodynamic data. A corresponding value of $6.42 \times 10^{4}$ was obtained when data from the First Order Method for Flexible Bodies is included. Including flexible body data increases the absolute value of the frequency response function by 30.8%. At $\omega = 0.20$ rad/sec, the phase lag for the rigid body aerodynamic case is 0.30 rad. The flexible body aerodynamic data yields a phase lag of 0.36 rad.

Saturn V dynamic calculations were also made using flexible body data obtained by multiplying the local rigid body normal force derivatives by the local angle-of-attack. In the frequency range considered, the Saturn V frequency response functions that were obtained were very similar to those computed using the data from First Order Method for Flexible Bodies. This is because of the similarity of the pitching moment about the center of gravity obtained from the two methods. As stated previously, this similarity of the pitching moment is considered by the authors to be a coincidence in the case of the Saturn V vehicle.

## V. CONCLUSIONS AND RECOMMENDATIONS

The following conclusions were reached as the result of this study:

- The equation of the disturbance velocity potential has been formulated in flexible body coordinates (see equation (2-33)) and is in the same mathematical form as in cylindrical coordinates.

- As a result of this similarity in form, the First Order Method described by Ferri and Van Dyke has been extended to determine the aerodynamic characteristics of flexible bodies.

- The First Order Method for Flexible Bodies developed in this study is shown in appendix C to be compatible with Dahm's Slender Body Method for flexible bodies.

- The First Order Method for Flexible Bodies yields results that are significantly different from those obtained using rigid body data modified to account for variations in local angle-of-attack. This is shown in figure (2-5) and by comparing figure (2-11) with (2-9) and by comparing figure (2-10) with figure (2-12).

- The characteristics of flexible bodies are linear in terms of the rigid body angle-of-attack and the normal acceleration of a vehicle. This is shown in equations (3-7), (3-39), (3-40), (3-41), (3-43), (3-44), (3-51), and (3-52).

- The flexible body aerodynamic forces significantly affect the performance of a vehicle. Static considerations indicate the pitching moment about the center of gravity is increased more than 16% for the Saturn V vehicle at the maximum dynamic pressure. A dynamic analysis indicates that the Saturn V flexible body aerodynamic forces can increase the engine gimbal angle by 30%.

- Flexible body calculations were made using the First Order Method for Flexible Bodies and also using rigid body data modified to account for variations in local angle-of-attack.

These two methods gave different results for the local normal force distribution. However, these differences occurred in relation to the Saturn V center of gravity, at time t = 79 sec, such that similar pitching moments are computed by both methods. This similarity in pitching moment resulted in similar vehicle dynamic response calculations. This is considered to be a fortunate coincidence in the case of the Saturn V vehicle.

The following recommendations are based on the results of this study:

- Wind tunnel tests should be conducted on bent models of simple geometry. These models would consist of combinations of ogives, cones, cone frustums, and cylinders.

- The First Order Method for Flexible Bodies should be applied to the flexible bodies currently being studied in wind tunnel tests by Aero-Astrodynamic Laboratory of MSFC.

- A noniterative computing scheme should be devised for computing the aeroelastic response of a flexible vehicle.

- The First Order Method for Flexible Bodies should be extended to the Hybrid Method for flexible bodies.

- The First Order Method for Flexible Bodies is probably valid for non-uniform cross flow. This should be investigated. Extensions should be made if necessary.

- The methods of this study should be integrated into a more exact dynamic simulation.

- The methods of analyzing separated flows developed by Korst should be included in the flexible body aerodynamic analysis.

- The First Order Method for Flexible Bodies should be extended to include time dependent terms.

## REFERENCES


1. Papadopoulos, James G., "Aeroelastic Load Growth Effects on Saturn Configurations," NASA TM X-53634, July 14, 1967.

2. Papadopoulos, James G., "Wind Penetration Effects on Flight Simulations," AIAA Paper No. 67-609, AIAA Guidance, Control, and Flight Dynamics Conference, Huntsville, Alabama, August 14-16, 1967.

3. Dahm, Werner K., "Approximate Longitudinal Normal Force Distribution on Slender Bodies and Body - Tail Configurations, Oscillating in Arbitrary Mode Shapes," Aeroballistics Internal Note 80, November 1, 1955.

4. Ferri, Antonio, Elements of Aerodynamics of Supersonic Flows. The Macmillan Company, New York, 1949.

5. Van Dyke, Milton D., "First- and Second-Order Theory of Supersonic Flow Past Bodies of Revolution," Journal of the Aeronautical Sciences, March 1951

6. Anonymous, "Static Aerodynamic Characteristics of the Apollo-Saturn V Vehicle," NASA TMX-53517, September 16, 1966.

7. Sears, W. R., General Theory of High Speed Aerodynamics. Princeton University Press, Princeton, 1954.

## APPENDIX A

The fact that equation (2-42) is a solution of equation (2-33) is demonstrated in this appendix. Consider equation (2-42):

$$\phi_a(x, r) = \int_{\cosh^{-1}\frac{x}{\beta r}}^{0} f(x - \beta r \cosh z)\, dz \tag{2-42}$$

Taking the derivative with respect to x yields:

$$\frac{\partial \phi a}{\partial x} = \int_{\cosh^{-1}\frac{x}{\beta r}}^{0} f'(x - \quad r \cosh z)\, dz - \frac{f(0)}{\beta r \sqrt{\left(\frac{x}{\beta r}\right)^2 - 1}} \tag{2-43}$$

For pointed bodies, the source strength, f, is zero at $x - \beta\ r \cosh z = 0$. Thus the last term in equation (2-41) is zero. Taking the second derivative yields:

$$\frac{\partial^2 \phi a}{\partial x^2} = \int_{\cosh^{-1}\frac{x}{\beta r}}^{0} f''(x - \beta r \cosh z)\, dz - \frac{f'(0)}{\beta r \sqrt{\left(\frac{x}{\beta r}\right)^2 - 1}} \tag{A-1}$$

Taking the derivatives of equation (2-41) with respect to r yields:

$$\frac{\partial \phi a}{\partial r} = -\beta \int_{\cosh^{-1}\frac{x}{\beta r}}^{0} f'(x - \beta r \cosh z) \cosh z\, dz + \frac{f(0)\left(\frac{x}{\beta r}\right)}{r\sqrt{\left(\frac{x}{\beta r}\right)^2 - 1}} \tag{2-44}$$

$$\frac{\partial^2 \phi a}{\partial r^2} = \beta^2 \int_{\cosh^{-1}\frac{x}{\beta r}}^{0} f''(x - \beta r \cosh z) \cosh^2 z\, dz - \frac{f'(0)\beta \left(\frac{x}{\beta r}\right)^2}{r\sqrt{\left(\frac{x}{\beta r}\right)^2 - 1}} \tag{A-2}$$

Taking the derivatives of equation (2-42) with respect to $\theta$ yields:

$$\frac{\partial \phi a}{\partial \theta} = 0 \qquad \text{(A-3)}$$

$$\frac{\partial^2 \phi a}{\partial \theta^2} = 0 \qquad \text{(A-4)}$$

Substituting equations (A-1), (2-44), (A-2), and (A-4) into equation (2-33) yields:

$$-\beta^2 \int_{\cosh^{-1}\frac{x}{\beta r}}^{0} f''(x - r\cosh z)\, dz + \beta^2 \int_{\cosh^{-1}\frac{x}{\beta r}}^{0} f''(x - \beta r \cosh z) \cosh^2 z\, dz$$

$$-\frac{1}{r}\,\beta \int_{\cosh^{-1}\frac{x}{\beta r}}^{0} f'(x - \beta r \cosh z)\cosh z\, dz = +\frac{f'(0)\,\beta\left[\left(\frac{x}{\beta r}\right)^2 - 1\right]}{r\sqrt{\left(\frac{x}{\beta r}\right)^2 - 1}} \qquad \text{(A-5)}$$

$$\beta^2 \int_{\cosh^{-1}\frac{x}{\beta r}}^{0} f''(x - \beta r\cosh z)\sinh^2 z\, dz - \frac{\beta}{r}\int_{\cosh^{-1}\frac{x}{\beta r}}^{0} f'(x - \beta r \cosh z)\cosh z\, dz$$

$$= \frac{\beta}{r} f'(0)\sqrt{\left(\frac{x}{\beta r}\right)^2 - 1} \qquad \text{(A-6)}$$

$$-\frac{\beta}{r} f'(x - \beta r\cosh z)\sinh z \Big]_{\cosh^{-1}\frac{x}{\beta r}}^{0} = \frac{\beta}{r} f'(0)\sqrt{\left(\frac{x}{\beta r}\right)^2 - 1} \qquad \text{(A-7)}$$

$$\frac{\beta}{r} f'(0)\sqrt{\left(\frac{x}{\beta r}\right)^2 - 1} = \frac{\beta}{r} f'(0)\sqrt{\left(\frac{x}{\beta r}\right)^2 - 1} \qquad \text{(A-8)}$$

which proves that equation (2-42) is a solution of equation (2-33).

## APPENDIX B

The fact that equation (2-61) is a solution of equation (2-33) is demonstrated in this appendix. Consider equation (2-61):

$$\phi_c(x, r, \theta) = -\cos\theta\,\beta \int_{\cosh^{-1}\frac{x}{\beta r}}^{0} m\,(x - \beta r \cosh z)\cosh z\,dz \qquad (2\text{-}61)$$

where m (0) = 0 for a closed pointed body. The function $m\,(x - \beta\, r \cosh z)$ must be chosen to fit the boundary conditions of the body. Consider the derivative of equation (2-61) with respect to x:

$$\frac{\partial \phi_c}{\partial x} = -\cos\theta\,\beta \int_{\cosh^{-1}\frac{x}{\beta r}}^{0} m'\,(x - \beta r \cosh z)\cosh z\,dz + \frac{m(0)}{r}$$

$$\frac{\cos\theta\left(\frac{x}{\beta r}\right)}{\sqrt{\left(\frac{x}{\beta r}\right)^2 - 1}} \qquad (2\text{-}62)$$

The last term is zero since m(0) = 0. Taking the second derivative with respect to x yields:

$$\frac{\partial^2 \phi_c}{\partial x^2} = -\cos\theta\,\beta \int_{\cosh^{-1}\frac{x}{\beta r}}^{0} m''\,(x - \beta\, r \cosh z)\cosh z\,dz + \frac{m'(0)}{r}\,\frac{\cos\theta\left(\frac{x}{\beta r}\right)}{\sqrt{\left(\frac{x}{\beta r}\right)^2 - 1}} \qquad (B\text{-}1)$$

Taking the cross derivative with respect to x and r yields: (B-2)

$$\frac{\partial^2 \phi_c}{\partial r\,\partial x} = +\cos\theta\,\beta^2 \int_{\cosh^{-1}\frac{x}{\beta r}}^{0} m''(x - \beta\, r \cosh z)\cosh^2 z\,dz - \frac{m'(0)}{r}\,\frac{\cos\theta\beta\left(\frac{x}{\beta r}\right)^2}{\sqrt{\left(\frac{x}{\beta r}\right)^2 - 1}}$$

The first and second derivatives with respect to r are given by:

$$\frac{\partial \phi_c}{\partial r} = + \cos\theta\,\beta^2 \int_{\cosh^{-1}\frac{x}{\beta r}}^{0} m'\,(x - \beta r \cosh z) \cosh^2 z\, dz - \frac{m'(0)}{r}$$

$$\frac{\cos\theta\,\beta \left(\frac{x}{\beta r}\right)^2}{\sqrt{\left(\frac{x}{\beta r}\right)^2 - 1}} \tag{2-63}$$

$$\frac{\partial^2 \phi_c}{\partial r^2} = - \cos\theta\,\beta^3 \int_{\cosh^{-1}\frac{x}{\beta r}}^{0} m''(x - \beta r \cosh z) \cosh^3 z\, dz + \frac{m'(0)}{r}$$

$$\frac{\cos\theta\beta^2 \left(\frac{x}{\beta r}\right)^3}{\sqrt{\left(\frac{x}{\beta r}\right)^2 - 1}} \tag{B-3}$$

And the second derivative with respect to $\theta$ is:

$$\frac{\partial^2 \phi_c}{\partial\theta^2} = + \cos\theta\,\beta \int_{\cosh^{-1}\frac{x}{\beta r}}^{0} m\,(x - \beta r \cosh z) \cosh z\, dz \tag{B-4}$$

Substituting equations (B-1), (2-63), (B-3), and (B-4) into equation (2-33) yields:

$$- \cos\theta\beta^3 \int_{\cosh^{-1}\frac{x}{\beta r}}^{0} m''(x - \beta r \cosh z) \cosh z \sinh^2 z\, dz + \frac{\cos\theta}{r}\,\beta^2$$

$$\int_{\cosh^{-1}\frac{x}{\beta r}}^{0} m'(x - \beta r \cosh z) \cosh^2 z\, dz + \frac{\cos\theta\beta}{r^2} \int_{\cosh^{-1}\frac{x}{\beta r}}^{0} m\,(x - \beta r \cosh z) \cosh z\, dz =$$

$$- \frac{m'(0)}{r}\; \frac{\cos\theta\,\beta^2 \left(\frac{x}{\beta r}\right) \left[\left(\frac{x}{\beta r}\right)^2 - 1\right]}{\sqrt{\left(\frac{x}{\beta r}\right)^2 - 1}} \tag{B-5}$$

Rearranging:

$$- \cos\theta\, \beta^2 \int_{\cosh^{-1}\frac{x}{\beta r}}^{0} \Big[ \beta m''(x - \beta r \cosh z) \cosh z \sinh^2 z - \frac{1}{r} m'(x - \beta r \cosh z)$$

$$(\cosh^2 z + \sinh^2 z) \Big] dz - \frac{\cos\theta}{r} \beta \int_{\cosh^{-1}\frac{x}{\beta r}}^{0} \Big[ \beta\, m'(x - \beta r \cosh z) \sinh^2 z - \frac{1}{r} m$$

$$(x - \beta r \cosh z) \cosh z \Big] dz = - \frac{m'(0)}{r} \frac{\cos\theta\, \beta^2 \left(\frac{x}{\beta r}\right) \left[\left(\frac{x}{\beta r}\right)^2 - 1\right]}{\sqrt{\left(\frac{x}{\beta r}\right)^2 - 1}} \tag{2-45}$$

Integrating this equation:

$$- \frac{\cos\theta}{r} \beta^2 m'(x - \beta r \cosh z) \cosh z \sinh z - \frac{\cos\theta}{r^2} \beta\, m(x - \beta r \cosh z)$$

$$\sinh z \Big]_{0}^{\cosh^{-1}\left(\frac{x}{\beta r}\right)} = - \frac{m'(0)}{r} \frac{\cos\theta\, \beta^2 \left(\frac{x}{\beta r}\right) \left[\left(\frac{x}{\beta r}\right)^2 - 1\right]}{\sqrt{\left(\frac{x}{\beta r}\right)^2 - 1}} \tag{2-46}$$

$$- \frac{m'(0) \cos\theta\, \beta^2 \left(\frac{x}{\beta r}\right) \sqrt{\left(\frac{x}{\beta r}\right)^2 - 1}}{r} - \frac{m(0)}{r^2} \cos\theta\, \beta \sqrt{\left(\frac{x}{\beta r}\right)^2 - 1}$$

$$= - \frac{m'(0) \cos\theta\, \beta^2 \left(\frac{x}{\beta r}\right) \sqrt{\left(\frac{x}{\beta r}\right)^2 - 1}}{r} \tag{2-47}$$

Since m (0) = 0, the second term in equation (2-47) is zero. The left side of the equation is then equal to the right side, which proves that equation (2-37) is a solution of the equation of the velocity potential, equation (2-33). This equation is written in bent body coordinates and is valid only for bodies with small curvature and with small rates of change of curvature.

APPENDIX C

The extension of the First Order Method developed for flexible bodies will reduce to Dahm's result ( reference 3) when the slender body restrictions are applied. This result is demonstrated in this appendix. The pressure coefficient in the slender body theory is:

$$C_p = -\frac{2\left(\frac{\partial \phi_c}{\partial x}\right)_R}{V_\infty} \qquad \text{(C-1)}$$

Thus, only the partial derivative of the cross flow disturbance potential with respect to x need be considered. In slender body theory for bent bodies, this derivative is given by:

$$\left(\frac{\partial \phi_c}{\partial x}\right)_R = \frac{\cos\theta}{R} \quad V_\infty \quad \frac{d(R^2 \sin\alpha)}{dx} \qquad \text{(C-2)}$$

The expression for the derivative in the First Order Method will be shown to reduce to this expression when the slender body restrictions are applied. These restrictions require that $\frac{\beta r_i}{x_i}$ and $\left(\frac{dr}{dx}\right)_n$ are negligibie in satisfying the boundary conditions. Consider equations (2-77) and (2-56):

$$\left(\frac{\partial \phi_c}{\partial x}\right)_n = -\cos\theta\,\beta \sum_{i=2}^{n} b_i\, Y_{n,i} \qquad \text{(2-77)}$$

$$Y_{n,i} = \sqrt{\psi_{n,1}^2 - 1} \quad - \sqrt{\psi_{n,1-1}^2 - 1} \qquad \text{(2-56)}$$

The slender body restrictions yield:

$$Y_{n,i} = -\frac{x_i - x_{i-1}}{\beta r_n} \qquad \text{(C-3)}$$

Substituting equations (C-3) into (2-77) yields:

$$\left(\frac{\partial \phi_c}{\partial x}\right)_n = + \frac{\cos\theta}{r_n} \sum_{i=2}^{n} b_i (x_i - x_{i-1}) \tag{C-4}$$

Now consider equation (2-80):

$$2(V_\infty \sin\alpha)_n = -\beta \sum_{i=2}^{n} b_i \left\{ 2\left(\frac{dr}{dx}\right)_n Y_{n,i} + \beta (X_{n,i} + Z_{n,i}) \right\} \tag{2-80}$$

From the slender body restrictions $\left(\frac{dr}{dx}\right)_n$ is negligible and $X_{n,i} \ll Z_{n,i}$. Thus equation (2-80) can be written:

$$(V_\infty \sin\alpha)_n = -1/2\ \beta^2 \sum_{i=2}^{n} b_i Z_{n,i} \tag{C-5}$$

From equation (2-76)

$$Z_{n,i} = \psi_{n,i}\sqrt{\psi^2_{n,i} - 1} - \psi_{n,i-1}\sqrt{\psi^2_{n,i-1} - 1} \tag{2-76}$$

Applying the slender body restrictions yields:

$$Z_{n,i} = \left(\frac{x_n - x_i}{\beta r_n}\right)^2 - \left(\frac{x_n - x_{i-1}}{\beta r_n}\right)^2 \tag{C-6}$$

Substituting this expression into equation (C-3) yields:

$$r_n^2 (V_\infty \sin\alpha)_n = -1/2 \sum_{i=2}^{n} b_i \left\{ (x_n - x_i)^2 - (x_n - x_{i-1})^2 \right\} \tag{C-7}$$

Likewise:

$$r^2_{n+1} (V_\infty \sin\alpha)_{n+1} = -1/2 \sum_{i=2}^{n+1} b_i \left\{ (x_{n+1} - x_i)^2 - (x_{n+1} - x_{i-1})^2 \right\} \tag{C-8}$$

Subtracting equation (C-8) from equation (C-7):

$$r_{n+1}^2 (V_\infty \sin\alpha)_{n+1} - r_n^2 (V_\infty \sin\alpha)_n = +1/2\, b_{n+1}(x_{n+1} - x_n)^2$$

$$- 1/2 \sum_{i=2}^{n} b_i \left\{ (x_{n+1} - x_i)^2 - (x_{n+1} - x_{i-1})^2 \right\} + 1/2 \sum_{i=2}^{n} b_i \left\{ (x_n - x_i)^2 \right. \quad \text{(C-9)}$$

$$\left. - (x_n - x_{i-1})^2 \right\}$$

$$r_n^2{}_{+1} (V_\infty \sin\alpha)_{n+1} - r_n^2 (V_\infty \sin\alpha)_n = +1/2\, b_{n+1} (x_{n+1} - x_n)^2 \quad \text{(C-10)}$$

$$+ \sum_{i=2}^{n} b_i (x_{n+1} - x_n)(x_i - x_{i-1})$$

Dividing by $(x_{n+1} - x_n)$:

$$\frac{r_{n+1}^2 (V_\infty \sin\alpha)_{n+1} - r_n^2 (V_\infty \sin\alpha)_n}{x_{n+1} - x_n} = 1/2\, b_n (x_{n+1} - x_n) + \sum_{i=2}^{n} b_i (x_i - x_{i-1}) \quad \text{(C-11)}$$

Since $1/2\, b_n (x_{n+1} - x_n)$ is small compared with the sum, equation (C-11) can be substituted into equation (C-4) to yield:

$$\left(\frac{\partial \phi_c}{\partial x}\right)_n = \frac{\cos\theta}{r_n} \left\{ \frac{r_{n+1}^2 (V_\infty \sin\alpha)_{n+1} - r_n^2 (V_\infty \sin\alpha)_n}{x_{n+1} - x_n} \right\} \quad \text{(C-12)}$$

which is equivalent to equation (C-2). Thus, applying the slender body restrictions to the First Order Method reduces it to the Slender Body Method for flexible bodies.

# APPENDIX D

This appendix contains the material used to compute the aerodynamic characteristics of a bent body as derived in section II. Specifically, it contains a definition of the key terms and the significant equations of the numerical analysis. It also contains a flow diagram of the analysis and a listing of the computer program. Sample input and output data are included. This computer program determines the following aerodynamic parameters of a bent axially symmetric body in the supersonic regime:

- The pressure coefficients around the body at each station
- Local normal force per foot
- Total normal force forward of a given body station
- Total body normal force
- Total forebody axial force
- Total body pitching moment
- Body center of pressure

The following parameters must be input to the program:

- Body velocity
- Specific heat ratio
- Dynamic pressure
- Body length
- Distance of the center of gravity from the body base
- Mach number
- Body geometry and local angle-of-attack at various body stations

The computation sequence used in this program requires that the last two body stations be identical; that is, X(NB) = X(NB-1), R(NB) = R(NB-1), and ALP(NB) = ALP(NB-1).

## DEFINITION OF SYMBOLS

| Symbol | Definition |
|---|---|
| U | Axial velocity component (ft/sec) |
| W | Radial velocity component (ft/sec) |
| CP | Pressure coefficient |
| QNFP | Local normal force per foot (lb /ft) |
| QNPS1 | Local normal force per foot caused by area change from slender body theory (lb /ft) |
| QNPS2 | Local normal force per foot caused by bending from slender body theory (lb /ft) |
| QNPS | Local normal force per foot from slender body theory (lb /ft) |
| QNF | Total normal force forward of station N (lb ) |
| QMF | Total pitching moment about the center of gravity (ft/lb ) |
| QNS | Total normal force forward of station N from slender body theory (lb ) |
| QMS | Total pitching moment about the center of gravity from slender body theory (ft/lb ) |
| V | Free stream velocity (ft/sec) |
| GAM | Specific heat ratio |
| Q | Dynamic pressure (lb /ft$^2$) |
| QL | Vehicle length (ft) |
| QLCG | Distance between body center of gravity and base (ft) |
| QM | Free stream Mach number |
| X | Distance of body station from body nose (ft) |
| R | Radius of body at body station (ft) |
| ALP | Local angle-of-attack at body station (ft) |
| QLCP | Distance between center of pressure and base (ft) |
| QLCS | Distance between center of pressure and base from slender body theory (ft) |

## SOLUTION OF EQUATIONS

1. $$BET = \sqrt{QM^2 - 1}$$

2. $$ZNIM = \frac{X(N)}{BET\ [R(N)]}$$

3. $$ZSIM = \sqrt{ZNIM^2 - 1}$$

4. $$ZNI = \frac{X(N) - \{X(I) - BET\ [R(I)]\}}{BET\ [R(N)]}$$

5. $$ZSI = \sqrt{ZNI^2 - 1}$$

6. $$XB(I) = ZNIM(ZSIM) - ZNI\ (ZSI) + \ln(2NIM + ZSIM) - \ln(ZNI + ZSI)$$

7. $$YB(I) = ZSIM - ZSI$$

8. $$ZB(I) = ZNIM\ \left[YB(I)\right] - 1/2\ XB(I)$$

9. $$SBX = SBX - \frac{B(I)\ XB(I)}{XB(N)}$$

10. $$B(N) = SBX + \frac{2V\ [ALP(N)]}{BET^2\ XB(N)}$$

11. $$SBY = SBY + BET\ \left[B(I)\right]\left[YB(I)\right]$$

12. $$SBZ = SBZ + BET^2\ \left[B(I)\right]\left[ZB(I)\right]$$

13. $U = V + SBY \left\{ \cos\left[\pi(0.02J - 0.01)\right]\right\}$

14. $W = \left\{ SBZ - V\left[ALP(N)\right]\right\} \sin\left[\pi(0.02J - 0.01)\right]$

15. $CP(J) = \frac{2}{GAM(QM)^2} \left\{ \left[1 + \frac{GAM - 1}{2} \; QM^2 \left(1 - \frac{U^2 + W^2}{V^2}\right)\right]^{\frac{GAM}{GAM - 1}} - 1 \right\}$

16. $QNFP = QNFP - 0.04\pi(Q) \left[R(N)\right] \; CP(J) \; \cos\left[\pi(0.02J + 0.01)\right]$

17. $QNPS1 = 4\pi(Q) \; ALP(N) \; R(N) \left[\frac{R(N+1) - R(N-1)}{X(N+1) - X(N-1)}\right]$

18. $QNPS2 = 2\pi(Q) \; R(N)^2 \left[\frac{ALP(N+1) - ALP(N-1)}{X(N+1) - X(N-1)}\right]$

19. $QNPS = QNPS1 + QNPS2$

20. $QNF = QNF + 1/2 \; QNFP\left[X(N+1) - X(N-1)\right]$

21. $QMF = QMF - 1/2 \; QNFP \left[X(N) - QL + QLCG\right]\left[X(N+1) - X(N-1)\right]$

22. $QNS = QNS + 1/2 \; QNPS \left[X(N+1) - X(N-1)\right]$

23. $QMS = QMS - 1/2 \; QNPS \left[X(N) - QL + QLCG\right] \left[X(N+1) - X(N-1)\right]$

24. $QLCP = QLCG + \frac{QMF}{QNF}$

25. $QLCS = QLCG + \frac{QMS}{QNS}$

## COMPUTER FLOW DIAGRAM

**INPUTS**

IPRT, QM, V, GAM, Q, QL, QLCG, NB, X(N), R(N), ALP(N), (52 values N)

↓

**PRINT INPUTS**

↓

$\pi = 3.14159265358979323846$

QNF = 0

QMF = 0

QAF = 0

QNS = 0

QMS = 0

QAS = 0     B(1) = 0,     CN(1) = 0,     A(1) = 0

$BET = \sqrt{QM^2 - 1}$

NBM = NB-1

GA = GAM/(GAM - 1.0)

DO 100 N=2, NBM

↓

DRDX = {R(N) - R(N-1)} /{X(N) - X(N-1)}

PNIM = X(N)/ {BET R(N)}

PN(1) = PNIM

$PSIM = \sqrt{PNIM^2 - 1}$

DO 10 I = 2, N

PN(I) = [X(N) - {X(I) - BET R(I)}] /{BET R(N)}

$PSI = \sqrt{PN(I)^2 - 1}$

XBN(I) = ln {PN(I) + PSI} - ln {PNIM + PSIM}

YBN(I) = PSI - PSIM

ZBM(I) = PN(I) x PSI - PNIM x PSIM

PNIM = PN(I)

10 PSIM = PSI

↓

```
SA = 0.0
SB = 0.0
NM = N-1
DO20 I = 2, NM
   SA = SA + A(I) [BET x YBN(I) + DRDX x XBN(I)]
20SB  = SB + B(I)  [2DRDX x YBN(I) + BET{ XBN(I) + ZBN(I)}]
   A(N) = - {DRDX x V + SA} / {BET x YBN(N) + DRDX x XBN(N)}
   B(N) = - {2V x ALP(N) + BET x SB} /[ 2BET x DRDX x YBN(N)
          + BET^2 {XBN(N) + ZBN(N)} ]
```

```
DO 30 I = 2, N
30 CN(I) = CN(I-1) + {B(I) - B(I-1)} PN(I-1)
```

```
SAX = 0
SAR = 0
SBX = 0
SBR = 0
SBT = 0
DO40 I = 2, N
   SAX = SAX + A(I) x XBN(I)
   SAR = SAR - BET x A(I) x YBN(I)
   SBX = SBX - BET x B(I) x YBN(I)
   SBR = SBR + 1/2 BET^2 B(I) {XBN(I) + ZBN(I)}
40SBT = SBT + 1/2 BET^2 [2CN(I) x YBN(I) - B(I) {XBN(I) + ZBN(I)}]
```

```
DO50 J = 1, 50
  U = V + SAX + SBX x cos {π (0.02 J -0.01)}
  VS = SAR + [V x ALP(N) + SBR] x cos {π (0.02 J - 0.01)}
  W = [SBT - V x ALP(N)] sin{π -(0.02 J - 0.01)}
```

$$50 \quad CP(J) = \{2/(GAM \times QM^2)\} \times \left\{ \left[ 1 + \frac{GAM-1}{2} QM^2 \left( 1 - \frac{U^2 + VS^2 + W^2}{V^2} \right. \right]^{GA} -1 \right\}$$

G1 = $1/4[\{R(N+1) + R(N)\}^2 - \{R(N) + R(N-1)\}^2]\,Q$

G2 = - 2QR(N)

SCP = 0

SCPC = 0

DO 60 J = 1, 50

SCP = SCP + 0.02 x $\pi$ CP(J)

60 SCPC = SCPC + 0.02 $\pi$ - CP(J) cos [$\pi$- (0.02 J - 0.01)]

AN = G1 x SCP

QNFP = G2 x SCPC

---

QNPS1 = 4$\pi$ Q ALP(N) R(N) DRDX

QNPS2 = 2$\pi$ Q $R(N)^2$ [{ALP(N+1) - ALP(N-1)} /{X(N+1) - X(N-1)}]

QNPS = QNPS1 + QNPS2

---

QAF = QAF + AN

QNF = QNF + 1/2 QNFP {X(N+1) - X(N-1)}

QMF = QMF - 1/2 QNFP{X(N) - QL + QLCG} x {X(N+1) - X(N-1)}

QNS = QNS + 1/2 QNPS{ X(N+1) - X(N-1)}

100 QMS = QMS - 1/2 QNPS {X(N) - QL + QLCG} x{X(N+1) - X(N-1)}

---

QLCP = QLCG + QMF/QNF

QLCS = QLCG + QMS/QNS

---

PRINT

N, A(N), B(N), QNFP, QNPS1, QNPS2, QNPS, CP(J) for each N

QLCP, QLCS, QMF, QNS, QMS, QAF for N = NB

each N QNF, X(N), R(N), ALP(N)

## PREPARATION OF DATA

The GE-415 FORTRAN Routine 4831-1108 has the capability of making a series of consecutive runs. The input for this routine consists of a Production Control Card, Title Card, two cards of initial data, and one data table.

### Production Control Card

The first card presented for each production run must be the Production Control Card, which specifies in column 10 the number of runs contained within the production run.

### Title Card

The title card is a card which lets the user identify the runs. The computer will print whatever is punched on this card. The title card must be present in every run even if it is blank.

### Data Cards

There are two input data cards. Card 1 contains NB, the number of cards contained in the data table, and IPRT, a print option. Card 2 contains V, GAM, Q, QL, QLCG, and QM. The definitions of the above symbols are given in the section on definition of symbols.

### Data Table

A data table must be presented for each run in a production run. The number of cards in the data table is equal to NB which is listed on the first data card of each run. The values given are X, R, and ALP. The definitions of the values contained in the data table are given in the section on definition of symbols.

### Data Presentation

The form of the data to be presented for Computer Routine 4831-1108 must be submitted as shown below.

Production Control Card | Format (8I10)

NRUNS

Title Card | Format (80H)

First Data Card | Format (8I10)

NB
IPRT

Second Data Card | Format (8E10.4)

V
GAM
Q
QL
QLCG
QM

Data Table | Format (8E10.4)

X(N)
R(N)
ALP(N)

All of the above data must be presented for the first of a series of consecutive runs. For each subsequent run, omit the Production Control Card.

The deck for a production run is prepared by simply stacking the runs consecutively with the table being the last card of a run and the title card as the first card of the next run.

# FORTRAN PROGRAM LISTING

```
      .JOB,TATE       48?2
      .PX
      .FORTRAN,OPT
              ENDOPT
$       SETMEM  00000000
C     PROGRAM NUMBER - 4831-1108
C     PROGRAM NAME - LOCAL ANGLE-OF-ATTACK AERODYNAMICS PROGRAM
      DIMENSION X(250),R(250),ALP(250),B(250),XB(250),YB(250),ZB(250)
      DIMENSION PN(250),A(250),CN(250),XBN(250),YBN(250),ZBN(250),CP(50)
      CN(1) = 0.0
      B(1) = 0.0
      A(1) = 0.0
      PRINT 98
      IRUNS = 0
      READ 500,NRUNS
      PRINT 104,NRUNS
  104 FORMAT (10X,37HTHE NUMBER OF RUNS TO BE PROCESSED IS,I3)
    1 PRINT 98
      IRUNS =  IRUNS + 1
      PRINT 600
      READ 1111
      PRINT 1111
 1111 FORMAT (80H
     1                                                                )
      PRINT 502
      READ 500,NB,IPRT
      PRINT 101,NB,IPRT
  101 FORMAT (10X,4HNB  ,I5,10X,4HIPRT,I5)
      READ 501,V,GAM,Q,QL,QLCG,QM
      PRINT 102,V,GAM,Q,QL,QLCG,QM
  102 FORMAT (10X,4HV   ,F16.8,5X,4HGAM ,F16.8,5X,4HQ   ,E16.8/
     1        10X,4HQL  ,F16.8,5X,4HQLCG,F16.8,5X,4HQM  ,E16.8)
      DO 2 N = 1,NB
      READ 501,X(N),R(N),ALP(N)
    2 PRINT 103,X(N),R(N),ALP(N)
  103 FORMAT (10X,4HX   ,F16.8,5X4HR   ,F16.8,5X4HALP ,F16.8)
      PRINT 98
      PRINT 600
  600 FORMAT (20X53HLOCAL ANGLE-OF-ATTACK AERODYNAMICS PROGRAM, 4831-110
     18//)
      PI = 3.1415926536
      QNF = QMF = QAF = QNS = QMS = QAS = 0.0
      BET = SQRT(QM**2-1.0)
      NBM = NB - 1
      GA = GAM/(GAM-1.0)
      DO 100 N = 2,NBM
      DRDX = (R(N)-R(N-1))/(X(N)-X(N-1))
      PNIM = X(N)/(BET*R(N))
      PN(1) = PNIM
      PSIM = SQRT(PNIM**2-1.0)
      DO 10 I = 2,N
      PN(I) = (X(N)-(X(I)-BET*R(I)))/(BET*R(N))
      PSI = SQRT(PN(I)**2-1.0)
      XBN(I) = ALOG(PN(I)+PSI)-ALOG(PNIM+PSIM)
      YBN(I) = PSI-PSIM
```

```
      ZBN(I) = PN(I)*PSI-PNIM*PSIM
      PNIM = PN(I)
      PSIM = PSI
      IF (IPRT .EQ. 0) GO TO 10
      PRINT 1001,XBN(I),YBN(I),ZBN(I)
 1001 FORMAT (5X,3HXBN,E16.8,5X,3HYBN,E16.8,5X,3HZBN,E16.8/)
   10 CONTINUE
      SA = SB = 0.0
      NM = N - 1
      DO 20 I = 2,NM
      SA = SA+A(I)*(BET*YBN(I)+DRDX*XBN(I))
      SB = SB+B(I)*(2.0*DRDX*YBN(I)+BET*(XBN(I)+ZBN(I)))
      IF (IPRT .EQ. 0) GO TO 20
      PRINT 1002,SA,SB
 1002 FORMAT (5X,3HSA ,E16.8,5X,3HSB ,E16.8/)
   20 CONTINUE
      A(N) = -(DRDX*V+SA)/(BET*YBN(N)+DRDX*XBN(N))
      B(N) = -(2.0*V*ALP(N)+BET*SB)/(2.0*BET*DRDX*YBN(N)+BET**2
     1*(XBN(N)+ZBN(N)))
      DO 30 I = 2,N
      CN(I) = CN(I-1)+(B(I)-B(I-1))*PN(I-1)
      IF (IPRT .EQ. 0) GO TO 30
      PRINT 5055
 5055 FORMAT (10X,2HCN/)
      PRINT 201,CN(1),CN(2)
   30 CONTINUE
      SAX = SAR = SBX = SBR = SBT = 0.0
      DO 40 I = 2,N
      SAX = SAX+A(I)*XBN(I)
      SAR = SAR-BET*A(I)*YBN(I)
      SBX = SBX-BET*B(I)*YBN(I)
      SBR = SBR+0.5*BET**2*B(I)*(XBN(I)+ZBN(I))
      SBT = SBT+0.5*BET**2*(2.0*CN(I)*YBN(I)-B(I)*(XBN(I)+ZBN(I)))
      IF (IPRT .EQ. 0) GO TO 40
      PRINT 1003,SAX,SAR,SBX,SBR,SBT
 1003 FORMAT (5X,3HSAX,E16.8,5X,3HSAR,E16.8,5X,3HSBX,E16.8,
     1          5X,3HSBY,E16.8,5X,3HSBT,E16.8/)
   40 CONTINUE
      DO 50 J = 1,50
      U = V+SAX+SBX*COS(PI*(0.02*J-0.01))
      VS = SAR+(V*ALP(N)+SBR)*COS(PI*(0.02*J-0.01))
      W = (SBT-V*ALP(N))*SIN(PI*(0.02*J-0.01))
      CP(J) = (2.0/(GAM*QM**2))*((1.0+((GAM-1.0)/2.0)*QM**2*
     1(1.0-((U**2+VS**2+W**2)/V**2)))**GA-1.0)
      IF (IPRT .EQ. 0) GO TO 50
      PRINT 777,U,W,VS
  777 FORMAT (10X,3HU  ,E16.8,5X,3HW  ,E16.8,5X,3HVS ,E16.8/)
   50 CONTINUE
      G1 = 0.25*((R(N+1)+R(N))**2-(R(N)+R(N-1))**2)*Q
      G2 = -2.0*Q*R(N)
      SCP = SCPC = 0.0
      DO 60 J = 1,50
      SCP = SCP+0.02*PI*CP(J)
   60 SCPC = SCPC+0.02*PI*CP(J)*COS(PI*(0.02*J-0.01))
      AN = G1*SCP
```

```
      QNFP = G2*SCPC
      QNPS1 = 4.0*PI*Q*ALP(N)*R(N)*DRDX
      QNPS2 = 2.0*PI*Q*R(N)**2*((ALP(N+1)-ALP(N-1))/(X(N+1)-X(N-1)))
      QNPS = QNPS1+QNPS2
      QAF = QAF+AN
      QNF = QNF+0.5*QNFP*(X(N+1)-X(N-1))
      QMF = QMF-0.5*QNFP*(X(N)-QL+QLCG)*(X(N+1)-X(N-1))
      QNS = QNS+0.5*QNPS*(X(N+1)-X(N-1))
      QMS = QMS-0.5*QNPS*(X(N)-QL+QLCG)*(X(N+1)-X(N-1))
      PRINT 200,N
  200 FORMAT (63X,3HN =,I3//)
      PRINT 2011
 2011 FORMAT (10X,2HCP/)
      PRINT 201,CP
      PRINT 502
  201 FORMAT (10E13.5)
      PRINT 202,QNFP,QNPS1,QNPS2,QNPS
  202 FORMAT (10X,5HQNFP ,E16.8,5X,5HQNPS1,E16.8,5X,5HQNPS2,E16.8,5X,5HQ
     1NPS ,E16.8//)
      PRINT 2022,A(N),B(N),QNF
 2022 FORMAT (10X,5HA    ,E16.8,5X,5HB    ,E16.8,5X,5HQNF  ,E16.8//)
      PRINT 2323,X(N),R(N),ALP(N)
 2323 FORMAT (10X,5HX    ,E16.8,5X,5HR    ,E16.8,5X,5HALP  ,E16.8//)
      IF (IPRT .EQ. 0) GO TO 100
      PRINT 203,QAF,QMF,QNS,QMS
  203 FORMAT (10X,5HQAF  ,E16.8,5X,5HQMF  ,E16.8,5X,5HQNS  ,E16.8,5X,5HQ
     1MS  ,E16.8//)
  100 CONTINUE
      QLCP = QLCG+(QMF/QNF)
      QLCS = QLCG+(QMS/QNS)
      PRINT 203,QAF,QMF,QNS,QMS
      PRINT 204,QLCP,QLCS
  204 FORMAT (10X,5HQLCP ,E16.8,5X,5HQLCS ,E16.8//)
  500 FORMAT (8I10)
   98 FORMAT (1H1)
  501 FORMAT (8E10.4)
  502 FORMAT (//)
      IF (IRUNS - NRUNS) 1,99,99
   99 STOP 1
      END
        .EOJ
```

SAMPLE INPUT

THE NUMBER OF RUNS TO BE PROCESSED IS 1

LOCAL ANGLE-OF-ATTACK AERODYNAMICS PROGRAM, 4831-110[illegible]

SATURN V ALPHA 8 DEG QM 1.20

| | | | | | |
|---|---|---|---|---|---|
| NB | 69 | IPRT | 0 | | |
| V | 0.16480000E+04 | GAM | 0.14000000E+01 | Q | 0.76000000E+03 |
| CL | 0.34834300E+03 | QLCG | 0.10000000E+03 | QM | 0.12000000E+01 |
| X | 0.00000000E+00 | R | 0.00000000E+00 | ALP | 0.13940000E+00 |
| X | 0.15410000E+01 | R | 0.54200000E+00 | ALP | 0.13940000E+00 |
| X | 0.30830000E+01 | R | 0.10830000E+01 | ALP | 0.13940000E+00 |
| X | 0.35000000E+01 | R | 0.10830000E+01 | ALP | 0.13940000E+00 |
| X | 0.40000000E+01 | R | 0.10830000E+01 | ALP | 0.13940000E+00 |
| X | 0.12000000E+02 | R | 0.10830000E+01 | ALP | 0.13940000E+00 |
| X | 0.21480000E+02 | R | 0.10830000E+01 | ALP | 0.13940000E+00 |
| X | 0.21670000E+02 | R | 0.12250000E+01 | ALP | 0.13940000E+00 |
| X | 0.22430000E+02 | R | 0.17660000E+01 | ALP | 0.13940000E+00 |
| X | 0.23380000E+02 | R | 0.25000000E+01 | ALP | 0.13940000E+00 |
| X | 0.24000000E+02 | R | 0.25000000E+01 | ALP | 0.13940000E+00 |
| X | 0.29210000E+02 | R | 0.25000000E+01 | ALP | 0.13940000E+00 |
| X | 0.30154000E+02 | R | 0.28920000E+01 | ALP | 0.13940000E+00 |
| X | 0.33930000E+02 | R | 0.44570000E+01 | ALP | 0.13940000E+00 |
| X | 0.38650000E+02 | R | 0.64150000E+01 | ALP | 0.13940000E+00 |
| X | 0.39000000E+02 | R | 0.64150000E+01 | ALP | 0.13940000E+00 |
| X | 0.44000000E+02 | R | 0.64150000E+01 | ALP | 0.13940000E+00 |
| X | 0.49000000E+02 | R | 0.64150000E+01 | ALP | 0.13940000E+00 |
| X | 0.53853000E+02 | R | 0.64150000E+01 | ALP | 0.13940000E+00 |
| X | 0.54000000E+02 | R | 0.64380000E+01 | ALP | 0.13940000E+00 |
| X | 0.55000000E+02 | R | 0.66960000E+01 | ALP | 0.13940000E+00 |
| X | 0.57000000E+02 | R | 0.69150000E+01 | ALP | 0.13940000E+00 |
| X | 0.60000000E+02 | R | 0.73850000E+01 | ALP | 0.13940000E+00 |
| X | 0.64000000E+02 | R | 0.80160000E+01 | ALP | 0.13940000E+00 |
| X | 0.68000000E+02 | R | 0.86470000E+01 | ALP | 0.13940000E+00 |
| X | 0.72000000E+02 | R | 0.92790000E+01 | ALP | 0.13940000E+00 |
| X | 0.76000000E+02 | R | 0.99100000E+01 | ALP | 0.13940000E+00 |
| X | 0.80000000E+02 | R | 0.10541000E+02 | ALP | 0.13940000E+00 |
| X | 0.81850000E+02 | R | 0.10833000E+02 | ALP | 0.13940000E+00 |
| X | 0.83000000E+02 | R | 0.10833000E+02 | ALP | 0.13940000E+00 |
| X | 0.93000000E+02 | R | 0.10833000E+02 | ALP | 0.13940000E+00 |
| X | 0.98000000E+02 | R | 0.10833000E+02 | ALP | 0.13940000E+00 |
| X | 0.10300000E+03 | R | 0.10833000E+02 | ALP | 0.13940000E+00 |
| X | 0.10800000E+03 | R | 0.10833000E+02 | ALP | 0.13940000E+00 |
| X | 0.11300000E+03 | R | 0.10833000E+02 | ALP | 0.13940000E+00 |
| X | 0.11700000E+03 | R | 0.10833000E+02 | ALP | 0.13940000E+00 |
| X | 0.12100000E+03 | R | 0.10833000E+02 | ALP | 0.13940000E+00 |
| X | 0.12451800E+03 | R | 0.10833000E+02 | ALP | 0.13940000E+00 |
| X | 0.12501800E+03 | R | 0.10833000E+02 | ALP | 0.13940000E+00 |
| X | 0.12851800E+03 | R | 0.12028000E+02 | ALP | 0.13940000E+00 |
| X | 0.13251800E+03 | R | 0.13224000E+02 | ALP | 0.13940000E+00 |
| X | 0.13651800E+03 | R | 0.14420000E+02 | ALP | 0.13940000E+00 |
| X | 0.14051800E+03 | R | 0.15615000E+02 | ALP | 0.13940000E+00 |
| X | 0.14347700E+03 | R | 0.16500000E+02 | ALP | 0.13940000E+00 |
| X | 0.14400000E+03 | R | 0.16500000E+02 | ALP | 0.13940000E+00 |
| X | 0.14700000E+03 | R | 0.16500000E+02 | ALP | 0.13940000E+00 |
| X | 0.15000000E+03 | R | 0.16500000E+02 | ALP | 0.13940000E+00 |
| X | 0.15500000E+03 | R | 0.16500000E+02 | ALP | 0.13940000E+00 |
| X | 0.16500000E+03 | R | 0.16500000E+02 | ALP | 0.13940000E+00 |
| X | 0.17500000E+03 | R | 0.16500000E+02 | ALP | 0.13940000E+00 |

| | | | | | |
|---|---|---|---|---|---|
| X | 0.19500000E+03 | R | 0.16500000E+02 | ALP | 0.13940000E+00 |
| X | 0.21000000E+03 | R | 0.16500000E+02 | ALP | 0.13940000E+00 |
| X | 0.23000000E+03 | R | 0.16500000E+02 | ALP | 0.13940000E+00 |
| X | 0.25000000E+03 | R | 0.16500000E+02 | ALP | 0.13940000E+00 |
| X | 0.28000000E+03 | R | 0.16500000E+02 | ALP | 0.13940000E+00 |
| X | 0.30000000E+03 | R | 0.16500000E+02 | ALP | 0.13940000E+00 |
| X | 0.31534300E+03 | R | 0.16500000E+02 | ALP | 0.13940000E+00 |
| X | 0.31539300E+03 | R | 0.16521000E+02 | ALP | 0.13940000E+00 |
| X | 0.31734300E+03 | R | 0.17340000E+02 | ALP | 0.13940000E+00 |
| X | 0.31934300E+03 | R | 0.18180000E+02 | ALP | 0.13940000E+00 |
| X | 0.32334300E+03 | R | 0.19860000E+02 | ALP | 0.13940000E+00 |
| X | 0.32734300E+03 | R | 0.21540000E+02 | ALP | 0.13940000E+00 |
| X | 0.33134300E+03 | R | 0.23220000E+02 | ALP | 0.13940000E+00 |
| X | 0.33534300E+03 | R | 0.24900000E+02 | ALP | 0.13940000E+00 |
| X | 0.33934300E+03 | R | 0.27300000E+02 | ALP | 0.13940000E+00 |
| X | 0.34334300E+03 | R | 0.28260000E+02 | ALP | 0.13940000E+00 |
| X | 0.34734300E+03 | R | 0.29940000E+02 | ALP | 0.13940000E+00 |
| X | 0.34834300E+03 | R | 0.30360000E+02 | ALP | 0.13940000E+00 |
| X | 0.34834300E+03 | R | 0.30360000E+02 | ALP | 0.13940000E+00 |

LOCAL ANGLE-OF-ATTACK AERODYNAMICS PROGRAM, 4831-1108

N = 2

CP

| | | | | | | | | | |
|---|---|---|---|---|---|---|---|---|---|
| 0.18343E+00 | 0.18358E+00 | 0.18388E+00 | 0.18435E+00 | 0.18499E+00 | 0.18582E+00 | 0.18686E+00 | 0.18814E+00 | 0.18968E+00 | 0.19151E+00 |
| 0.19365E+00 | 0.19615E+00 | 0.19902E+00 | 0.20230E+00 | 0.20602E+00 | 0.21021E+00 | 0.21488E+00 | 0.22007E+00 | 0.22578E+00 | 0.23204E+00 |
| 0.23885E+00 | 0.24622E+00 | 0.25414E+00 | 0.26260E+00 | 0.27159E+00 | 0.28108E+00 | 0.29105E+00 | 0.30146E+00 | 0.31225E+00 | 0.32338E+00 |
| 0.33480E+00 | 0.34642E+00 | 0.35819E+00 | 0.37001E+00 | 0.38181E+00 | 0.39350E+00 | 0.40499E+00 | 0.41618E+00 | 0.42697E+00 | 0.43728E+00 |
| 0.44700E+00 | 0.45605E+00 | 0.46434E+00 | 0.47180E+00 | 0.47833E+00 | 0.48388E+00 | 0.48840E+00 | 0.49182E+00 | 0.49413E+00 | 0.49529E+00 |

| | | | | | | | |
|---|---|---|---|---|---|---|---|
| QNFP | 0.20030030E+03 | QNPS1 | 0.25379448E+03 | QNPS2 | 0.00000000E+00 | QNPS | 0.25379448E+03 |
| A | 0.16487897E+03 | B | 0.42762123E+02 | QNF | 0.30876291E+03 | | |
| X | 0.15410000E+01 | R | 0.54200000E+00 | ALP | 0.13940000E+00 | | |

N = 3

CP

| | | | | | | | | | |
|---|---|---|---|---|---|---|---|---|---|
| 0.18260E+00 | 0.18275E+00 | 0.18305E+00 | 0.18351E+00 | 0.18415E+00 | 0.18497E+00 | 0.18601E+00 | 0.18728E+00 | 0.18881E+00 | 0.19063E+00 |
| 0.19277E+00 | 0.19525E+00 | 0.19811E+00 | 0.20138E+00 | 0.20509E+00 | 0.20926E+00 | 0.21392E+00 | 0.21909E+00 | 0.22480E+00 | 0.23104E+00 |
| 0.23784E+00 | 0.24519E+00 | 0.25310E+00 | 0.26155E+00 | 0.27052E+00 | 0.28001E+00 | 0.28996E+00 | 0.30036E+00 | 0.31114E+00 | 0.32226E+00 |
| 0.33367E+00 | 0.34528E+00 | 0.35704E+00 | 0.36886E+00 | 0.38065E+00 | 0.39233E+00 | 0.40381E+00 | 0.41500E+00 | 0.42579E+00 | 0.43609E+00 |
| 0.44581E+00 | 0.45486E+00 | 0.46315E+00 | 0.47060E+00 | 0.47713E+00 | 0.48268E+00 | 0.48719E+00 | 0.49062E+00 | 0.49293E+00 | 0.49408E+00 |

| | | | | | | | |
|---|---|---|---|---|---|---|---|
| QNFP | 0.39974312E+03 | QNPS1 | 0.50585678E+03 | QNPS2 | 0.00000000E+00 | QNPS | 0.50585678E+03 |
| A | 0.16405426E+03 | B | 0.42594429E+02 | QNF | 0.70031130E+03 | | |
| X | 0.30830000E+01 | R | 0.10830000E+01 | ALP | 0.13940000E+00 | | |

N = 4

CP

| | | | | | | | | | |
|---|---|---|---|---|---|---|---|---|---|
| -.45665E+00 | -.45651E+00 | -.45623E+00 | -.45581E+00 | -.45522E+00 | -.45447E+00 | -.45354E+00 | -.45240E+00 | -.45105E+00 | -.44945E+00 |
| -.44760E+00 | -.44546E+00 | -.44301E+00 | -.44024E+00 | -.43711E+00 | -.43362E+00 | -.42973E+00 | -.42543E+00 | -.42070E+00 | -.41554E+00 |
| -.40994E+00 | -.40389E+00 | -.39739E+00 | -.39044E+00 | -.38306E+00 | -.37526E+00 | -.36706E+00 | -.35849E+00 | -.34959E+00 | -.34038E+00 |
| -.33093E+00 | -.32128E+00 | -.31148E+00 | -.30161E+00 | -.29174E+00 | -.28193E+00 | -.27226E+00 | -.26283E+00 | -.25369E+00 | -.24495E+00 |
| -.23669E+00 | -.22898E+00 | -.22190E+00 | -.21552E+00 | -.20992E+00 | -.20516E+00 | -.20128E+00 | -.19833E+00 | -.19635E+00 | -.19535E+00 |

| | | | | | | | |
|---|---|---|---|---|---|---|---|
| QNFP | 0.10852062E+05 | QNPS1 | 0.16741228E+05 | QNPS2 | 0.00000000E+00 | QNPS | 0.16741228E+05 |
| A | 0.41649365E+03 | B | 0.58611659E+02 | QNF | 0.40358296E+06 | | |
| X | 0.34734300E+03 | R | 0.29940000E+02 | ALP | 0.13940000E+00 | | |

N = 68

CP

| | | | | | | | | | |
|---|---|---|---|---|---|---|---|---|---|
| 0.33144E+00 | 0.33161E+00 | 0.33195E+00 | 0.33246E+00 | 0.33317E+00 | 0.33408E+00 | 0.33522E+00 | 0.33661E+00 | 0.33826E+00 | 0.34021E+00 |
| 0.34249E+00 | 0.34512E+00 | 0.34812E+00 | 0.35154E+00 | 0.35538E+00 | 0.35969E+00 | 0.36448E+00 | 0.36976E+00 | 0.37556E+00 | 0.38189E+00 |
| 0.38875E+00 | 0.39614E+00 | 0.40406E+00 | 0.41250E+00 | 0.42144E+00 | 0.43085E+00 | 0.44071E+00 | 0.45098E+00 | 0.46161E+00 | 0.47254E+00 |
| 0.48373E+00 | 0.49511E+00 | 0.50660E+00 | 0.51813E+00 | 0.52961E+00 | 0.54097E+00 | 0.55211E+00 | 0.56295E+00 | 0.57340E+00 | 0.58336E+00 |
| 0.59275E+00 | 0.60148E+00 | 0.60946E+00 | 0.61664E+00 | 0.62292E+00 | 0.62826E+00 | 0.63260E+00 | 0.63589E+00 | 0.63811E+00 | 0.63922E+00 |

| | | | | | | | |
|---|---|---|---|---|---|---|---|
| QNFP | 0.11086187E+05 | QNPS1 | 0.16976075E+05 | QNPS2 | 0.00000000E+00 | QNPS | 0.16976075E+05 |
| A | 0.35225677E+03 | B | 0.67544533E+02 | QNF | 0.40892606E+06 | | |
| X | 0.34834300E+03 | R | 0.30360000E+02 | ALP | 0.13940000E+00 | | |
| QAF | 0.97455709E+06 | QMF | 0.10020301E+08 | QNS | 0.61063131E+06 | QMS | -.10358953E+08 |
| QLCP | 0.12450394E+03 | QLCS | 0.83035667E+02 | | | | |

## APPENDIX E

The computation of the structural flexing of the vehicle is described here. The necessary equations are derived in section III. Key terms are defined and the significant equations of the numerical analysis are given. Also described are the flow diagrams of the numerical analysis and a listing of the computer programs. Sample input and output data are included.

This computer program determines the parameters AKBB, BKBB, PKB, QKB, PK, QK which must be evaluated for the following equations:

$$\frac{d^2yk}{dx^2} = AKBB\ \alpha_r + BKBB\ \ddot{w}$$

$$\frac{dyk}{dx} = PKB\ \alpha_r + QKB\ \ddot{w}$$

$$yk = PK\ \alpha_r + QK\ \ddot{w}$$

The input for this program consists of:

- Rigid body normal force distribution
- Incremental aerodynamic loading caused by body flexing due to aerodynamic forces
- Incremental aerodynamic loading caused by body flexing due to normal acceleration
- Body mass distribution
- Body stiffness distribution

This computer program is based on simple beam theory. It is used in conjunction with the flexible body aerodynamic program in an iterative procedure to establish the deflections and the aerodynamic characteristics of a flexible body.

## DEFINITION OF SYMBOLS

| Symbol | Definition |
|---|---|
| XNPRA | Derivative of rigid body local normal force distribution (lb/ft rad) |
| XNPKA | Derivative of incremental local normal force distribution caused by bending due to aerodynamic forces (lb/ft rad) |
| XNPKW | Derivative of incremental local normal force distribution caused by bending due to normal acceleration ($sec^2$)(lb $sec^2/ft^2$) |
| XJ | Distance from nose, where the three parameters above are input, at station J (ft) |
| XMP | Body mass distribution (slug /ft) |
| EI | Body stiffness ($ft^2$ lb) |
| XL | Distance from nose, where the two above parameters are input, at station L (ft) |
| X | Distance from nose (ft) |
| DX | Interpolation parameter |
| DJ | Interpolation parameter |
| DL | Interpolation parameter |
| XNPRAN | Value of XNPRA at station XN (lb/ft rad) |
| XNPKAN | Value of XNPKA at station XN (lb/ft rad) |
| XNPKWN | Value of XNPKW at station XN (lb $sec^2/ft^2$) |
| XMPN | Value of XMP at station XN (slug /ft) |
| EIN | Value of EI at station XN ($ft^2$ lb) |
| X[illegible] | Ratio of X(N)/X(N-1) |
| X[illegible] | Distance from nose at station N (ft) |
| AKBB | Partial derivative of $d^2yk/dx^2$ with respect to $\alpha_r$ (1/ft) |
| BKBB | Partial derivative of $d^2yk/dx^2$ with respect to $\ddot{w}$ ($sec^2/ft^2$) |
| GAK | Integration constant |
| HAK | Integration constant (ft) |
| GBK | Integration constant (lb/$sec^2$) |
| HBK | Integration constant (1/$sec^2$) |
| PKB | Partial derivative of dyk/dx with respect to $\alpha_r$ |
| PK | Partial derivative of yk with respect to $\alpha_r$ (ft) |
| QKB | Partial derivative of dyk/dx with respect to $\ddot{w}$ (ft/$sec^2$) |
| QK | Partial derivative of yk with respect to $\ddot{w}$ (1/$sec^2$) |

## SOLUTION OF EQUATIONS

1. $DJ = \dfrac{X(N) - XJ(J-1)}{XJ(J) - XJ(J-1)}$

2. $DL = \dfrac{X(N) - XL(L-1)}{XL(L) - XJ(L-1)}$

3. $XNPRAN = (1-DJ)\{XNPRA(J-1)\} + DJ\{XNPRA(J)\}$

4. $XNPKAN = (1-DJ)\{XNPKA(J-1)\} + DJ\{XNPKA(J)\}$

5. $XNPKWN = (1-DJ)\{XNPKW(J-1)\} + DJ\{XNPKW(J)\}$

6. $XMPN = (1-DL)\{XMP(L-1)\}+ DL\{XMP(L)\}$

7. $EIN = (1-DL)\{EI(L-1)\} + DL\{EI(L)\}$

8. $EINM = EIN$

9. $GAK = \dfrac{(XIAXK)(XIMK) - (XIAK)(XIMLK)}{XIMLK^2 - (XIMK)(XIMLLK)}$

10. $HAK = \dfrac{(XIAK)(XIMLLK) - (XIAXK)(XIMLK)}{XIMLK^2 - (XIMK)(XIMLLK)}$

11. $GBK = \dfrac{(XIBXK)(XIMK) - (XIBK)(XIMLK)}{XIMLK^2 - (XIMK)(XIMLLK)}$

12. $HBK = \dfrac{(XIBK)(XIMLLK) - (XIBXK)(XIMLK)}{XIMLK^2 - (XIMK)(XIMLLK)}$

13. $PKB(N) = AKB(N) + GAK$

14. PK(N) = AK(N) + X(N) GAK + HAK

15. QKB(N) = BKB(N) + GBK

16. QK(N) = BK(N) + X(N) GBK + HBK

COMPUTER FLOW DIAGRAM

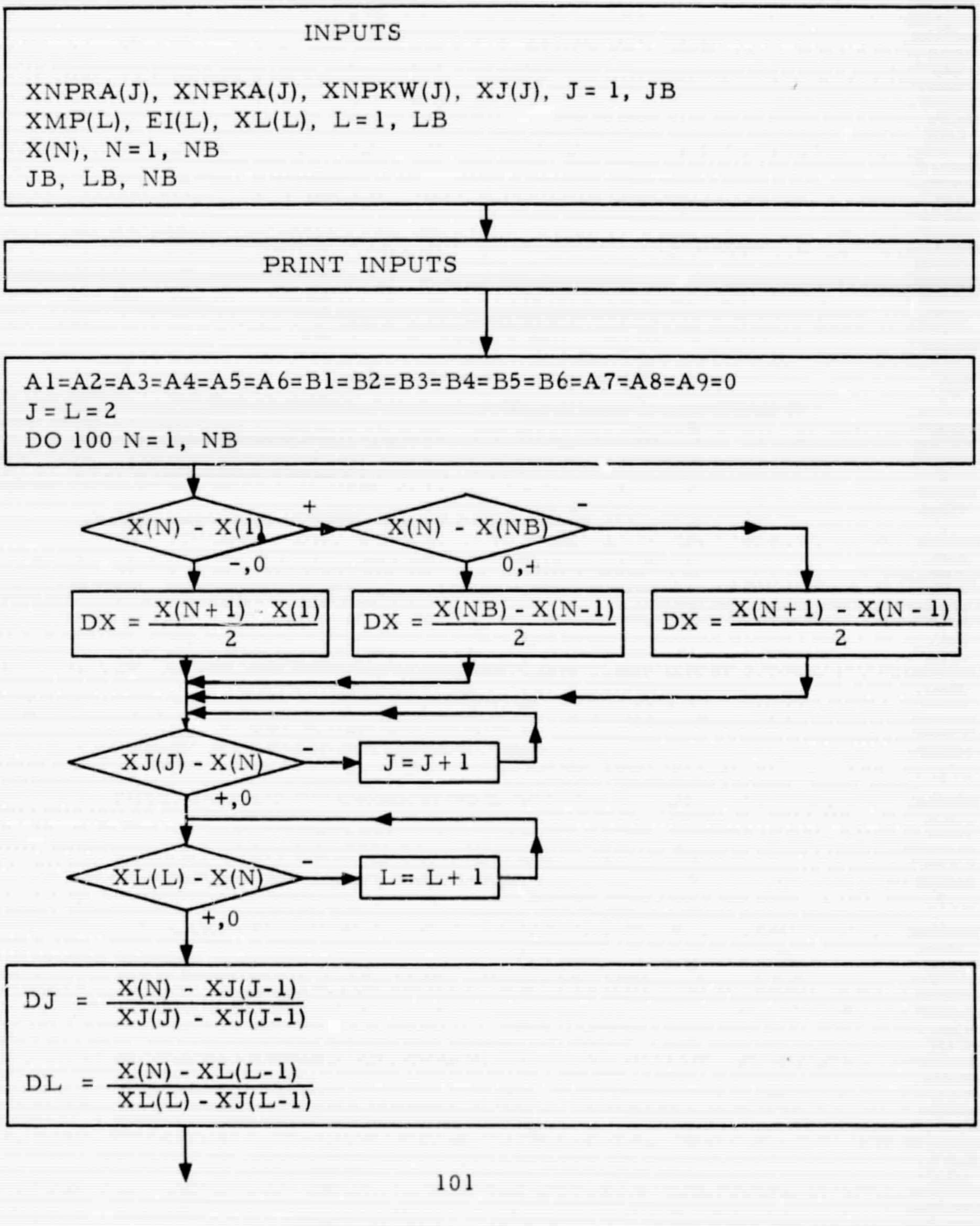

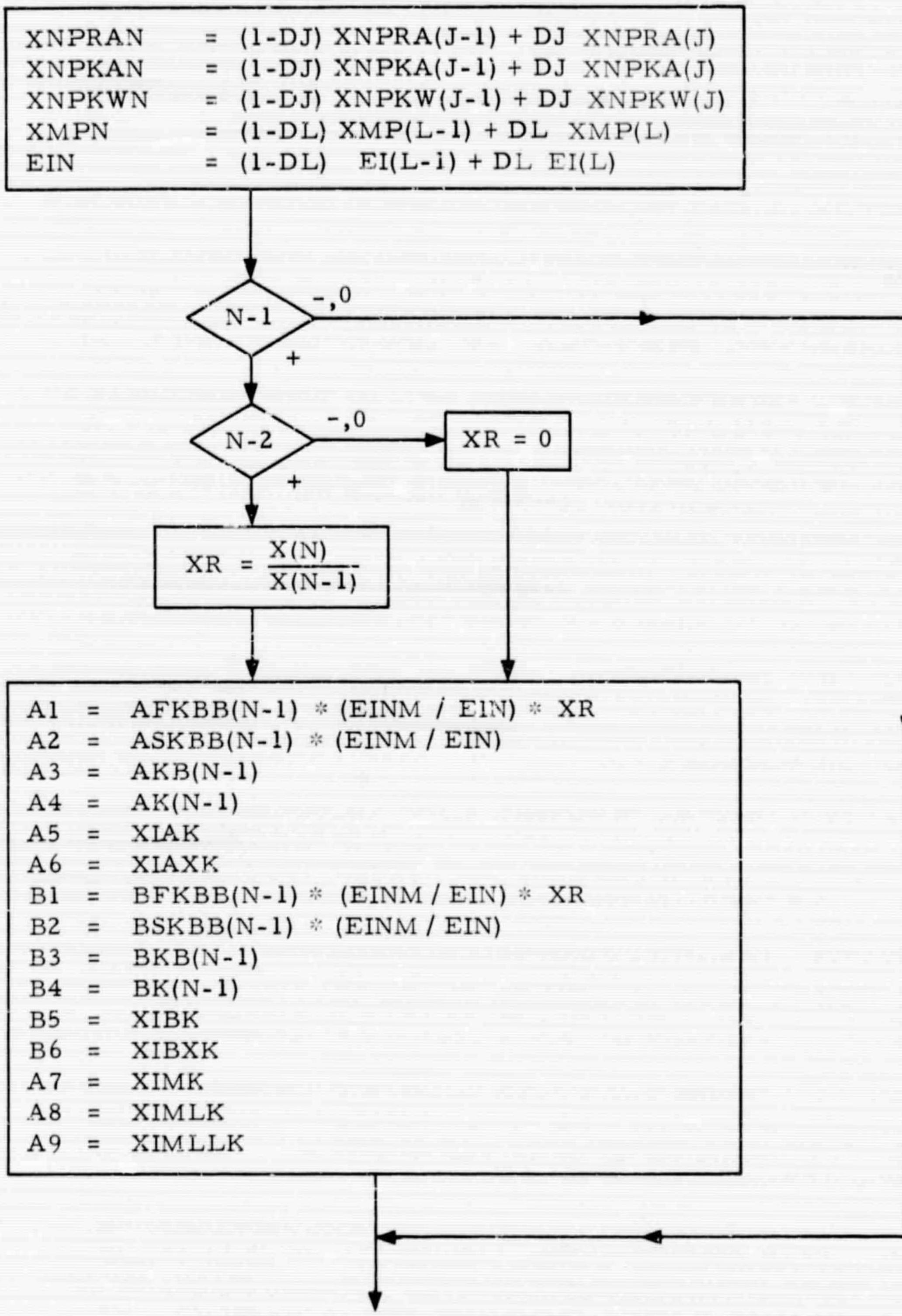

XNPRAN = (1-DJ) XNPRA(J-1) + DJ XNPRA(J)
XNPKAN = (1-DJ) XNPKA(J-1) + DJ XNPKA(J)
XNPKWN = (1-DJ) XNPKW(J-1) + DJ XNPKW(J)
XMPN = (1-DL) XMP(L-1) + DL XMP(L)
EIN = (1-DL) EI(L-1) + DL EI(L)
N-1
-,0
+
N-2
-,0
XR = 0
+
XR = X(N) / X(N-1)
A1 = AFKBB(N-1) * (EINM / EIN) * XR
A2 = ASKBB(N-1) * (EINM / EIN)
A3 = AKB(N-1)
A4 = AK(N-1)
A5 = XIAK
A6 = XIAXK
B1 = BFKBB(N-1) * (EINM / EIN) * XR
B2 = BSKBB(N-1) * (EINM / EIN)
B3 = BKB(N-1)
B4 = BK(N-1)
B5 = XIBK
B6 = XIBXK
A7 = XIMK
A8 = XIMLK
A9 = XIMLLK

```
AFKBB(N)    =  A1 - (X(N)/EIN) (XNPRAN + XNPKAN) DX
ASKBB(N)    =  A2 + (X(N)/EIN) (XNPRAN + XNPKAN) DX
AKBB(N)     =  AFKBB(N) + ASKBB(N)
BFKBB(N)    =  B1 + (X(N)/EIN) (XMPN - XNPKWN) DX
BSKBB(N)    =  B2 - (X(N)/EIN) (XMPN - XNPKWN) DX
BKBB(N)     =  BFKBB(N) + BSKBB(N)
AKB(N)      =  A3 + AKBB(N) * DX
BKB(N)      =  B3 + BKBB(N) * DX
AK(N)       =  A4 + AKB(N) * DX
BK(N)       =  B4 + BKB(N) * DX
```

```
XIAK        =  A5 + XMPN * AK(N) DX
XIAXK       =  A6 + XMPN * AK(N) * X(N) * DX
XIBK        =  B5 + XMPN * BK(N) * DX
XIBXK       =  B6 + XMPN * BK(N) * X(N) * DX
XIMK        =  A7 + XMPN * DX
XIMLK       =  A8 + XMPN * X(N) * DX
XIMLLK      =  A9 + XMPN * X(N)^2 * DX
EINM        =  EIN
```

```
                     PRINT

N, X(N), L, J, XNPRAN, XNPKAN, XNPKWN, XMPN, EIN,
AFKBB(N), ASKBB(N), AKBB(N), BFKBB(N), BSKBB(N),
BKBB(N), AKB(N), BKB(N), AK(N), BK(N), XIAK
XIAXK, XIBK, XIBXK, XIMK, XIMLK, XIMLLK
100 CONTINUE
```

```
GAK  =  [XIAXK * XIMK - XIAK * XIMLK] / [XIMLK^2 - XIMK * XIMLLK]

HAK  =  [XIAK * XIMLLK - XIAXK * XIMLK] / [XIMLK^2 - XIMK *
         XIMLLK]

GBK  =  [XIBXK * XIMK - XIBK * XIMLK] / [XIMLK^2 - XIMK * XIMLLK]

HBK  =  [XIBK * XIMLLK - XIBXK * XIMLK] / [XIMLK^2 - XIMK *
         XIMLLK]
```

```
PRINT

GAK, HAK, GBK, HBK
```

```
DO 1000 N  =  1, NB
PKB(N)     =  AKB(N) + GAK
PK(N)      =  AK(N) + X(N) * GAK + HAK
QKB(N)     =  BKB(N) + GBK
QK(N)      =  BK(N) + X(N) * GBK + HBK
```

```
PRINT

X(N), PKB(N), PK(N), QKB(N), QK(N), N = 1, KB

1000 CONTINUE
```

## PREPARATION OF DATA

The GE-415 FORTRAN Routine 4831-1109 has the capability of making a series of consecutive runs. The input for this routine consists of a Production Control Card, Title Card, Control Card, and three data tables.

### Production Control Card

The first card presented for each production run must be the Production Control Card, which specifies in column 10 the number of runs contained within the production run.

### Title Card

The title card is a card which lets the user identify the runs. The computer will print whatever is punched on this card. The title card must be present in every run even if it is blank.

### Control Card

This card contains the values of JB, LB, and NB which determine the number of cards in the three data tables. JB = number of cards in data table 1; LB = number of cards in data table 2; NB = number of cards in data table 3.

### Data Tables

There are three input data tables. Data Table 1 contains XNPRA(J), XNPKA(J), XNPKW(J), and XJ(J). Data Table 2 contains XMP(L), EI(L), and XL(L). Data Table 3 contains X(N). The definitions of the above symbols are given in the section on definition of symbols.

### Data Presentation

The form of the data to be presented for Computer Routine 4831-1109 must be submitted as shown below:

Production Control Card Format (8I10)

NRUNS

| | |
|---|---|
| Title Card | Format (80H) |
| Control Card | Format (8I10) |
| JB | |
| LB | |
| NB | |
| First Data Table | Format (8E10. 4) |
| XNPRA(J) | |
| XNPKA(J) | |
| XNPKW(J) | |
| XJ(J) | |
| Second Data Table | Format (8E10. 4) |
| XMP(L) | |
| EI(L) | |
| XL(L) | |
| Third Data Table | Format (8E10. 4) |
| X(N) | |

All of the above data must be presented for the first of a series of consecutive runs. For each subsequent run, omit the Production Control Card.

The deck for a production run is prepared by simply stacking the runs consecutively.

# FORTRAN PROGRAM LISTING

```
          .JOB,TATE       4832
          .FORTRAN,OPT
                    ENDOPT
C       PROGRAM NUMBER - 4831-1109
C       PROGRAM NAME - LOCAL VEHICLE DEFLECTION PROGRAM
        DIMENSION XNPRA(100),XNPKA(100),XNPKW(100),XJ(100),XMP(100)
        DIMENSION X(100),AFKBB(100),ASKBB(100),AKBB(100),BFKBB(100)
        DIMENSION BSKBB(100),BKBB(100),AKB(100),BKB(100),AK(100),BK(100)
        DIMENSION PK(100),QKB(100),QK(100),PKB(100),XL(100),EI(100)
        PRINT 98
        IRUNS = 0
        READ 500,NRUNS
        PRINT 104,NRUNS
  104   FORMAT (10X37HTHE NUMBER OF RUNS TO BE PROCESSED IS,I5)
    1   PRINT 98
        IRUNS = IRUNS + 1
        PRINT 600
  600   FORMAT (20X43HLOCAL VEHICLE DEFLECTION PROGRAM, 4831-1109//)
        READ 1111
        PRINT 1111
 1111   FORMAT (80H
     1                                                                  )
        PRINT 97
        READ 500,JB,LB,NB
        PRINT 101,JB,LB,NB
  101   FORMAT (10X2HJB,I10,5X2HLB,I10,5X2HNB,I10)
        DO 2 J = 1,JB
        READ 501,XNPRA(J),XNPKA(J),XNPKW(J),XJ(J)
    2   PRINT 102,XNPRA(J),XNPKA(J),XNPKW(J),XJ(J)
  102   FORMAT (10X5HXNPRA,F16.8,5X5HXNPKA,E16.8,5X5HXNPKW,F16.8,
     1          5X5HXJ   ,F16.8)
        DO 3 L = 1,LB
        READ 501,XMP(L),EI(L),XL(L)
    3   PRINT 103,XMP(L),EI(L),XL(L)
  103   FORMAT (10X5HXMP  ,F16.8,5X5HEI   ,E16.8,5X5HXL   ,E16.8)
        DO 4 N = 1,NB
        READ 501,X(N)
    4   PRINT 105,X(N)
  105   FORMAT (10X5HX    ,F16.8)
        PRINT 98
        PRINT 600
        A1 = A2 = A3 = A4 = A5 = A6 = B1 = B2 = B3 = B4 = B5 = B6 = 0.0
        A7 = A8 = A9 = 0.0
        J = 2
        L = 2
        DO 100 N = 1,NB
        IF (X(N)-X(1) .GT. 0.0) GO TO 5
        DX = (X(N+1)-X(1))/2.0
        GO TO 7
    5   IF (X(N)-X(NB) .LT. 0.0) GO TO 6
        DX = (X(NB)-X(N-1))/2.0
        GO TO 7
    6   DX = (X(N+1)-X(N-1))/2.0
    7   IF (XJ(J)-X(N) .GE. 0.0) GO TO 9
        J = J + 1
```

```
      GO TO 7
    9 IF (XL(L)-X(N) .GE. 0.0) GO TO 11
      L = L + 1
      GO TO 9
   11 DJ = (X(N)-XJ(J-1))/(XJ(J)-XJ(J-1))
      DL = (X(N)-XL(L-1))/(XL(L)-XJ(L-1))
      XNPRAN = (1.0-DJ)*XNPRA(J-1)+DJ*XNPRA(J)
      XNPKAN = (1.0-DJ)*XNPKA(J-1)+DJ*XNPKA(J)
      XNPKWN = (1.0-DJ)*XNPKW(J-1)+DJ*XNPKW(J)
      XMPN = (1.0-DL)*XMP(L-1)+DL*XMP(L)
      EIN = (1.0-DL)*EI(L-1)+DL*EI(L)
      IF (N - 1 .LE. 0) GO TO 8
      IF (N - 2 .GT. 0) GO TO 10
      XR = 0.0
      GO TO 12
   10 XR = X(N)/X(N-1)
   12 A1 = AFKBB(N-1)*(EINM/EIN)*XR
      A2 = ASKBB(N-1)*(EINM/EIN)
      A3 = AKB(N-1)
      A4 = AK(N-1)
      A5 = XIAK
      A6 = XIAXK
      B1 = BFKBB(N-1)*(EINM/EIN)*XR
      B2 = BSKBB(N-1)*(EINM/EIN)
      B3 = BKB(N-1)
      B4 = BK(N-1)
      B5 = XIBK
      B6 = XIBXK
      A7 = XIMK
      A8 = XIMLK
      A9 = XIMLLK
    8 AFKBB(N) = A1-(X(N)/EIN)*(XNPRAN+XNPKAN)*DX
      ASKBB(N) = A2+(X(N)/EIN)*(XNPRAN+XNPKAN)*DX
      AKBB(N) = AFKBB(N)+ASKBB(N)
      BFKBB(N) = B1+(X(N)/EIN)*(XMPN-XNPKWN)*DX
      BSKBB(N) = B2-(X(N)/EIN)*(XMPN-XNPKWN)*DX
      BKBB(N) = BFKBB(N)+BSKBB(N)
      AKB(N) = A3+AKBB(N)*DX
      BKB(N) = B3+BKBB(N)*DX
      AK(N) = A4+AKB(N)*DX
      BK(N) = B4+BKB(N)*DX
      XIAK = A5+XMPN*AK(N)*DX
      XIAXK = A6+XMPN*AK(N)*X(N)*DX
      XIBK = B5+XMPN*BK(N)*DX
      XIBXK = B6+XMPN*BK(N)*X(N)*DX
      XIMK = A7+XMPN*DX
      XIMLK = A8+XMPN*X(N)*DX
      XIMLLK = A9+XMPN*X(N)**2*DX
      EINM = EIN
      PRINT 106,N,L,J
  106 FORMAT (10X3HN =,I5,10X3HL =,I5,10X3HJ =,I5/)
      PRINT 107,X(N),XNPRAN,XNPKAN,XNPKWN,XMPN
  107 FORMAT (5X6HX      ,F16.8,5X6HXNPRAN,E16.8,5X6HXNPKAN,E16.8,
     1        5X6HXNPKWN,F16.8,5X6HXMPN  ,E16.8)
      PRINT 108,EIN,AFKBB(N),ASKBB(N),AKBB(N),BFKBB(N)
```

```
 108 FORMAT (5X6HEIN    ,F16.8,5X6HAFKBB ,E16.8,5X6HASKBB ,E16.8,
    1          5X6HAKBB  ,F16.8,5X6HBFKBB ,E16.8)
     PRINT 109,BSKBB(N),BKBB(N),AKB(N),BKB(N),AK(N)
 109 FORMAT (5X6HBSKBB ,F16.8,5X6HBKBB  ,E16.8,5X6HAKB   ,E16.8,
    1          5X6HBKB   ,F16.8,5X6HAK    ,E16.8)
     PRINT 110,BK(N),XIAK,XIAXK,XIBK,XIBXK
 110 FORMAT (5X6HBK    ,F16.8,5X6HXIAK  ,E16.8,5X6HXIAXK ,E16.8,
    1          5X6HXIBK  ,F16.8,5X6HXIBXK ,E16.8)
     PRINT 1099,XIMK,XIMLK,XIMLLK
1099 FORMAT (5X6HXIMK  ,F16.8,5X6HXIMLK ,E16.8,5X6HXIMLLK,F16.8//)
 100 CONTINUE
     GAK = (XIAXK*XIMK-XIAK*XIMLK)/(XIMLK**2-XIMK*XIMLLK)
     HAK = (XIAK*XIMLLK-XIAXK*XIMLK)/(XIMLK**2-XIMK*XIMLLK)
     GBK = (XIBXK*XIMK-XIBK*XIMLK)/(XIMLK**2-XIMK*XIMLLK)
     HBK = (XIBK*XIMLLK-XIBXK*XIMLK)/(XIMLK**2-XIMK*XIMLLK)
     PRINT 111,GAK,HAK,GBK,HBK
 111 FORMAT (5X6HGAK   ,F16.8,5X6HHAK   ,E16.8,5X6HGBK   ,F16.8,
    1          5X6HHBK   ,F16.8//)
     DO 1000 N = 1,NB
     PKB(N) = AKB(N)+GAK
     PK(N) = AK(N)+X(N)*GAK+HAK
     QKB(N) = BKB(N)+GBK
     QK(N) = BK(N)+X(N)*GBK+HBK
     PRINT 112,N
 112 FORMAT (10X3HN =,I5//)
     PRINT 113,PKB(N),PK(N),QKB(N),QK(N),X(N)
 113 FORMAT (5X6HPKB   ,F16.8,5X6HPK    ,E16.8,5X6HQKB   ,E16.8,
    1          5X6HQK    ,E16.8,5X6HX     ,E16.8//)
1000 CONTINUE
     PRINT 97
  98 FORMAT (1H1)
 500 FORMAT (8I10)
 501 FORMAT (8E10.4)
  97 FORMAT (//)
     IF (IRUNS - NRUNS) 1,99,99
  99 STOP 1
     END
       ,FOJ
```

SAMPLE INPUT

```
THE NUMBER OF RUNS TO BE PROCESSED IS  1
```

LOCAL VEHICLE DEFLECTION PROGRAM, 4831-1109

SATURN V K # 3

| JB | 67 LR | 63 | NB 67 | | | | |
|---|---|---|---|---|---|---|---|
| XNPRA | 0.14072970E+04 | XNPKA | 0.19018207E+03 | XNPKW | -.13984135E+01 | XJ | 0.15410000E+01 |
| XNPRA | 0.28087999E+04 | XNPKA | 0.37960983E+03 | XNPKW | -.32232983E+00 | XJ | 0.30830000E+01 |
| XNPRA | 0.21145593E+04 | XNPKA | 0.28513430E+03 | XNPKW | -.22931733E+01 | XJ | 0.35000000E+01 |
| XNPRA | 0.16774925E+04 | XNPKA | 0.22568733E+03 | XNPKW | -.27377639E+01 | XJ | 0.40000000E+01 |
| XNPRA | -.75875178E+03 | XNPKA | -.10479809E+03 | XNPKW | 0.20558609E+00 | XJ | 0.12000000E+02 |
| XNPRA | 0.17636729E+03 | XNPKA | 0.25653551E+02 | XNPKW | 0.47936510E-01 | XJ | 0.21480000E+02 |
| XNPRA | 0.11107953E+04 | XNPKA | 0.14936801E+03 | XNPKW | -.90977872E+00 | XJ | 0.21670000E+02 |
| XNPRA | 0.40205554E+04 | XNPKA | 0.53438272E+03 | XNPKW | -.38240427E+01 | XJ | 0.22430000E+02 |
| XNPRA | 0.73895251E+04 | XNPKA | 0.98014233E+03 | XNPKW | -.71941848E+01 | XJ | 0.23380000E+02 |
| XNPRA | 0.67731289E+04 | XNPKA | 0.89182501E+03 | XNPKW | -.65265669E+01 | XJ | 0.24000000E+02 |
| XNPRA | 0.32102698E+04 | XNPKA | 0.40066353E+03 | XNPKW | -.29231198E+01 | XJ | 0.29210000E+02 |
| XNPRA | 0.51190295E+04 | XNPKA | 0.61559604E+03 | XNPKW | -.43811511E+01 | XJ | 0.30154000E+02 |
| XNPRA | 0.10978111E+05 | XNPKA | 0.13202942E+04 | XNPKW | -.94061507E+01 | XJ | 0.33930000E+02 |
| XNPRA | 0.17284196E+05 | XNPKA | 0.20808878E+04 | XNPKW | -.14854754E+02 | XJ | 0.38650000E+02 |
| XNPRA | 0.15466515E+05 | XNPKA | 0.18399058E+04 | XNPKW | -.13180752E+02 | XJ | 0.39000000E+02 |
| XNPRA | 0.10924814E+05 | XNPKA | 0.12342203E+04 | XNPKW | -.89706264E+01 | XJ | 0.44000000E+02 |
| XNPRA | 0.69233552E+04 | XNPKA | 0.68729065E+03 | XNPKW | -.52236456E+01 | XJ | 0.49000000E+02 |
| XNPRA | 0.38466391E+04 | XNPKA | 0.28417840E+03 | XNPKW | -.24176289E+01 | XJ | 0.53853000E+02 |
| XNPRA | 0.41763044E+04 | XNPKA | 0.29030057E+03 | XNPKW | -.25305116E+01 | XJ | 0.54000000E+02 |
| XNPRA | 0.54104414E+04 | XNPKA | 0.37953139E+03 | XNPKW | -.33009311E+01 | XJ | 0.55000000E+02 |
| XNPRA | 0.55986558E+04 | XNPKA | 0.35289495E+03 | XNPKW | -.32202692E+01 | XJ | 0.57000000E+02 |
| XNPRA | 0.70101427E+04 | XNPKA | 0.43204942E+03 | XNPKW | -.39734478E+01 | XJ | 0.60000000E+02 |
| XNPRA | 0.86740874E+04 | XNPKA | 0.53557486E+03 | XNPKW | -.49101060E+01 | XJ | 0.64000000E+02 |
| XNPRA | 0.10173649E+05 | XNPKA | 0.61416945E+03 | XNPKW | -.56822949E+01 | XJ | 0.68000000E+02 |
| XNPRA | 0.11545763E+05 | XNPKA | 0.67855360E+03 | XNPKW | -.63602663E+01 | XJ | 0.72000000E+02 |
| XNPRA | 0.12803147E+05 | XNPKA | 0.72502388E+03 | XNPKW | -.69329650E+01 | XJ | 0.76000000E+02 |
| XNPRA | 0.13977673E+05 | XNPKA | 0.77670923E+03 | XNPKW | -.75209346E+01 | XJ | 0.80000000E+02 |
| XNPRA | 0.14498890E+05 | XNPKA | 0.79721133E+03 | XNPKW | -.77731558E+01 | XJ | 0.81850000E+02 |
| XNPRA | 0.12552358E+05 | XNPKA | 0.53468678E+03 | XNPKW | -.60239503E+01 | XJ | 0.83000000E+02 |
| XNPRA | 0.71793345E+04 | XNPKA | 0.11958223E+03 | XNPKW | -.26374150E+01 | XJ | 0.93000000E+02 |
| XNPRA | 0.49765019E+04 | XNPKA | -.58650515E+02 | XNPKW | -.12241584E+01 | XJ | 0.98000000E+02 |
| XNPRA | 0.31596545E+04 | XNPKA | -.17079492E+03 | XNPKW | -.20838091E+00 | XJ | 0.10300000E+03 |
| XNPRA | 0.17232843E+04 | XNPKA | -.26166106E+03 | XNPKW | 0.60278520E+00 | XJ | 0.10800000E+03 |
| XNPRA | 0.63527922E+03 | XNPKA | -.32555786E+03 | XNPKW | 0.11977109E+01 | XJ | 0.11300000E+03 |
| XNPRA | -.11484219E+02 | XNPKA | -.37374938E+03 | XNPKW | 0.15967959E+01 | XJ | 0.11700000E+03 |
| XNPRA | -.48994712E+03 | XNPKA | -.40977375E+03 | XNPKW | 0.19105909E+01 | XJ | 0.12100000E+03 |
| XNPRA | -.79141886E+03 | XNPKA | -.40967025E+03 | XNPKW | 0.20240034E+01 | XJ | 0.12451800E+03 |
| XNPRA | -.82554452E+03 | XNPKA | -.45623196E+03 | XNPKW | 0.22613480E+01 | XJ | 0.12501800E+03 |
| XNPRA | 0.69245787E+04 | XNPKA | -.14206833E+03 | XNPKW | -.13920404E+01 | XJ | 0.12851800E+03 |
| XNPRA | 0.13543199E+05 | XNPKA | 0.99696127E+02 | XNPKW | -.42686779E+01 | XJ | 0.13251800E+03 |
| XNPRA | 0.19330174E+05 | XNPKA | 0.30791662E+03 | XNPKW | -.67033601E+01 | XJ | 0.13651800E+03 |
| XNPRA | 0.24500751E+05 | XNPKA | 0.47800539E+03 | XNPKW | -.87367468E+01 | XJ | 0.14051800E+03 |
| XNPRA | 0.28028880E+05 | XNPKA | 0.60412913E+03 | XNPKW | -.10183967E+02 | XJ | 0.14347700E+03 |
| XNPRA | 0.25189253E+05 | XNPKA | 0.48861015E+03 | XNPKW | -.87727812E+01 | XJ | 0.14400000E+03 |
| XNPRA | 0.23287489E+05 | XNPKA | 0.36500376E+03 | XNPKW | -.74527788E+01 | XJ | 0.14700000E+03 |
| XNPRA | 0.21411991E+05 | XNPKA | 0.25967936E+03 | XNPKW | -.62603198E+01 | XJ | 0.15000000E+03 |
| XNPRA | 0.18373910E+05 | XNPKA | 0.13778774E+03 | XNPKW | -.46776469E+01 | XJ | 0.15500000E+03 |
| XNPRA | 0.12875845E+05 | XNPKA | -.37710362E+02 | XNPKW | -.21274611E+01 | XJ | 0.16500000E+03 |
| XNPRA | 0.82696728E+04 | XNPKA | -.27284287E+03 | XNPKW | 0.78763781E+00 | XJ | 0.17500000E+03 |
| XNPRA | 0.19787524E+04 | XNPKA | -.48498994E+03 | XNPKW | 0.39847749E+01 | XJ | 0.19500000E+03 |
| XNPRA | -.49364977E+03 | XNPKA | -.62839280E+03 | XNPKW | 0.59645985E+01 | XJ | 0.21000000E+03 |
| XNPRA | -.18572993E+04 | XNPKA | -.76582003E+03 | XNPKW | 0.86343592E+01 | XJ | 0.23000000E+03 |

| | | | | | | | |
|---|---|---|---|---|---|---|---|
| XNPRA | -.19317953E+04 | XNPKA | -.91196134E+03 | XNPKW | 0.11820861E+02 | XJ | 0.25000000E+03 |
| XNPRA | -.12851604E+04 | XNPKA | -.70913745E+03 | XNPKW | 0.11366403E+02 | XJ | 0.28000000E+03 |
| XNPRA | -.77797188E+03 | XNPKA | -.82142919E+03 | XNPKW | 0.16602491E+02 | XJ | 0.30000000E+03 |
| XNPRA | -.47532897E+03 | XNPKA | -.67110953E+03 | XNPKW | 0.15355329E+02 | XJ | 0.31534300E+03 |
| XNPRA | -.34632932E+03 | XNPKA | -.75211144E+03 | XNPKW | 0.17210259E+02 | XJ | 0.31539300E+03 |
| XNPRA | 0.53597989E+04 | XNPKA | -.10513619E+04 | XNPKW | 0.22341211E+02 | XJ | 0.31734300E+03 |
| XNPRA | 0.10861396E+05 | XNPKA | -.14039847E+04 | XNPKW | 0.28912376E+02 | XJ | 0.31934300E+03 |
| XNPRA | 0.20968183E+05 | XNPKA | -.20125815E+04 | XNPKW | 0.40150920E+02 | XJ | 0.32334300E+03 |
| XNPRA | 0.30132287E+05 | XNPKA | -.25971029E+04 | XNPKW | 0.51307633E+02 | XJ | 0.32734300E+03 |
| XNPRA | 0.38571061E+05 | XNPKA | -.31182281E+04 | XNPKW | 0.61202721E+02 | XJ | 0.33134300E+03 |
| XNPRA | 0.46439905E+05 | XNPKA | -.36119497E+04 | XNPKW | 0.70697375E+02 | XJ | 0.33534300E+03 |
| XNPRA | 0.57825955E+05 | XNPKA | -.43192262E+04 | XNPKW | 0.84012946E+02 | XJ | 0.33934300E+03 |
| XNPRA | 0.60907064E+05 | XNPKA | -.45390199E+04 | XNPKW | 0.88786961E+02 | XJ | 0.34334300E+03 |
| XNPRA | 0.67565970E+05 | XNPKA | -.49425464E+04 | XNPKW | 0.96434706E+02 | XJ | 0.34734300E+03 |
| XNPRA | 0.69214357E+05 | XNPKA | -.50423141E+04 | XNPKW | 0.98317149E+02 | XJ | 0.34834300E+03 |
| XMP | 0.00000000E+00 | EI | 0.00000000E+00 | XL | 0.00000000E+00 | | |
| XMP | 0.80460000E+01 | EI | 0.11000000E+09 | XL | 0.33990000E+01 | | |
| XMP | 0.75880000E+01 | EI | 0.18000000E+09 | XL | 0.67330000E+01 | | |
| XMP | 0.75880000E+01 | EI | 0.10000000E+09 | XL | 0.83990000E+01 | | |
| XMP | 0.75880000E+01 | EI | 0.30000000E+09 | XL | 0.10066000E+02 | | |
| XMP | 0.12488000E+02 | EI | 0.30000000E+09 | XL | 0.15066000E+02 | | |
| XMP | 0.12488000E+02 | EI | 0.30000000E+09 | XL | 0.20066000E+02 | | |
| XMP | 0.12488000E+02 | EI | 0.21000000E+09 | XL | 0.21732000E+02 | | |
| XMP | 0.31600000E+01 | EI | 0.90000000E+09 | XL | 0.23399000E+02 | | |
| XMP | 0.31600000E+01 | EI | 0.26000000E+09 | XL | 0.25066000E+02 | | |
| XMP | 0.31600000E+01 | EI | 0.29000000E+09 | XL | 0.28399000E+02 | | |
| XMP | 0.36436000E+02 | EI | 0.32000000E+09 | XL | 0.31732000E+02 | | |
| XMP | 0.36436000E+02 | EI | 0.22900000E+10 | XL | 0.35899000E+02 | | |
| XMP | 0.29773000E+02 | EI | 0.38900000E+10 | XL | 0.39233000E+02 | | |
| XMP | 0.29773000E+02 | EI | 0.17400000E+10 | XL | 0.40066000E+02 | | |
| XMP | 0.29773000E+02 | EI | 0.39900000E+10 | XL | 0.45066000E+02 | | |
| XMP | 0.98161000E+02 | EI | 0.39900000E+10 | XL | 0.47566000E+02 | | |
| XMP | 0.98161000E+02 | EI | 0.26000000E+10 | XL | 0.53399000E+02 | | |
| XMP | 0.34210000E+01 | EI | 0.50300000E+10 | XL | 0.57566000E+02 | | |
| XMP | 0.34210000E+01 | EI | 0.12330000E+11 | XL | 0.70066000E+02 | | |
| XMP | 0.57800000E+01 | EI | 0.14930000E+11 | XL | 0.74233000E+02 | | |
| XMP | 0.57800000E+01 | EI | 0.19970000E+11 | XL | 0.80483000E+02 | | |
| XMP | 0.25711000E+02 | EI | 0.21530000E+11 | XL | 0.82566000E+02 | | |
| XMP | 0.25711000E+02 | EI | 0.41670000E+11 | XL | 0.86733000E+02 | | |
| XMP | 0.56057000E+02 | EI | 0.36110000E+11 | XL | 0.90899000E+02 | | |
| XMP | 0.56057000E+02 | EI | 0.72220000E+11 | XL | 0.99233000E+02 | | |
| XMP | 0.56057000E+02 | EI | 0.72220000E+11 | XL | 0.11381600E+03 | | |
| XMP | 0.49333400E+03 | EI | 0.72220000E+11 | XL | 0.11589900E+03 | | |
| XMP | 0.49333400E+03 | EI | 0.65970000E+11 | XL | 0.12423300E+03 | | |
| XMP | 0.49333400E+03 | EI | 0.63890000E+11 | XL | 0.12839900E+03 | | |
| XMP | 0.28163000E+02 | EI | 0.87500000E+11 | XL | 0.13256600E+03 | | |
| XMP | 0.28163000E+02 | EI | 0.18750000E+12 | XL | 0.14923300E+03 | | |
| XMP | 0.12853000E+03 | EI | 0.34722000E+12 | XL | 0.15339900E+03 | | |
| XMP | 0.12853000E+03 | EI | 0.34722000E+12 | XL | 0.17839900E+03 | | |
| XMP | 0.12317500E+03 | EI | 0.34722000E+12 | XL | 0.18256600E+03 | | |
| XMP | 0.12317500E+03 | EI | 0.34722000E+12 | XL | 0.19089900E+03 | | |
| XMP | 0.15955750E+04 | EI | 0.34722000E+12 | XL | 0.19506600E+03 | | |
| XMP | 0.15955750E+04 | EI | 0.47222000E+12 | XL | 0.19923300E+03 | | |
| XMP | 0.15955750E+04 | EI | 0.40278000E+12 | XL | 0.20339900E+03 | | |
| XMP | 0.95321000E+03 | EI | 0.41667000E+12 | XL | 0.20756600E+03 | | |
| XMP | 0.10317400E+03 | EI | 0.41667000E+12 | XL | 0.21173300E+03 | | |
| XMP | 0.10317400E+03 | EI | 0.41667000E+12 | XL | 0.21673300E+03 | | |
| XMP | 0.46610000E+02 | EI | 0.44444000E+12 | XL | 0.22423300E+03 | | |
| XMP | 0.46610000E+02 | EI | 0.37500000E+12 | XL | 0.22506600E+03 | | |
| XMP | 0.25833200E+03 | EI | 0.43750000E+12 | XL | 0.23673300E+03 | | |
| XMP | 0.18948630E+04 | EI | 0.49999000E+12 | XL | 0.26173300E+03 | | |
| XMP | 0.18867470E+04 | EI | 0.54861000E+12 | XL | 0.27839900E+03 | | |
| XMP | 0.12056050E+04 | EI | 0.48611000E+12 | XL | 0.28256600E+03 | | |
| XMP | 0.12056050E+04 | EI | 0.41319000E+12 | XL | 0.28673300E+03 | | |
| XMP | 0.43368000E+02 | EI | 0.41319000E+12 | XL | 0.29089900E+03 | | |
| XMP | 0.43368000E+02 | EI | 0.41319000E+12 | XL | 0.29506600E+13 | | |

| | | | | | |
|---|---|---|---|---|---|
| XMP | 0.14832300E+03 | FI | 0.41319000E+12 | XL | 0.30339900E+03 |
| XMP | 0.14832300E+03 | FI | 0.44097000E+12 | XL | 0.31173300E+03 |
| XMP | 0.13587880E+04 | FI | 0.45139000E+12 | XL | 0.31589900E+03 |
| XMP | 0.13587880E+04 | FI | 0.45833000E+12 | XL | 0.32006600E+03 |
| XMP | 0.12722090E+04 | FI | 0.45833000E+12 | XL | 0.32423300E+03 |
| XMP | 0.12722090E+04 | FI | 0.76389000E+12 | XL | 0.32839900E+03 |
| XMP | 0.35935500E+03 | FI | 0.97222000E+12 | XL | 0.33256600E+03 |
| XMP | 0.35935500E+03 | FI | 0.12153000E+13 | XL | 0.33673300E+03 |
| XMP | 0.41657900E+03 | FI | 0.15278000E+13 | XL | 0.34089900E+03 |
| XMP | 0.41657900E+03 | FI | 0.17361000E+13 | XL | 0.34506600E+03 |
| XMP | 0.17602700E+03 | FI | 0.17361000E+13 | XL | 0.34714900E+03 |
| XMP | 0.17602700E+03 | FI | 0.17361000E+13 | XL | 0.35339900E+03 |
| X | 0.15410000E+01 | | | | |
| X | 0.30830000E+01 | | | | |
| X | 0.35000000E+01 | | | | |
| X | 0.40000000E+01 | | | | |
| X | 0.12000000E+02 | | | | |
| X | 0.21480000E+02 | | | | |
| X | 0.21670000E+02 | | | | |
| X | 0.22430000E+02 | | | | |
| X | 0.23380000E+02 | | | | |
| X | 0.24000000E+02 | | | | |
| X | 0.29210000E+02 | | | | |
| X | 0.30154000E+02 | | | | |
| X | 0.33930000E+02 | | | | |
| X | 0.38650000E+02 | | | | |
| X | 0.39000000E+02 | | | | |
| X | 0.44000000E+02 | | | | |
| X | 0.49000000E+02 | | | | |
| X | 0.53853000E+02 | | | | |
| X | 0.54000000E+02 | | | | |
| X | 0.55000000E+02 | | | | |
| X | 0.57000000E+02 | | | | |
| X | 0.60000000E+02 | | | | |
| X | 0.64000000E+02 | | | | |
| X | 0.68000000E+02 | | | | |
| X | 0.72000000E+02 | | | | |
| X | 0.76000000E+02 | | | | |
| X | 0.80000000E+02 | | | | |
| X | 0.81850000E+02 | | | | |
| X | 0.83000000E+02 | | | | |
| X | 0.93000000E+02 | | | | |
| X | 0.98000000E+02 | | | | |
| X | 0.10300000E+03 | | | | |
| X | 0.10800000E+03 | | | | |
| X | 0.11300000E+03 | | | | |
| X | 0.11700000E+03 | | | | |
| X | 0.12100000E+03 | | | | |
| X | 0.12451800E+03 | | | | |
| X | 0.12501800E+03 | | | | |
| X | 0.12851800E+03 | | | | |
| X | 0.13251800E+03 | | | | |
| X | 0.13651800E+03 | | | | |
| X | 0.14051800E+03 | | | | |
| X | 0.14347700E+03 | | | | |
| X | 0.14400000E+03 | | | | |
| X | 0.14700000E+03 | | | | |
| X | 0.15000000E+03 | | | | |
| X | 0.15500000E+03 | | | | |
| X | 0.16500000E+03 | | | | |
| X | 0.17500000E+03 | | | | |
| X | 0.19500000E+03 | | | | |
| X | 0.21000000E+03 | | | | |
| X | 0.23000000E+03 | | | | |
| X | 0.25000000E+03 | | | | |
| X | 0.28000000E+03 | | | | |

| | |
|---|---|
| x | 0.39000000E+03 |
| x | 0.31534300E+03 |
| x | 0.31539300E+03 |
| x | 0.31734300E+03 |
| x | 0.31934300E+03 |
| x | 0.32334300E+03 |
| x | 0.32734300E+03 |
| x | 0.33134300E+03 |
| x | 0.33534300E+03 |
| x | 0.33934300E+03 |
| x | 0.34334300E+03 |
| x | 0.34734300E+03 |
| x | 0.34834300E+03 |

SAMPLE OUTPUT

```
LOCAL VEHICLE DEFLECTION PROGRAM, 4831-1109

    N =    1          L =    2          J =    2

X      0.15410000E+01    XNPRAN  0.14072970E+04    XNPKAN  0.19018207E+03    XNPKWN  -.13984135E+01    XMPN   0.66732433E+01
EIN    0.91232508E+08    AFKBB   -.20803796E-04    ASKBB   0.20803796E-04    AKBB    0.00000000E+00    BFKBB  0.10511630E-06
BSKBB  -.10511630E-06    BKBB    0.00000000E+00    AKB     0.00000000E+00    BKB     0.00000000E+00    AK     0.00000000E+00
BK     0.00000000E+00    XIAK    0.00000000E+00    XIAXK   0.00000000E+00    XIBK    0.00000000E+00    XIBXK  0.00000000E+00
XIMK   0.51450706E+01    XIMLK   0.79285537E+01    XIMLLK  0.12217901E+02

    N =    2          L =    2          J =    2

X      0.30830000E+01    XNPRAN  0.28087999E+04    XNPKAN  0.37960983E+03    XNPKWN  -.32232983E+00    XMPN   0.13350817E+02
EIN    0.18252422E+09    AFKBB   -.52751109E-04    ASKBB   0.63149632E-04    AKBB    0.10398523E-04    BFKBB  0.22621737E-06
BSKBB  -.27875847E-06    BKBB    -.52541105E-07    AKB     0.10185354E-04    BKB     -.51464012E-07    AK     0.99765544E-05
BK     -.50409000E-07    XIAK    0.13046465E-03    XIAXK   0.40222252E-03    XIBK    -.65920481E-06    XIBXK  -.20323284E-05
XIMK   0.18222196E+02    XIMLK   0.48245331E+02    XIMLLK  0.13651453E+03

    N =    3          L =    3          J =    3

X      0.35000000E+01    XNPRAN  0.21145593E+04    XNPKAN  0.28513430E+03    XNPKWN  -.22931733E+01    XMPN   0.80333266E+01
EIN    0.11193698E+09    AFKBB   -.13205263E-03    ASKBB   0.13737413E-03    AKBB    0.53214915E-05    BFKBB  0.56680476E-06
BSKBB  -.60258566E-06    BKBB    -.35780907E-07    AKB     0.12625258E-04    BKB     -.67869558E-07    AK     0.15765235E-04
BK     -.81527193E-07    XIAK    0.18853243E-03    XIAXK   0.60545975E-03    XIBK    -.95949231E-06    XIBXK  -.30833347E-05
XIMK   0.21905476E+02    XIMLK   0.61136812E+02    XIMLLK  0.18163471E+03

    N =    4          L =    3          J =    4

X      0.40000000E+01    XNPRAN  0.16774925E+04    XNPKAN  0.22568733E+03    XNPKWN  -.27377639E+01    XMPN   0.79705868E+01
EIN    0.12152602E+09    AFKBB   -.40524063E-03    ASKBB   0.39276609E-03    AKBB    -.12474543E-04    BFKBB  0.20946307E-05
BSKBB  -.20530054E-05    BKBB    0.41625379E-07    AKB     -.40391552E-04    BKB     0.10903830E-06    AK     -.15589886E-03
BK     0.38188559E-06    XIAK    -.50925405E-02    XIAXK   -.20518832E-01    XIBK    0.11976879E-04    XIBXK  0.48662153E-04
XIMK   0.55780470E+02    XIMLK   0.19663679E+03    XIMLLK  0.72363461E+03

    N =    5          L =    6          J =    5

X      0.12000000E+02    XNPRAN  -.75875178E+03    XNPKAN  -.10479809E+03    XNPKWN  0.20558609E+00    XMPN   0.10678867E+02
EIN    0.30000000E+09    AFKBB   -.19057581E-03    ASKBB   -.14279269E-03    AKBB    -.33336850E-03    BFKBB  0.62069807E-05
BSKBB  -.44931045E-05    BKBB    0.17138762E-05    AKB     -.29540323E-02    BKB     0.15088317E-04    AK     -.25974141E-01
BK     0.13225377E-03    XIAK    -.24293449E+01    XIAXK   -.29111547E+02    XIBK    0.12355658E-01    XIBXK  0.14817284E+00
XIMK   0.14911377E+03    XIMLK   0.13166364E+04    XIMLLK  0.14163630E+05

    N =    6          L =    8          J =    6

X      0.21480000E+02    XNPRAN  0.17636729E+03    XNPKAN  0.25653551E+02    XNPKWN  0.47936510E-01    XMPN   0.12488000E+02
EIN    -.17525806E+10    AFKBB   0.70364948E-04    ASKBB   0.12471193E-04    AKBB    0.82836141E-04    BFKBB  -.26390349E-05
BSKBB  0.15062954E-05    BKBB    -.11327394E-05    AKB     -.25535195E-02.   BKB     0.96115212E-05    AK     -.38320408E-01
BK     0.17872548E-03    XIAK    -.47431112E+01    XIAXK   -.78811247E+02    XIBK    0.23147010E-01    XIBXK  0.37997107E+00
XIMK   0.20949325E+03    XIMLK   0.26135877E+04    XIMLLK  0.42022143E+05

    N =    7          L =    8          J =    7

X      0.21670000E+02    XNPRAN  0.11107953E+04    XNPKAN  0.14936801E+03    XNPKWN  [illegible]       XMPN   [illegible]
```

```
PKB    -.60542993E-01    PK    -.11703342E+01    QKB    0.10837895E-02    QK    0.23873674E-01    X    0.33534300E+03

     N =   64

PKB    -.61740565E-01    PK    -.14172965E+01    QKB    0.11181061E-02    QK    0.28346098E-01    X    0.33934300E+03

     N =   65

PKB    -.62730875E-01    PK    -.16682200E+01    QKB    0.11470854E-02    QK    0.32934440E-01    X    0.34334300E+03

     N =   66

PKB    -.63297984E-01    PK    -.16212962E+01    QKB    0.11639785E-02    QK    0.34353831E-01    X    0.34734300E+03

     N =   67

PKB    -.63412155E-01    PK    -.15846127E+01    QKB    0.11673927E-02    QK    0.34440675E-01    X    0.34834300E+03
```

# APPENDIX F

This appendix contains the necessary information to determine the integrated vehicle dynamics of a flexible vehicle. It contains a flow diagram of the numerical analysis of the equations derived in section IV. It also contains a listing of the computer program and sample inputs and outputs.

This computer program determines the absolute values and phase angles of the following flexible vehicle frequency response functions:

- Wind velocity to vehicle normal acceleration
- Wind velocity to engine gimbal angle
- Wind velocity to vehicle yaw angle

The input for this program consists of:

- Flexible body aerodynamic terms
- Flexible body slope parameters
- Mass data
- Engine thrust and control parameters

This flexible body control program is based on a basic control analysis. It is valid only at frequencies below the control frequency of the vehicle. However it does include flexible body aerodynamic terms and it also includes the effects of vehicle flexing on the attitude sensors.

## DEFINITION OF SYMBOLS

| Symbol | Definition |
|---|---|
| XNRAN | Rigid body normal force derivative, lb /rad |
| XNKAN | Derivative of the incremental normal force caused by flexing due to the aerodynamic loading, lb /rad |
| XNKWN | Derivative of the incremental normal force caused by flexing due to the acceleration loading, lb $sec^2$/ft |
| XMRAN | Rigid body yawing moment derivative, ft lb /rad |
| XMKAN | Derivative of the incremental yawing moment caused by flexing due to the aerodynamic loading, ft lb /rad |
| XMKWN | Derivative of the incremental yawing moment caused by flexing due to the acceleration loading, lb/$sec^2$ |
| XI | Moment of inertia, slug $ft^2$ |
| XL | Vehicle length, ft |
| XCG | Distance from vehicle nose to the center of gravity, ft |
| F | Gimbled thrust, lb |
| V | Vehicle velocity, ft/sec |
| XM | Vehicle mass, slug |
| AO | Control gain |
| Al | Control gain, sec |
| PKBXB | Flexing parameter at I. U. |
| PKBL | Flexing parameter at vehicle base |
| QKBXB | Flexing parameter at I. U., ft/$sec^2$ |
| QKBL | Flexing parameter at base, ft/$sec^2$ |
| DELW | Incremental frequency, rad/sec |
| WB | Frequency cutoff, rad/sec |
| ABFPV | Absolute value of the frequency response function of wind velocity to yaw angle, rad sec/ft |
| ABFWV | Absolute value of the frequency response function of wind velocity to vehicle normal acceleration, 1/sec |
| ABFBV | Absolute value of the frequency response function of wind velocity to engine gimbal angle, rad sec/ft |

## SOLUTION OF EQUATIONS

1. $S1 = -(XMRAN + XMKAN) + (XL - XCG)\ F\ [AO(1 + PKBXB) + PKBL]$

2. $S2 = -XMKWN + (XL - XCG)\ F\ [AO(QKBXB) + QKBL]$

3. $S3 = -(XMRAN + XMKAN) + (XL - XCG)\ F\ [AO(PKBXB) + PKBL]$

4. $T1 = XNRAN + XNKAN + F[AO(1 + PKBXB) + PKBL]$

5. $T2 = XNKWN - XM + F[AO(QKBXB) + QKBL]$

6. $T3 = XNRAN + XNKAN + F[AO(PKBXB) + PKBL]$

7. $$PH1V = \frac{\frac{1}{V}\Big[S2(T3)-S3(T2)\Big]\Big[S1(T2)-S2(T1)-T2(XI)(W^2)\Big]}{\Big[S1(T2)-S2(T1)-T2(XI)W^2\Big]^2 + A1^2F^2\Big[T2(XL-XCG) - S2\Big]^2 W^2}$$

8. $$PH2V = \frac{-\Big[\frac{1}{V}\Big\{S2(T3)-S3(T2)\Big\}A1(F)\Big\{T2(XL-XCG)-S2\Big\}W\Big]}{\Big[S1(T2)-S2(T1)-T2(XI)W^2\Big]^2 + A1^2F^2\Big[T2(XL-XCG)-S2\Big]^2W^2}$$

9. $ABFPV = +\sqrt{PH1V^2 + PH2V^2}$

10. $THPV = TAN^{-1}\left[\frac{-PH2V}{PH1V}\right]$

11. $W1V = A1(F)(W)\left[\frac{PH2V}{T2}\right] - T1\left[\frac{PH1V}{T2}\right] - \left[\frac{T3}{T2(V)}\right]$

12. $W2V = -A1(F)(W)\left[\frac{PH1V}{T2}\right] - T1\left[\frac{PH2V}{T2}\right]$

13. $$ABFWV = \pm \sqrt{W1V^2 + W2V^2}$$

14. $$THWV = TAN^{-1}\left[\frac{-W2V}{W1V}\right]$$

15. $$BET1V = [A0 + A0(PKBXB)]\ PH1V - A1(W)(PH2V) + A0(QKBXB)\ (W1V)$$
$$+ A0(PKBXB)$$

16. $$BET2V = [A0 + A0(PKBXB)]\ PH2V + A1(W)(PH1V) + A0(QKBXB)(W2V)$$

17. $$ABFBV = \pm \sqrt{BET1V^2 + BET2V^2}$$

18. $$THBV = TAN^{-1}\left[\frac{-BET2V}{BET1V}\right]$$

## COMPUTER FLOW DIAGRAM

**INPUTS**

XNRAN, XNKAN, XNKWN, XMRAN, XMKAN, XMKWN
XI, XL, XCG, F, V, XM, AO, A1, PKBXB, PKBL, QKBXB, QKBL,
DELW, WB

**PRINT INPUTS**

S1 = -(XMRAN + XMKAN) + (XL-XCG)* F * (AO(1+PKBXB) + PKBL)

S2 = -XMKWN + (XL-XCG) * F * (AO * QKBXB + QKBL)

S3 = -(XMRAN + XMKAN) + (XL-XCG) * F * (AO * PKBXB + PKBL)

T1 = XNRAN + XNKAN + F * (AO (1 + PKBXB) + PKBL)

T2 = XNKWN-XM + F * (AO * QKBXB + QKBL)

T3 = XNRAN + XNKAN * F * (AO * PKBXB + PKBL)

W = - DELW

W = W + DELW

$$PH1V = [(1/V)(S2 * T3 - S3 * T2)(S1 * T2 - S2 * T1 - T2 * XI * W^2)] \,/\, [(S1 * T2 - S2 * T1 - T2 * XI * W^2)^2 + A1^2 * F^2 * (T2 * (XL-XCG) - S2)^2 * W^2]$$

$$PH2V = - [(1/V)(S2*T3 - T2)*A1*F*(T2*(XL-XCG) - S2)\ W] \,/\, [(S1*T2 - S2*T1 - T2*XI*W^2)^2 + A1^2*F^2*(T2*(XL-XCG)-S2)^2*W^2]$$

1

(1)

$$ABFPV = +\sqrt{PH1V^2 + PH2V^2}$$

$$THPV = \tan^{-1}\left[\frac{-PH2V}{PH1V}\right]$$

W1V = A1 * F * W * PH2V/T2 - T1 * PH1V / T2 - T3 / (T2 * V)

W2V = -A1 * F * W * PH1V / T2 - T1 * PH2V / T2

$$ABFWV = +\sqrt{W1V^2 + W2V^2}$$

$$THWV = \tan^{-1}\left[\frac{-W2V}{W1V}\right]$$

BET1V = [AO+AO*PKBXB] *PH1V - A1*W*PH2V+AO*QKBXB*W1V +AO*PKBXB/V

BET2V = (AO+AO*PKBXB)*PH2V+A1*W*PH1V+AO*QKBXB*W2V

$$ABFBV = +\sqrt{BET1V^2 + BET2V^2}$$

$$THBV = \tan^{-1}\left[\frac{-BET2V}{BET1V}\right]$$

PRINT

W, PH1V, PH2V, ABFPV, THPV, ABFWV, THWV, ABFBV, THBV

WB-W

PRINT S1, S2, S3, T1, T2, T3

STOP

## PREPARATION OF DATA

The GE 415 FORTRAN Routine 4831-1110 has the capability of making a series of consecutive runs. The input for this routine consists of a Production Control Card, Title Card, and four data cards.

### Production Control Card

The first card presented for each production run must be the Production Control Card, which specifies in column 10 the number of runs contained within the production run.

### Title Card

The title card is a card which lets the user identify the runs. The computer will print whatever is punched on this card. The title card must be present in every run even if it is blank.

### Data Cards

There are four input data cards. Card 1 contains XNRAN, XNKAN, XNKWN, XMRAN, and XMKAN. Card 2 contains XMKWN, XI, XL, XCG, and F. Card 3 contains V, XM, AO, A1, and PKBXB. Card 4 contains PKBL, QKBXB, QKBL, DELW, and WB. The definitions of the above symbols are given in the section on definition of symbols.

### Data Presentation

The form of the data to be presented for Computer Routine 4831-1110 must be submitted as shown below:

| | |
|---|---|
| Production Control Card | Format (8I10) |
| NRUNS | |
| Title Card | Format (80H) |
| First Data Card | Format (8E10. 4) |

XNRAN
XNKAN
XNKWN
XMRAN
XMKAN

Second Data Card — Format (8E10. 4)

XMKWN
XI
XL
XCG
F

Third Data Card — Format (8E10. 4)

V
XM
AO
A1
PKBXB

Fourth Data Card — Format (8E10. 4)

PKBL
QKBXB
QKBL
DELW
WB

All of the above data must be presented for the first of a series of consecutive runs. For each subsequent run, omit the Production Control Card.

The deck for a production run is prepared by simply stacking the runs consecutively.

```
      .JOB,TATE
      .PX
      .FORTRAN,OPT
               ENDOPT
C     PROGRAM NUMBER - 4831-1110
C     PROGRAM NAME - INTEGRATED VEHICLE DYNAMICS PROGRAM
      PRINT 98
      IRUNS = 0
      READ 500,NRUNS
      PRINT 104,NRUNS
  104 FORMAT (10X37HTHE NUMBER OF RUNS TO BE PROCESSED IS,I3)
    1 PRINT 98
      IRUNS = IRUNS + 1
      PRINT 600
  600 FORMAT (20X46HINTEGRATED VEHICLE DYNAMICS PROGRAM, 4831-1110//)
      READ 1111
      PRINT 1111
 1111 FORMAT (80H
     1                                                                )
      PRINT 97
      READ 501,XNRAN,XNKAN,XNKWN,XMRAN,XMKAN
      PRINT 101,XNRAN,XNKAN,XNKWN,XMRAN,XMKAN
  101 FORMAT (10X5HXNRAN,E16.8,5X5HXNKAN,E16.8,5X5HXNKWN,E16.8,
     1           5X5HXMRAN,E16.8,5X5HXMKAN,E16.8)
      READ 501,XMKWN,XI,XL,XCG,F
      PRINT 102,XMKWN,XI,XL,XCG,F
  102 FORMAT (10X5HXMKWN,E16.8,5X5HXI    ,E16.8,5X5HXL    ,E16.8,
     1           5X5HXCG   ,E16.8,5X5HF     ,E16.8)
      READ 501,V,XM,A0,A1,PKBXB
      PRINT 103,V,XM,A0,A1,PKBXB
  103 FORMAT (10X5HV     ,E16.8,5X5HXM    ,E16.8,5X5HA0    ,E16.8,
     1           5X5HA1    ,E16.8,5X5HPKBXB,E16.8)
      READ 501,PKBL,QKBXB,QKBL,DELW,WB
      PRINT 105,PKBL,QKBXB,QKBL,DELW,WB
  105 FORMAT (10X5HPKBL  ,E16.8,5X5HQKBXB,E16.8,5X5HQKBL  ,E16.8,
     1           5X5HDELW  ,E16.8,5X5HWB    ,E16.8)
      PRINT 98
      PRINT 600
      S1= -(XMRAN+XMKAN)+(XL-XCG)*F*(A0*(1.0+PKBXB)+PKBL)
      S2 = -XMKWN+(XL-XCG)*F*(A0*QKBXB+QKBL)
      S3 = -(XMRAN+XMKAN)+(XL-XCG)*F*(A0*PKBXB+PKBL)
      T1 = XNRAN+XNKAN+F*(A0*(1.0+PKBXB)+PKBL)
      T2 = XNKWN-XM+F*(A0*QKBXB+QKBL)
      T3 = XNRAN+XNKAN+F*(A0*PKBXB+PKBL)
      W = -DELW
    2 W = W+DELW
      PH1V = ((1.0/V)*(S2*T3-S3*T2)*(S1*T2-S2*T1-T2*XI*W**2))/
     1((S1*T2-S2*T1-T2*XI*W**2)**2+A1**2*F**2*(T2*(XL-XCG)-S2)**2*W**2)
      PH2V =-((1.0/V)*(S2*T3-S3*T2)*A1*F*(T2*(XL-XCG)-S2)*W)/
     1((S1*T2-S2*T1-T2*XI*W**2)**2+A1**2*F**2*(T2*(XL-XCG)-S2)**2*W**2)
      ABFPV = SQRT(PH1V**2+PH2V**2)
      THPV = ATAN(-PH2V/PH1V)
      W1V = A1*F*W*PH2V/T2-T1*PH1V/T2-T3/(T2*V)
      W2V = -A1*F*W*PH1V/T2-T1*PH2V/T2
      ABFWV = SQRT(W1V**2+W2V**2)
```

```
      THWV = ATAN(-W2V/W1V)
      BET1V = (A0+A0*PKBXB)*PH1V-A1*W*PH2V+A0*QKBXB*W1V+A0*PKBXB/V
      BET2V = (A0+A0*PKBXB)*PH2V+A1*W*PH1V+A0*QKBXB*W2V
      ABFBV = SQRT(BET1V**2+BET2V**2)
      THBV = ATAN(-BET2V/BET1V)
      PRINT 106,W,PH1V,PH2V,ABFPV,THPV
  106 FORMAT (10X5HW     ,F16.8,5X5HPH1V ,F16.8,5X5HPH2V ,F16.8,
     1            5X5HABFPV,F16.8,5X5HTHPV ,F16.8)
      PRINT 107,ABFWV,THWV,ABFBV,THBV
  107 FORMAT (10X5HABFWV,F16.8,5X5HTHWV ,E16.8,5X5HABFBV,F16.8,
     1            5X5HTHBV ,F16.8)
      PRINT 97
      IF (WB - W .GE. 0.0) GO TO 2
      PRINT 900,S1,S2,S3
      PRINT 901,T1,T2,T3
  900 FORMAT (10X5HS1    ,F16.8,5X5HS2    ,E16.8,5X5HS3    ,E16.8//)
  901 FORMAT (10X5HT1    ,F16.8,5X5HT2    ,F16.8,5X5HT3    ,E16.8//)
      IF (IRUNS - NRUNS) 1,99,99
   98 FORMAT (1H1)
  500 FORMAT (8I10)
  501 FORMAT (8E10.4)
   97 FORMAT (//)
   99 STOP 1
      END
```

SAMPLE INPUT

```
THE NUMBER OF RUNS TO BE PROCESSED IS  1
```

INTEGRATED VEHICLE DYNAMICS PROGRAM. 4831-1110

FLEXIBLE BODY DATA

| | | | | | | | | | |
|---|---|---|---|---|---|---|---|---|---|
| XNRAN | 0.27800000E+07 | XNKAN | -.14898000E+06 | XNKWN | 0.27210000E+04 | XMRAN | 0.12607000E+09 | XMKAN | 0.15998000E+08 |
| XMKWN | -.29540000E+06 | XI | 0.55500000E+09 | XL | 0.35340000E+03 | XCG | 0.25260000E+03 | F | 0.30000000E+07 |
| V | 0.16480000E+04 | XM | 0.14829500E+06 | A0 | 0.86000000E+00 | A1 | 0.11500000E+01 | PKBXP | 0.32508000E-01 |
| PKBL | -.63412100E-01 | QKBXB | -.41270000E-03 | QKBL | 0.11674000E-02 | DELW | 0.10000000E-01 | WB | 0.20000000E+06 |

SAMPLE OUTPUT

```
INTEGRATED VEHICLE DYNAMICS PROGRAM, 4831-1110

W      0.00000000E+00    PH1V   0.71813940E-03    PH2V   0.00000000E+00    ABFPV  0.71813940E-03    THPV   0.00000000E+00
ABFWV  0.36313599E-01    THWV   0.00000000E+00    ABFBV  0.64175245E-03    THBV   0.00000000E+00

W      0.10000000E-01    PH1V   0.71784956E-03    PH2V   -.20969104E-04    ABFPV  0.71815576E-03    THPV   0.29202697E-01
ABFWV  0.36312866E-01    THWV   0.15829631E-01    ABFBV  0.64181853E-03    THBV   0.15831278E-01

W      0.20000000E-01    PH1V   0.71697813E-03    PH2V   -.41943838E-04    ABFPV  0.71820396E-03    THPV   0.58434261E-01
ABFWV  0.36310626E-01    THWV   0.31682291E-01    ABFBV  0.64201599E-03    THBV   0.31695464E-01

W      0.30000000E-01    PH1V   0.71551946E-03    PH2V   -.62929330E-04    ABFPV  0.71828142E-03    THPV   0.87723435E-01
ABFWV  0.36306758E-01    THWV   0.47580882E-01    ABFBV  0.64234247E-03    THBV   0.47625333E-01

W      0.40000000E-01    PH1V   0.71346417E-03    PH2V   -.83929699E-04    ABFPV  0.71838383E-03    THPV   0.11709870E+00
ABFWV  0.36301059E-01    THWV   0.63548052E-01    ABFBV  0.64279406E-03    THBV   0.63653391E-01

W      0.50000000E-01    PH1V   0.71079926E-03    PH2V   -.10494754E-03    ABFPV  0.71850510E-03    THPV   0.14658817E+00
ABFWV  0.36293242E-01    THWV   0.79606060E-01    ABFBV  0.64336523E-03    THBV   0.79811731E-01

W      0.60000000E-01    PH1V   0.70750827E-03    PH2V   -.12598346E-03    ABFPV  0.71863744E-03    THPV   0.17621940E+00
ABFWV  0.36282944E-01    THWV   0.95776635E-01    ABFBV  0.64404887E-03    THBV   0.96131888E-01

W      0.70000000E-01    PH1V   0.70357141E-03    PH2V   -.14703545E-03    ABFPV  0.71877128E-03    THPV   0.20601929E+00
ABFWV  0.36269715E-01    THWV   0.11208082E+00    ABFBV  0.64483619E-03    THBV   0.11264468E+00

W      0.80000000E-01    PH1V   0.69896590E-03    PH2V   -.16809850E-03    ABFPV  0.71889529E-03    THPV   0.23601391E+00
ABFWV  0.36253028E-01    THWV   0.12853886E+00    ABFBV  0.64571678E-03    THBV   0.12938007E+00

W      0.90000000E-01    PH1V   0.69366616E-03    PH2V   -.18916399E-03    ABFPV  0.71899635E-03    THPV   0.26622831E+00
ABFWV  0.36232274E-01    THWV   0.1451690[illegible]E+00    ABFBV  0.64667850E-03    THBV   0.14636691E+00

W      0.10000000E+00    PH1V   0.68764426E-03    PH2V   -.21021920E-03    ABFPV  0.71905962E-03    THPV   0.29668636E+00
ABFWV  0.36206765E-01    THWV   0.16199210E+00    ABFBV  0.64770753E-03    THBV   0.16363287E+00

W      0.11000000E+00    PH1V   0.68087032E-03    PH2V   -.23124682E-03    ABFPV  0.71906844E-03    THPV   0.3274[illegible]55E+00
ABFWV  0.36175735E-01    THWV   0.17902197E+00    ABFBV  0.64878831E-03    THBV   0.18120412E+00
```

| | | | | | | | | | |
|---|---|---|---|---|---|---|---|---|---|
| W | 0.12000000E+00 | PH1V | 0.67331304E-03 | PH2V | -.25222445E-03 | ABFPV | 0.71900461E-03 | THPV | 0.35842174E+00 |
| ABFWV | 0.36138344E-01 | THWV | 0.19627458E+00 | ABFBV | 0.64990354E-03 | THBV | 0.19910517E+00 | | |
| W | 0.13000000E+00 | PH1V | 0.66494035E-03 | PH2V | -.27312414E-03 | ABFPV | 0.71884801E-03 | THPV | 0.38973899E+00 |
| ABFWV | 0.36093679E-01 | THWV | 0.21376316E+00 | ABFBV | 0.65103420E-03 | THBV | 0.21735864E+00 | | |
| W | 0.14000000E+00 | PH1V | 0.65572003E-03 | PH2V | -.29391203E-03 | ABFPV | 0.71857709E-03 | THPV | 0.42137929E+00 |
| ABFWV | 0.36040763E-01 | THWV | 0.23149885E+00 | ABFBV | 0.65215956E-03 | THBV | 0.23598497E+00 | | |
| W | 0.15000000E+00 | PH1V | 0.64562061E-03 | PH2V | -.31454797E-03 | ABFPV | 0.71816878E-03 | THPV | 0.45335729E+00 |
| ABFWV | 0.35978555E-01 | THWV | 0.24949049E+00 | ABFBV | 0.65325725E-03 | THBV | 0.25500221E+00 | | |
| W | 0.16000000E+00 | PH1V | 0.63461218E-03 | PH2V | -.33498530E-03 | ABFPV | 0.71759862E-03 | THPV | 0.48568507E+00 |
| ABFWV | 0.35905965E-01 | THWV | 0.26774434E+00 | ABFBV | 0.65430331E-03 | THBV | 0.27442573E+00 | | |
| W | 0.17000000E+00 | PH1V | 0.62266744E-03 | PH2V | -.35517070E-03 | ABFPV | 0.71684097E-03 | THPV | 0.51837184E+00 |
| ABFWV | 0.35821857E-01 | THWV | 0.28626382E+00 | ABFBV | 0.65527232E-03 | THBV | 0.29426793E+00 | | |
| W | 0.18000000E+00 | PH1V | 0.60976271E-03 | PH2V | -.37504418E-03 | ABFPV | 0.71586919E-03 | THPV | 0.55142370E+00 |
| ABFWV | 0.35725063E-01 | THWV | 0.30504925E+00 | ABFBV | 0.65613754E-03 | THBV | 0.31453802E+00 | | |
| W | 0.19000000E+00 | PH1V | 0.59587910E-03 | PH2V | -.39453923E-03 | ABFPV | 0.71465593E-03 | THPV | 0.58484336E+00 |
| ABFWV | 0.35614406E-01 | THWV | 0.32409759E+00 | ABFBV | 0.65687110E-03 | THBV | 0.33524167E+00 | | |
| W | 0.20000000E+00 | PH1V | 0.58100366E-03 | PH2V | -.41358315E-03 | ABFPV | 0.71317339E-03 | THPV | 0.61862987E+00 |
| ABFWV | 0.35488678E-01 | THWV | 0.34340217E+00 | ABFBV | 0.65744424E-03 | THBV | 0.35638083E+00 | | |
| W | 0.21000000E+00 | PH1V | 0.56513060E-03 | PH2V | -.43209761E-03 | ABFPV | 0.71139366E-03 | THPV | 0.65277842E+00 |
| ABFWV | 0.35346723E-01 | THWV | 0.36295250E+00 | ABFBV | 0.65782756E-03 | THBV | 0.37795346E+00 | | |
| S1 | 0.10427434E+09 | S2 | 0.54109335E+06 | S3 | -.15578966E+09 | | | | |
| T1 | 0.51046543E+07 | T2 | -.14313657E+06 | T3 | 0.25246543E+07 | | | | |

TECHNICAL REPORT HSM-R111-68
October 7, 1968

# STUDY PROGRAM OF LOCAL ANGLE-OF-ATTACK EFFECTS ON VEHICLE DYNAMIC RESPONSE


By: George F. McCanless, Jr.

George F. McCanless, Jr.

By: Dale Bradley

Dale Bradley

Approved: M. L. Bell

M. L. Bell
Manager, Aero-Space Mechanics Branch

Approved: H. Bader, Jr.

H. Bader, Jr.
Chief Engineer, Structures and Mechanics Engineering Department